SYNTHESIS OF AMINOMETHYLTHIAZOLE ANALOGUES FOR EVALUATION AS ANTIPLASMODIAL AGENTS

A Dissertation submitted to the

UNIVERSITY OF CAPE TOWN

In fulfilment of the requirements for the degree of

MASTER OF SCIENCE

By

PETER M. CHEUKA

Supervisor: Professor KELLY CHIBALE

DEPARTMENT OF CHEMISTRY
UNIVERSITY OF CAPE TOWN
RONDEBOSCH 7701
CAPE TOWN
SOUTH AFRICA

DECEMBER 2013

TABLE OF CONTENTS

Chapter 3: Synthesis and Characterisation of Target Compounds

Chapter 4: Pharmacological Evaluation, Solubility, and Discussion

Chapter 5: Experimental

DECLARATION

I know the meaning of plagiarism and declare that all of the work in the dissertation, save for that which is properly acknowledged, is my own.

Date:

Signature:

ACKNOWLEDGEMENTS

Let me take this opportunity to extend my heartfelt thanks to my supervisor and indeed great mentor Professor Kelly Chibale for his guidance from the beginning of the research to its conclusion. He is also very much appreciated for funding of the entire research through a Medicinal Chemistry Scholarship. I would also love to acknowledge the following: Dr. Diego Gonzalez Cabrera and Dr. Tanya Paquet for their useful suggestions and concrete direction they offered on the chemistry aspect and proof reading of the dissertation; Dr. Marlene Espinoza Moraga, Shankari Nair, and Nicholas Njuguna for assisting in conducting solubility assays for the target compounds; Dr. Claire Le Manach for performing HPLC purity check experiments on some target compounds. I am also indeed grateful to the other Kelly Chibale research group members for their support.

Professor Peter Smith of University of Cape Town Division of Pharmacology is greatly acknowledged for the biological testing of the compounds.

I am also highly indebted to the Departments of Chemistry of the University of Zambia and University of Cape Town for their critically important support during my entire period of study.

My wife Martha including my daughter Merit are also acknowledged for their love and support they have shown.

Finally, the many Malaria victims especially of Sub-Saharan Africa are greatly acknowledged for giving me the impetus to contribute to the fight against this disease through this research project. This dissertation is dedicated to them.

PUBLICATIONS AND CONFERENCES

A Part of this dissertation was presented at the conference below:

- **Oral presentation:** Drug Discovery Re-Invented: Emerging Role of Biotechs, Academics and Non-Profits; October 16 - 19, 2013 at Hilton Scottsdale Resort & Villas, Scottsdale, Arizona, USA; *Aminomethylthiazoles as Orally Active Antimalarial Agents*.

ABSTRACT

The World Health Organisation has estimated that about 219 million cases of malaria occurred in 2010 with an estimated 660,000 fatalities resulting. The disease is caused by five species of protozoan parasites of the genus *Plasmodium* with *Plasmodium falciparum* being the most virulent. Among the many shortfalls of current antimalarial drugs, the emergence of drug resistant strains of the malaria parasites is the most disturbing. Thus, there is an urgent need to develop new chemotherapeutic agents which can potentially target drug resistant strains of these parasites. Undertaking structure activity relationship (SAR) studies around biologically active compounds is one strategy that can identify analogues with superior activity and/or novel modes of action to circumvent drug resistance. In this dissertation, the synthesis, characterisation, and antiplasmodial evaluation of aminomethylthiazoles and related analogues are reported.

The target compounds were synthesised by diverse protocols. The aminomethylheteroaryl pyrazole carboxamides **PCM1-006** and **PCM1-012** were synthesised by a three step synthetic protocol. This involved an acid-amine coupling step, followed by reduction of the cyano functionality and *in situ* boc-protection of the resulting primary amine. Deprotection with trifluoroacetic acid (TFA) delivered the desired aminomethylheteroaryl pyrazole carboxamides. A unique protocol was, however, employed to synthesise the lead compound **MMV010539**. The acid-amine coupling step was followed by a nucleophilic substitution of the chloro group with the azide group. A Staudinger reduction of the azide gave the free amine.

Analogues **PCM1-031** – **PCM1-051**, **PCM1-083**, **PCM1-085**, and **PCM1-087** were synthesised by coupling various carboxylic acids to a common amino intermediate followed by the deprotection of the amino functionality with TFA.

The aminomethylthiazole pyrazole carboxamides **PCM1-056** – **PCM1-073**, and **PCM1-089** were synthesised using a different strategy. The first step involved an acid-amine coupling reaction, which was followed by an *N*-benzylation step before deprotection of the amino group with TFA.

The synthesised compounds were characterised by a range of spectroscopic and analytical techniques. Nuclear magnetic resonance (NMR) spectroscopy, mass spectrometry (MS), infrared (IR) spectroscopy, high performance liquid chromatography (HPLC), thin layer chromatography (TLC) and melting point (m.p.) measurements were employed to fully characterise the target compounds.

The synthesised target compounds were assayed for aqueous solubility using the turbidimetric solubility assay and were found to have mean solubility values in the range 10 to > 200 μM at physiological pH (pH 7.4)

Relative to the lead compound **MMV010539** (IC_{50} = 0.0203 μM), all the analogues generally exhibited inferior *in vitro* antiplasmodial activity against the drug sensitive strain (NF54) of the parasite. The *in vitro* antiplasmodial activities were in the range IC_{50} = 0.125 to 173 μM with analogue **PCM1-006** retaining sub-μM activity (IC_{50} = 0.125 μM).

The SAR studies undertaken revealed that the thiazole moiety in the lead compound **MMV010539** is crucial for potent *in vitro* antiplasmodial activity but other aromatic heterocycles seem tolerable. Replacement of the *N*-benzylpyrazole moiety was found to be detrimental to activity. Moreover, introduction of substituents on the aromatic portion of the benzyl group as well as replacement of the *tert*-butyl group with other substituents was found to compromise activity albeit not drastically.

ABBREVIATIONS

1°	Primary
δ	Chemical shift
ACTs	Artemisinin-based combination therapies
ADME	Absorption, distribution, metabolism, and excretion
AQ	Amodiaquine
Ar	Aromatic
AR	Analytical reagent
ATQ	Atovaquone
BC	Before Christ
BCE	Before the Christian era
Bn	Benzyl
Boc_2O	Di-*tert*-butyl dicarbonate
br s	Broad singlet
$CDCl_3$	Deuterated chloroform
CD_3OD	Deuterated methanol
CE	Common Era
CH_2Cl_2	Dichloromethane
CH_3OH	Methanol
CO_2	Carbon dioxide
Co_2B	Cobalt(II) boride
CQ	Chloroquine
CQR	Chloroquine resistant
CQS	Chloroquine susceptible
$CS(NH_2)_2$	Thiourea
CYP1A2	Cytochrome P450 1A2
CYP2D6	Cytochrome P450 2D6
d	Doublet
$[D_6]$DMSO	Deuterated dimethyl sulfoxide
DCM	Dichloromethane
DDT	Dichlorodiphenyltrichloroethane
DIEA	*N*,*N*-diisopropylethylamine

DMAP	4-Dimethylaminopyridine
DMF	*N,N*-Dimethylformamide
DNA	Deoxyribonucleic acid
DX	Doxycycline
E1	Unimolecular elimination
EDCI	1-Ethyl-3-(3-dimethylaminopropyl) carbodiimide
EI-MS	Electron impact mass spectrometry
eq	Equivalent
ER	Endoplasmic reticulum
EtOAc	Ethyl acetate
FGI	Functional group interconversion
FTIR	Fourier transform infrared
FV	Food vacuole
HAP	Histo-aspartic protease
Hb	Haemoglobin
hERG	**h**uman ***E**ther-à-go-go*-**R**elated **G**ene
HIV	Human immunodeficiency virus
HOBt	1-Hydroxybenzotriazole
HPLC	High performance liquid chromatography
Hz	Hertz
MHz	Megahertz
IC_{50}	Concentration of a drug that is required for 50% inhibition *in vitro*
IRS	Insecticide indoor residual spraying
ITNs	Insecticide treated nets
K1	Chloroquine and multidrug resistant strain
K_2CO_3	Potassium carbonate
KBr	Potassium bromide
m	Multiplet
μM	Micromolar
MDR	Multidrug Resistance
Me	Methyl
MEP	Mepacrine
MFQ	Mefloquine
m.p	Melting point

MS	Mass spectrometry
m/z	Mass to charge ratio
$NaBH_4$	Sodium borohydride
NaCl	Sodium chloride
$NaHCO_3$	Sodium hydrogen carbonate
NaN_3	Sodium azide
NF54	Drug-sensitive strain of *Plasmodium falciparum*
NH_4Cl	Ammonium chloride
Ni_2B	Nickel(II) boride
NMR	Nuclear magnetic resonance
P. Berghei	*Plasmodium Berghei*
PBS	Phosphate buffer saline
PEXEL	*Plasmodium* export element
P. falciparum	*Plasmodium falciparum*
PG	Proguanil
Ph	Phenyl
pH	Power of hydrogen
PK	Pharmacokinetics
PM	Pamaquine
P. knowlesi	*Plasmodium knowlesi*
P. malariae	*Plasmodium malariae*
P. ovale	*Plasmodium ovale*
PPh_3	Triphenylphosphine
ppm	Parts per million
PQ	Primaquine
p-tolyl	*para*-tolyl
P. vivax	*Plasmodium vivax*
PY	Pyrimethamine
QC	Quinocide
QN	Quinine
RBCs	Red blood cells
R_f	Retardation factor
rt	Room temperature
s	Singlet

SAR	Structure activity relationship
SiO_2	Silicon dioxide (silica)
S_N2	Bimolecular nucleophilic substitution
SP	Sulphadoxine-pyrimethamine
t	Triplet
TB	Tuberculosis
t-Bu	*tertiary*-butyl
TEA	Triethylamine
Tert	*Tertiary*
TFA	Trifluoroacetic acid
THF	Tetrahydrofuran
TLC	Thin layer chromatography
TM	Target molecule
t_r	Retention time
WHO	World Health Organisation

CHAPTER 1

INTRODUCTION

1.1 Malaria: History and Introduction

The term malaria is derived from an Italian word mal'aria, meaning "bad air" and its occurrence can be traced back to about 40 centuries ago with the Chinese, Romans, and Greeks, particularly Hippocrates, documenting the symptoms from 2700 BCE – 340CE.[1] Ancient Roman infections were thought to be the result of walking in the night air.[2] Hippocrates later described the characteristics of malaria and pointed out its correlation with seasons and location.[3] He gave insight into the association of malaria with stagnant waters, which later prompted the Romans to embark on drainage programs. These preventive measures were amongst the first ones aimed at combating malaria in the Roman Empire.[3]

For many centuries, malaria has been a major health problem in Europe and Africa. Generally, the spread of malaria was fuelled by travelling tradesmen, settlers, and conquering forces. Over four centuries of slave trade saw millions of Africans die from the disease and it has been thought that the transportation of slaves facilitated the spread of malaria to the New World.[3] Malaria generally thrives in the tropical regions of the world, but it also had a profound impact on the early settlers of America, where it was commonly known as the "fever and ague." In 1875, its incidence in America peaked, and in 1914 over 600,000 cases were reported.[3]

Over the centuries, the understanding of malaria has evolved from myths to a clear scientific insight due to ground-breaking advances in medicine and dedicated efforts of individual scientists. Charles Louis Alphonse Laveran, a French army surgeon, is credited for discovering malaria parasites in the blood of infected patients.[4] Camillo Golgi, an Italian neurophysiologist, later established the existence of two forms of the disease. He noted that the first form of the disease was associated with tertian periodicity – fever every other day. The second form of the disease was associated with quartan periodicity – fever every third day. He further established that there was a concomitant appearance of the fever symptoms with the rupture of merozoites and their release into the blood stream.[4] Moreover, the mystery of the transmission of malaria was unravelled by Giovanni Batista Grassi and co-workers (1898-1899) who clearly demonstrated that the female *Anopheles* mosquito was responsible for the transmission of malaria from one human to another.[4]

The origins of malaria and particularly *Plasmodium falciparum* (*P. falciparum*) associated malaria, the most severe form of malaria, have been a subject of great controversy. Some studies have found Egyptian mummified remains, dating back to 1500-500 BC, containing *P. falciparum* DNA.[5] Other studies revealed that malaria originated from gorillas and not humans, which have led to the thought that the occurrence of *P. falciparum* in humans could have been a result of transmission from these apes.[6]

Malaria has clearly ravaged human populations from time immemorial, and still does today. The resurgence of malaria today has been fuelled by the advent of drug resistant parasites, which have significantly hampered efforts aimed at control and possible eradication of the disease. The recent unravelling of the *P. falciparum* genome, however, has given hope and promise to scientists for the design and development of novel and more effective chemotherapeutic remedies to malaria.[7]

1.2 Malaria epidemiology

Malaria has continued to be amongst the most devastating infectious diseases of our time and closely rivals HIV and tuberculosis (TB) in being a lead killer disease, mainly in tropical and subtropical regions (Figure 1.1).[8] According to the World Health Organisation (WHO) estimates, about 219 million cases occurred in 2010 (uncertainty range: 154 million to 289 million) with about 660,000 cases resulting in fatalities (uncertainty range: 490 000 to 836 000).[9] The vast majority of cases (80%) and deaths (91%) occurred in Sub-Saharan Africa with 86% of deaths occurring in children under the age of 5.[10] Pregnant women are also highly vulnerable. About 125 million pregnant women are at risk of malaria infection. In Sub-Saharan Africa, an estimated 200,000 infant deaths result from maternal malaria every year.[11] Moreover, in Western Europe and the United States there are respectively about 10,000 and 1300-1500 malaria cases per year.[12] In Europe, about 900 people died from the disease between 1993 and 2003.[13]

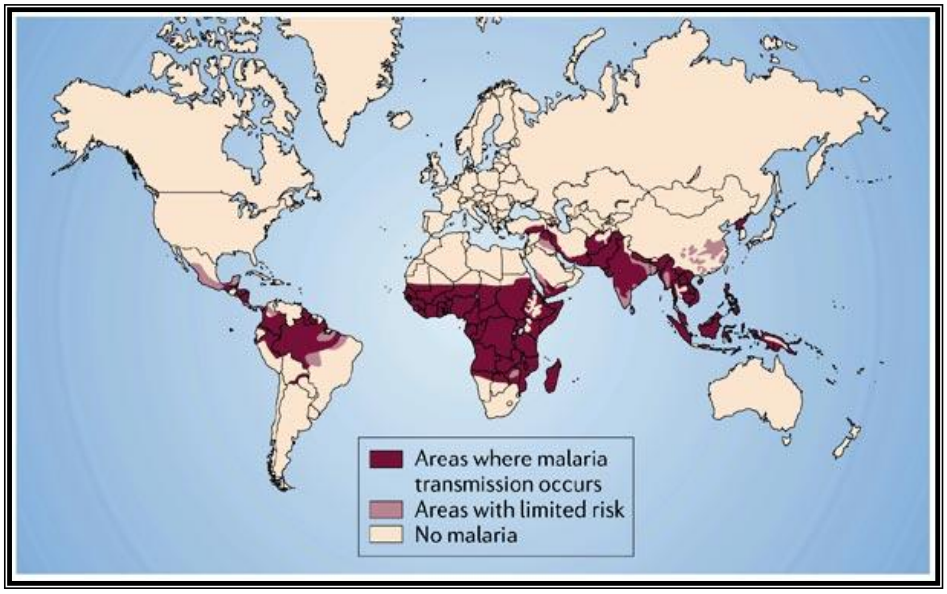

Figure 1.1 Geographic distribution of malaria[14]

Malaria transmission is more intense in warmer regions closer to the equator where the malaria vector can survive and multiply. High rainfall, humidity and stagnant waters in areas closer to the equator provide a conducive environment for continuous breeding of mosquitoes.[15] Malaria is therefore presently endemic in a broad band around the equator (Figure 1.1). Endemic areas include the Americas, many parts of Asia, and much of Africa. *P. falciparum,* the most virulent malaria parasite, however, cannot complete its growth cycle at temperatures below 20 ºC. Therefore, in cooler regions of the world, transmission is less intense and more seasonal. In addition, improved public health measures and economic development in many temperate areas, such as Western Europe and the United States of America (USA), have succeeded in combating malaria to some extent. Most of these areas, however, have *Anopheles* mosquitoes which have the potential to transmit malaria and hence there is a constant risk of disease reintroduction.[16]

Generally, rural areas suffer more incidences of malaria than cities. For instance, the cities of the Greater Mekong Subregion of Southeast Asia are essentially malaria free, whereas the disease is prevalent in rural parts of this region including international borders. Malaria is, however, prevalent in both urban and rural areas in Africa though there is reduced risk in larger cities.[17,18] According to the WHO 2012 world malaria report, malaria is currently endemic in 104 countries. In addition, every year around 30,000 out of about 125 million international travellers visiting these countries contract the disease.[13]

Global incidences of malaria and resulting mortalities have declined in recent years. According to the WHO, about 985,000 deaths were attributed to malaria in 2000. From 2000-2010, however, deaths due to malaria decreased by a third mainly as a result of the wide spread use of insecticide-treated nets (ITNs) and artemisinin-based combination therapies (ACTs).[19]

1.3 Malaria Parasite: Biology and Life Cycle

Four species of *Plasmodium* parasites are responsible for malaria infection in humans. These include *P. falciparum, P. vivax, P. malariae,* and *P. ovale* of which *P. falciparum* and *P. vivax* are the most common. *P. falciparum* is the most deadly. Recently, *P. knowlesi*, a malaria parasite species that infects monkeys and prevalent in certain forested areas of South-East Asia, has been reported to infect humans.[20]

Understanding the biology and life cycle of the malaria parasite is key to devising more rational control mechanisms and developing chemotherapeutic remedies against the disease.[21] The biology and life cycle of *P. falciparum* is the most studied and best understood of the parasites that infect humans.[22]

1.3.1 Life Cycle of the Malaria Parasite

The malaria parasite naturally infects a human host and a female *Anopheles* mosquito vector. Parasites are transmitted to the human host through a bite by an *Anopheles* mosquito. Within the human host, the parasites grow and multiply in liver cells, before invading red blood cells (RBCs). Parasites are transmitted back to the female *Anopheles* mosquito while in the blood stage.[23]

Malaria parasites are first introduced into the human host during a blood meal of a female *Anopheles* mosquito. The parasites are introduced as sporozoites, which quickly invade liver cells (Figure 1.2).

In the liver, sporozoites undergo rapid growth and division to produce tens of thousands of merozoites per liver cell. This growth and division takes place over 5 – 16 days, depending on the specific malaria parasite species.[24] It is during the liver stage that some parasite species go into dormancy, which results in relapse weeks or months later. The infected hepatocytes (liver cells) eventually burst open, releasing merozoites into the blood stream where they begin a cycle of invasion of RBCs. In the RBCs, merozoites undergo asexual replication, which results in

multiplication and concomitant lysis of the RBCs to release the newly formed merozoites.[24] The released merozoites attack new RBCs and the cycle of RBC infection continues in this manner. The RBC infection cycle completes every 1 – 3 days depending on the parasite species. Blood stage multiplication of the parasites eventually leads to thousands of RBCs becoming infected and giving rise to the symptoms and complications associated with malaria. The illness and complications can last for months if not treated or if the host's immune system does not intervene.[24]

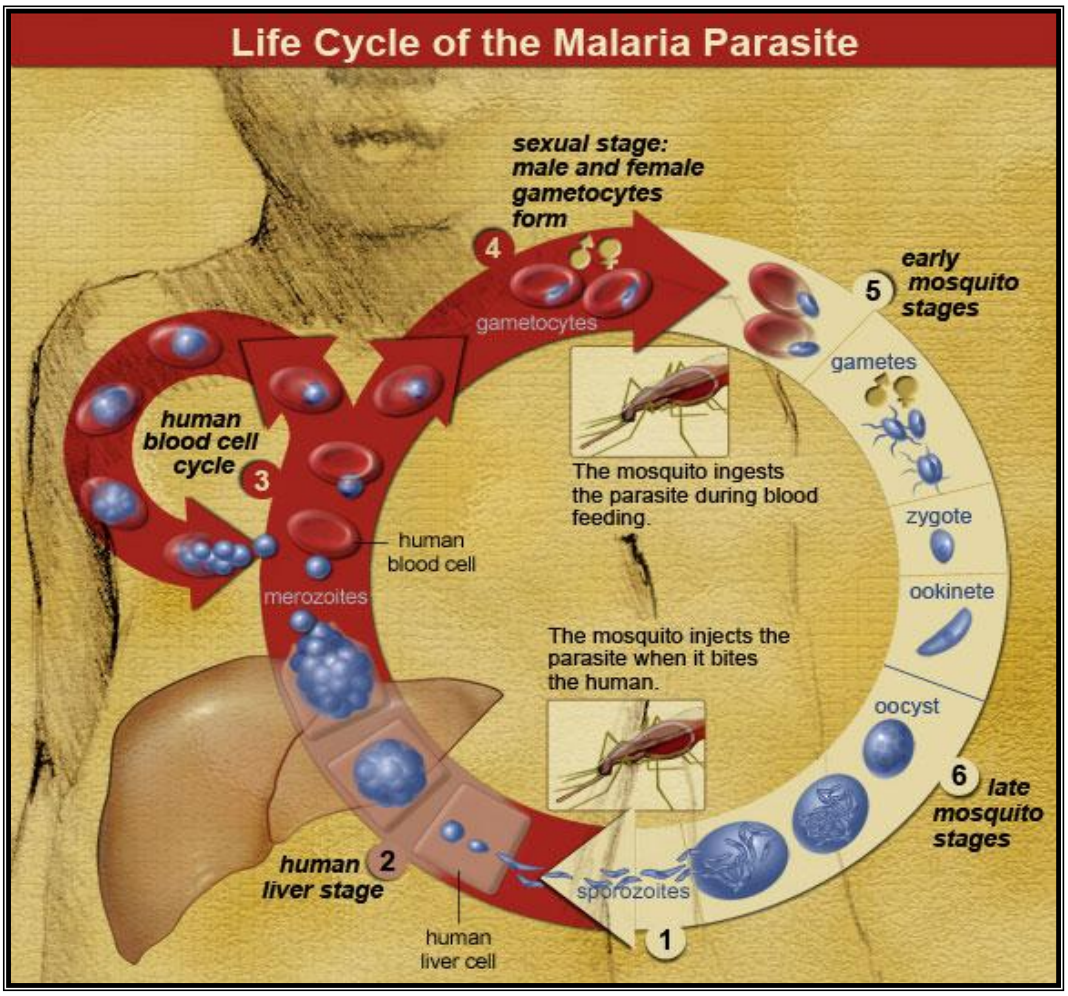

Figure 1.2 Life cycle of the malaria parasite[24]

During asexual replication, some merozoites develop into sexual male and female gametocytes, which continue their circulation in the blood stream. It is these sexual forms of the parasite that are ingested into the mosquito when feeding on an infected host.[24] Once in the mosquito, gametocytes are released into the gut where further development into mature sex cells, called gametes occurs. Diploid zygotes are formed following the fusion of male and female gametes.

Zygotes develop into mobile ookinetes, which travel to the mosquito midgut where they further develop into oocysts (Figure 1.2). After 8 – 15 days,[24] depending on the parasite species, the oocyst grows and divides, producing thousands of sporozoites which are released into the body cavity of the mosquito. The sporozoites invade the salivary glands of the mosquito, ready to continue the cycle of human infection.

1.3.2 Biochemistry of the Plasmodium Parasite

1.3.2.1 Background

The malaria parasite in the erythrocytes (RBCs) needs to nourish itself with nutrients, which it can then convert to other molecules and energy in order to maintain its homeostasis.[25a] The molecules also serve as raw materials for parasite growth and reproduction.[25a] For the parasite to grow and multiply, it needs bulk amounts of macromolecules and other biochemicals to maintain cellular structure and function. The parasite unfortunately degrades the host's macromolecules in order to manufacture its own macromolecules and biochemicals. Both the anabolic and catabolic processes that take place in the parasite are mediated by its enzymes.[25a]

The metabolic pathways of the malaria parasite have evolved over time due to its unique life cycle and microenvironment and, therefore, differ significantly from those of its human host.[25a] The presence of unique pathways in the parasite metabolism makes rational target-based drug design efforts tenable. In this light, drug or therapeutic strategies could be designed to disrupt unique parasite metabolic pathways. Some antimalarials are for instance known to cause parasite death by accumulating in the food vacuole (FV) which is a specialised parasite organelle for digestion of host haemoglobin (Hb).[25a]

1.3.2.2 The *P. falciparum* Food Vacuole and Haemoglobin Degradation

Therapeutic intervention of *P. falciparum* infection remains of paramount importance as it has been implicated in virtually all human malaria deaths.[26] *P. falciparum* and *P. vivax* are also responsible for the majority of infections.[26] In addition, the availability of methodologies for *in vitro* culture of *P. falciparum* for some decades, effected thorough scientific investigation that provided a deeper understanding of its biochemistry more than its counterparts (*P. vivax, P. malariae*, *P. ovale* and *P. knowlesi*).[22] Further discussions around FV biochemistry and Hb degradation pathways will be based on the *P. falciparum* malaria parasite.

As the malaria parasite invades the human host, pathogenic effects are only manifested during the blood stages of the parasite life cycle. The blood cycle involves four stages of which the trophozoite stage is metabolically the most active.[27] In the RBCs, the malaria parasite has to acquire amino acids in order to synthesise its proteins. The parasite suffers from its incapability to synthesise the amino acids in a *de novo* manner or uptake them exogenously. Consequently, the parasite resorts to catabolism of Hb to gain the necessary amino acids for its protein synthesis and maturation.[28-32] During the trophozoite stage, the parasite ingests and degrades about 60 – 80% of the Hb initially contained in the RBC.[33-35] There is evidence suggesting that only a small percentage of these amino acids are actually used for protein synthesis.[31,36] It has therefore been thought that apart from degrading Hb to obtain amino acids, degradation also serves to create space for the parasite within the RBC and to ensure osmotic stability of the RBC.[37,38]

The RBC cytosol is first transported into the FV of the parasite via the cytostome and some transport vesicles (Figure 1.3).[27]

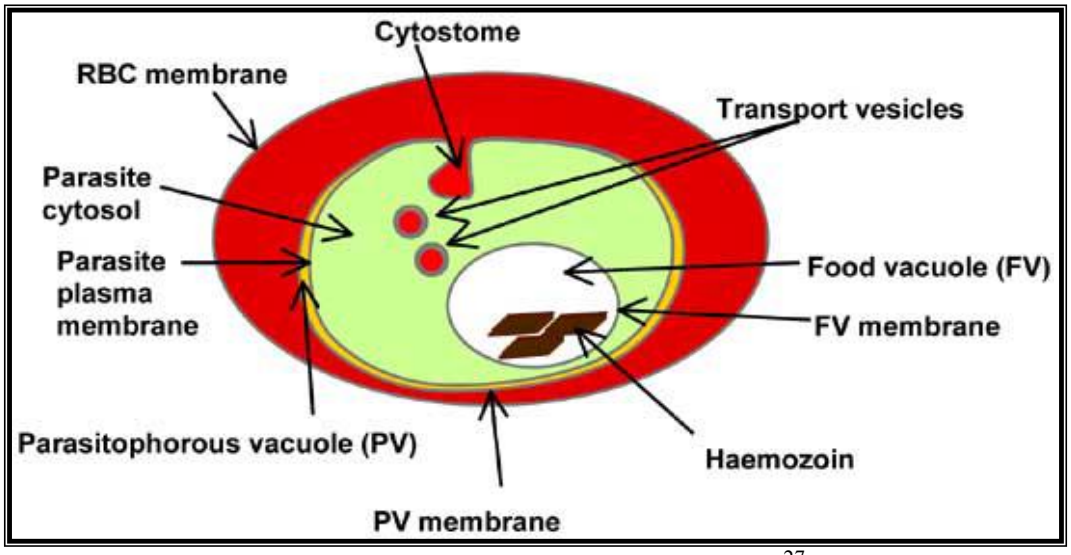

Figure 1.3 Structure of an infected RBC[27]

In the FV, Hb undergoes degradation by a series of proteolytic enzymes, which function optimally under the acidic conditions of the FV. The FV is widely believed to have a pH in the range of 5.0-5.5, though the actual pH and biochemistry of this compartment has recently been debated.[39-42] Bray *et al* reported the dependence of the fluorometrically determined pH of the FV on the pKa of the fluorophore. Therefore, contrary to what was previously believed, they suggested that the pH of this compartment may be variable, or weakly controlled.[42] They have also radically proposed that the transport vesicles may be the sites for Hb degradation, albeit

more tangible evidence is required to support this proposition.[43] On the other hand, more concrete evidence of haemoglobinase enzymes being located in the FV[44,45] strongly suggests Hb catabolism does indeed occur in the FV, although the process may begin in the transport vesicles.[46]

Three classes of protease enzymes have been identified in the FV. The first class is a group of four aspartic proteases, which comprise of plasmepsins-I, II and IV, and histo-aspartic protease (HAP).[44] The second class is a group of three cysteine proteases, generally referred to as falcipains, and includes falcipains-I, II and III.[47] The third class is represented by a zinc metalloprotease called falcilysin.[48]

Complete Hb degradation is accomplished by the sequential action of all three classes of proteolytic enzymes (Figure 1.4).[49a] However, there remains uncertainty on the physiological role of falcipain I in asexual blood stages of the parasite.[49b]

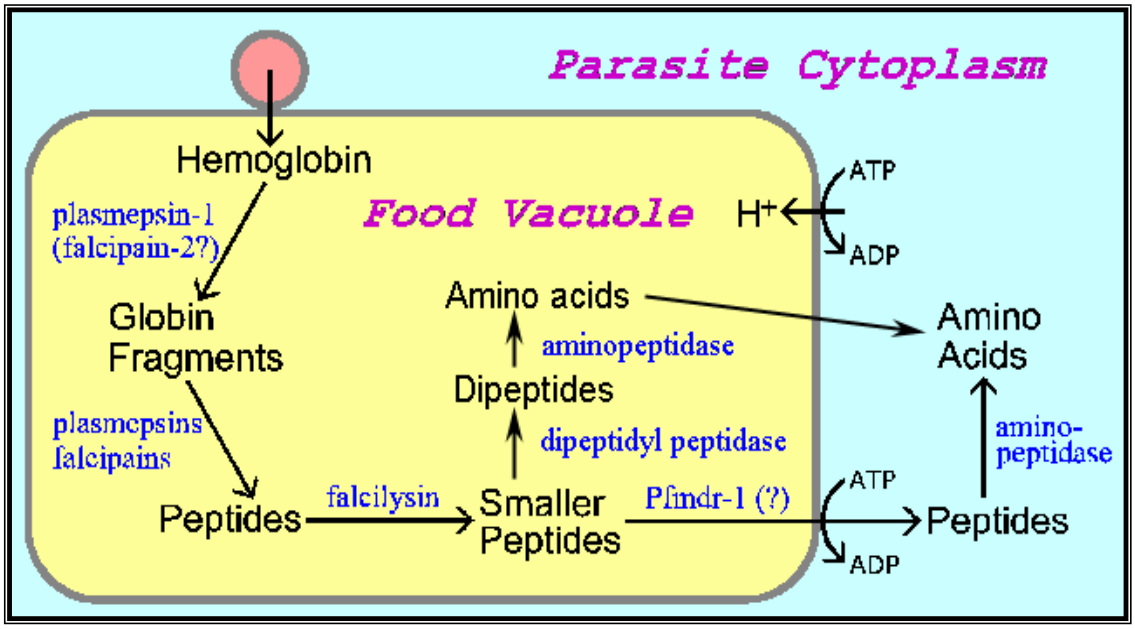

Figure 1.4 Hb degradation path way in the parasite FV[25]

Undenatured Hb is susceptible to cleavage by plasmepsins-I and II between phenylalanine and leucine residues at positions 33 and 34 of the alpha-globin chains.[45,50] The region on the globin chains on which the two residues are located is believed to be very important in giving stability to the overall Hb structure.[45,50] This cleavage causes the globin subunits to dissociate (Figure 1.4) and partially unfold, thereby exposing more protease sites to degradation. Further degradation, mediated by other plasmepsins, including falcipains, therefore, occurs on the large

globin fragments (Figure 1.4). Falcipain-II and possibly falcipain-III, have the capability of digesting native Hb, and have, therefore, been thought to be involved in the initial cleavage of Hb.[45,50] Falcilysin however, lacks the ability to digest either native Hb or denatured globin.[25a] It does however, cleave polypeptides produced from the action of the plasmepsins and falcipains.[25a] The action of falcilysin results in the formation of small peptides containing 6-8 amino acids (oligomers), which are further broken down to free amino acids by amino peptidases in the FV (Figure 1.4).[51] It has also been shown that a neutral amino peptidase activity occurs in the cytoplasm of several *Plasmodium* species,[52,53] implying that some of the peptide oligomers are transported out of the FV to the parasite cytoplasm prior to their digestion.[54]

In summary, the overall process of Hb digestion process seems to involve initial break down of Hb into large fragments by plasmepsins-I and II (and possibly falcipain-II). Combinations of several plasmepsins and falcipains then carry out further catabolism to smaller polypeptide fragments, which are further acted on by falcilysin. Amino peptidase enzymes finally hydrolyse the small peptides into free amino acids (Figure 1.4).[25a]

More recently, an important aspartic protease enzyme critical for parasite viability, plasmepsin-V, has been implicated in the cleavage of 200-300 effector proteins at a common conserved site [*Plasmodium* export element (PEXEL) motif]. This cleavage facilitates export of effector proteins out of the parasite into the cytosol of the infected erythrocyte,[25b,25e] thereby altering certain properties of the host RBC. Such altered properties include permeability to a number of substances, enhanced rigidity, and adherence to endothelial cells.[25c] Contrary to the plasmepsins that have been previously characterised and reported in literature as well as discussed in this dissertation, plasmepsin-V has been associated with a physiologically distinct role[25d] and is considered an interesting enzyme for antimalarial drug development.[25b] Moreover, unlike plasmepsins-I, II and IV, which are located in the FV,[44] plasmepsin-V's location is in the endoplasmic reticulum (ER) of the parasite, makes its participation in haemoglobin degradation highly unlikely.[25d]

1.3.2.3 Detoxification of Haem

The process of Hb degradation releases haem (ferroprotoporphyrin IX or Fe(II)PPIX) (Figure 1.5).[55] The iron centre of haem undergoes oxidation, likely through spontaneous autoxidation by molecular oxygen, which results in the formation of haematin (aqua/hydroxoferriprotoporphyrin IX or H_2O/HOFe (III)PPIX) (Figure 1.6).[46]

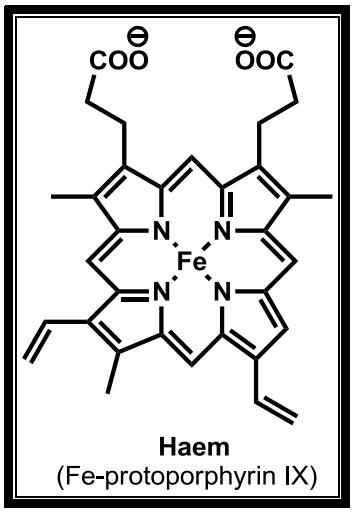

Figure 1.5 Structure of Haem [55]

Haem has been shown to be toxic to various organisms ranging from bacteria to vertebrates.[56,57] Vertebrates, however, have specialised defence proteins called haemopexins, which counteract these toxic effects by sequestration of free haem. It, therefore, seems logical to conclude that the malaria parasite must possess a defence mechanism against the toxic effects of haematin. It has been known for over a century that haematin gets converted into haemozoin.[46,58] Haemozoin is a microcrystalline substance with poor solubility present in the FV of the parasite.[46] Great strides have recently been made to unravel the fate of haem in the malaria parasite quantitatively by Egan and co-workers.[46]

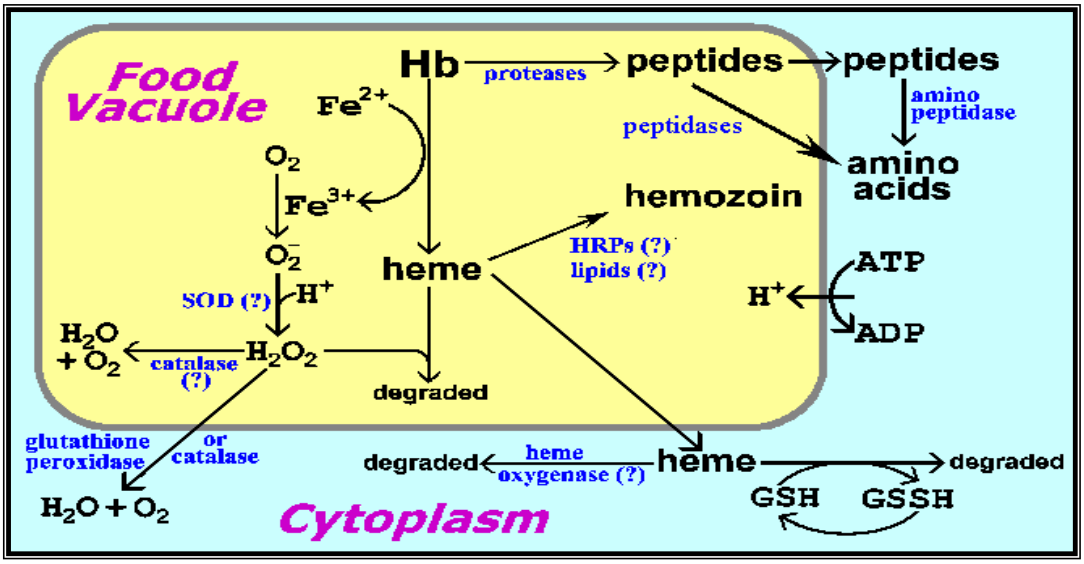

Figure 1.6 Hb degradation and Haem detoxification path way in the parasite FV[32]

Some studies have led to the conclusion that only 30% of the iron obtained from Hb degradation is sequestered in haemozoin.[33,34] It was on this initial finding, that Ginsburg and co-workers based their hypothesis that the remaining haematin undergoes transportation out of the FV into the parasite cytosol, where it undergoes degradation in a glutathione-dependent process.[33] It has also been shown that such a process is chemically feasible.[59] However, Tilley and co-workers have maintained that hydrogen peroxide generated by the autoxidation of haem is responsible for the degradation of haematin, and that this degradation occurs in the FV (Figure 1.6).[34] On the other hand, a study employing three independent physical and chemical techniques (Colorimetry, Mössbauer spectroscopy, and electron spectroscopic imaging) conclusively established that at least 95% of the haem generated through Hb degradation is incorporated into haemozoin.[60] Degradation of a small portion of haem, however, cannot be ruled out.

1.4 Malaria Control, Prevention and Treatment

A number of strategies have been employed in an attempt to control and prevent transmission of malaria. These range from vector control programmes to prophylactic and other chemotherapeutic remedies.

1.4.1 Current Preventive Measures

Prevention of infection and transmission plays a pivotal role in the fight against malaria. A number of preventive measures are employed in an effort to protect individuals in disease endemic areas.[61]

1.4.1.1 Vector Control Programmes

Mosquito vector control strategies are aimed at reducing the mosquito population. They incorporate the use of household insecticide indoor residual spraying (IRS), larval control, and insecticide treated nets (ITNs). With the availability of effective insecticides against adult *Anopheles* mosquitoes, IRS and ITNs have become the most valuable mosquito vector control measures.[62] Before dichlorodiphenyltrichloroethane (DDT) was known, the eradication and control of malaria in several tropical areas was achieved by removal or poisoning of mosquito breeding grounds, and the aquatic habitats of larva stages. For example, places with standing water were filled or had oil applied on them. However, for over half a century, there has been little application of these eradication methods in Africa.[61]

1.4.1.2 Prophylaxis

Prophylaxis is another strategy employed in the prevention of malaria. This involves administration of drugs on a daily or weekly basis to prevent possible infection. Contrary to the treatment of a malaria patient, prophylactic administration of drugs is done at a much lower dose.[61] However, in malaria endemic areas this practice is impractical owing to the exorbitant cost of the drugs and negative side effects associated with long term use.[61] These factors, coupled with the difficulty to obtain effective antimalarial drugs in poor countries hamper the prophylactic use of antimalarial drugs in malaria endemic areas.[61] Prophylactic use of antimalarial drugs is therefore restricted to individuals travelling to malarial regions on a short term basis.[61]

Mefloquine (MFQ) (**Lariam**), doxycycline (DX), and the combination of atovaquone (ATQ) and proguanil (PG) hydrochloride (**Malarone**) are some of the preventive drugs in modern use.[61] Parasite resistance in the area to be visited, side effects, and other considerations, have to be taken into account when choosing the drug for prophylactic use.[61] It is also important to note that the prophylactic effect takes some time to begin after starting taking the drugs. Temporary visitors to malaria endemic regions therefore have to start taking prophylactic agents

one to two weeks prior to their arrival. The medication must also continue for four weeks after leaving malaria endemic zones.[61] ATQ and PG combinations are the exception in that medication has to start two days before the visit and only continued for seven days afterwards.[61]

1.4.1.3 Vaccination

There is currently no effective vaccine against malaria, but a variety of candidates are under development.[61] However, vaccine development has largely been hampered by the complex nature of the malaria parasite.[61] The most clinically advanced vaccine candidate, RTS,S/AS01, has recently undergone large scale phase III trials and has been found to protect children as well as infants from clinical malaria for up to 18 months after vaccination. The WHO has since indicated the possibility of a policy recommendation for RTS,S/AS01 as early as 2015.[63] The largest group of vaccines being researched are pre-erythrocytic vaccines which target the parasite before it reaches the blood stages. Other groups of vaccine candidates are also being investigated.[61]

1.4.1.4 Other methods

Education in recognising the symptoms of malaria in endemic areas has played a critical role in the fight against the disease. In some areas of East Africa for example, education resulted in the reduction of the number of cases by as much as 20%.[61] People are also informed through education of the need to cover areas of stagnant and still water, which are ideal breeding grounds for mosquitoes.[61]

Computing power has also come on board in the fight against malaria. Health effects and transmission dynamics of the disease have been simulated in an attempt to come up with the best method, or combination of methods for malaria control.[61] Other approaches to malaria control include the use of natural predators for larval control, case management (diagnosis and treatment), and mass drug administration including mass fever treatment.[64,65]

1.4.2 Chemotherapeutic Interventions and Challenges

1.4.2.1 Introduction

Malaria has been one of the worst public health problems which has ravaged humankind for centuries. The situation was exacerbated by the lack of specific treatments for this disease for many centuries.[66] In the 17th century, quinine (QN) was successfully extracted from a tree bark from Peru, and in turn gave rise to the development of other synthetic alternatives. Of these synthetic alternatives, chloroquine (CQ) was the most successful antimalarial, but it suffered widespread resistance by the 1970s. The antimalarial drug artemisinin came on the scene in the same decade when Chinese scientists extracted it from the sweet wormwood plant. Artemisinin has since been very effective against chloroquine resistant parasites. With the effective use of ACTs, there has been renewed hope for the eradication of malaria.[66] However, the emergence of multidrug resistant (MDR) strains of *P. falciparum* has rendered antimalarial chemotherapy challenging and complex.[66,67] For example, affordable antimalarial drugs such as CQ and sulphadoxine-pyrimethamine (SP) have suffered widespread resistance hampering the fight against malaria. Because of their low cost and availability, these drugs still find use in Africa, albeit 30% of treatments fail. For countries were resistance to conventional monotherapies such as CQ or SP is evident, the WHO has recommended the use of ACTs for *P. falciparum* malaria.[68] Because of being costly however, the artemisinins have limited use in the developing world.[69] Moreover, disturbing evidence has emerged suggesting the existence of malaria parasites resistant to combination therapies that include artemisinins.[70,71]

There seems to be hope for malaria chemotherapy with recent ground-breaking advances such as the successful sequencing of the *P. falciparum* genome. The genomics of *P. falciparum* is expected to play a crucial role in the development of new therapeutic approaches.[72-74] In addition, understanding of the biochemistry of the *P. falciparum* parasite has led to unravelling the modes of action of current antimalarial drugs, and also has helped to identify novel potential therapeutic targets.[75,76]

1.4.2.2 Classification of Clinically Established Antimalarial Drugs

The current antimalarial drugs in clinical use can be classified according to their mode of action.[77,78] They can also be classified on the basis of the malaria parasite life cycle stage they

therapeutically act on in the human host.[77,78] The later classification will be discussed in greater detail.

1.4.2.2.1 Classification based on Parasite Life Cycle Stage Targeted

Antimalarial drugs can be classified into five groups according to their therapeutic action on the relevant malaria parasite life cycle stage. These groups include causal prophylactic drugs, schizontocidal drugs, gametocytocidal drugs, sporontocidal drugs, and anti-relapse drugs or secondary tissue schizontocides.[79]

i) Causal prophylactic drugs. Also called primary tissue schizontocides, these drugs are known to act on the primary tissue phase (pre-erythrocytic forms) of the malaria parasite.[79] Primaquine (PQ), pamaquine (PM) and possibly quinocide (QC) (Figure 1.7) are examples of drugs that act on primary tissue schizonts of *P. falciparum* and *P. vivax*. However, their use as prophylactic drugs is impractical due to possible side effects. Proguanil (PG) hydrochloride and pyrimethamine (PY) (Figure 1.7) on the other hand, possess higher activity against primary tissue forms of *P. falciparum*. They are also known to have some activity on the primary tissue forms of *P. vivax*.[79]

ii) Schizontocidal drugs. These drugs are also known as blood schizontocides and have therapeutic action against all species of malaria parasites on the asexual erythrocytic stage. Typical schizontocidal drugs include QN, mepacrine (MEP), CQ, and amodiaquine (AQ) (Figure 1.7). Owing to their potency and rapid action, these drugs find use in the treatment and temporary prevention (suppression) of clinical symptoms associated with malaria.[79]

iii) Gametocytocidal drugs. The 8-aminoquinolines, such as PM, PQ, and QC outlined in figure 1.7, are the most active of this class of antimalarials.[79] These act on the sexual forms of all species of malaria parasites with PQ and QC being much less toxic than the others. Other antimalarials such as AQ, CQ, MEP, and QN (Figure 1.7), also possess activity against the sexual forms of *P. malariae* and *P. vivax*, but are devoid of direct activity on the gametocytes of *P. falciparum*.[79]

iv) Sporontocidal drugs. The antimalarial activity of these drugs arises from their inhibition of parasite development at the sporogonic phase in the mosquito. PG, chloroproguanil, and

particularly PY are some examples of antimalarial drugs that exert this " anti-sporogonic action " effect.[79]

v) Anti-relapse drugs (secondary tissue schizontocides). The activity of these drugs is mainly on the secondary exo-erythrocytic phase of *P. vivax* and *P. malariae* infections in the liver. PM, PQ, and QC are the only antimalarial drugs with high enough activity. Usually, administration of these drugs is done after treatment of the primary attack and they are responsible for the cure of all relapsing infections. However, these drugs can also be administered at the time of latency or during a relapse.[79]

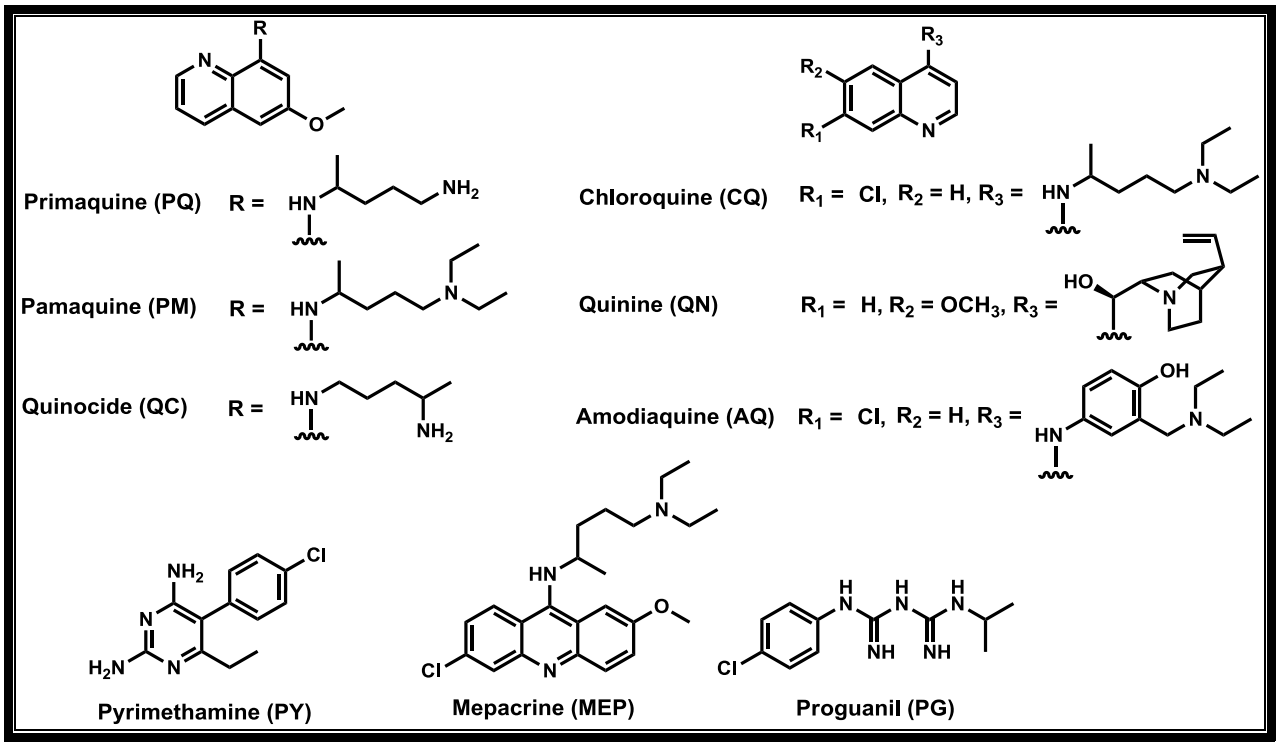

Figure 1.7 Chemical structures of drugs acting on different parasite life cycle stages

In conclusion, malaria remains a major cause of death for the impoverished countries of Sub-Saharan Africa and other tropical regions. Poverty and poor living conditions in Sub-Saharan Africa have exacerbated the situation. Antimalarial drug development programmes need to take this fact into account and ensure drugs that finally make it to the clinic are affordable. Resistance to antimalarial drugs no matter how novel they act also seems to be an inevitable fact. This calls for continued drug discovery efforts to identify new generations of antimalarial agents. Many classes of compounds have shown promise as novel antimalarial agents. These include compounds containing the thiazole heterocycle which are the central focus of the next chapter.

1.5 References

1. http://www.austincc.edu/microbio/2704x/pf.htm (Accessed on June 28, 2013)
2. http://www3.nd.edu/~haldarlb/intro_malaria.htm (Accessed on July 03, 2013)
3. http://www.infoplease.com/cig/dangerous-diseases-epidemics/malaria.html (Accessed on July 03, 2013).
4. http://www.cdc.gov/malaria/about/history/ (Accessed on July 16, 2013).
5. Nerlich, A.G.; Schraut, B.; Dittrich, S.; Jelinek, T.; Zink, A.R. *Emerg Infect Dis*. **2008**, *14*, 1317–1319.
6. Liu, W.; Li, Y.; Learn, G.H.; Rudicell, R.S.; Robertson, J.D.; Keele, B.F.; Ndjango, J.B.N.; Sanz, C.M.; Morgan, D.B.; Locatelli, S.; Gonder, M.K.; Kranzusch, P.J.; Walsh, P.D.; Delaporte, E.; Mpoudi-Ngole, E.; Georgiev, A.V.; Muller, M.N.; Shaw, G.M.; Peeters, M.; Sharp, P.M.; Rayner, J.C.; Hahn, B.H. *Nature*. **2010**, *467*, 420–25.
7. Gardner, M.J.; Hall, N.; Fung, E.; White, O.; Berriman, M.; Hyman, R.W.; Carlton, J.M.; Pain, A.; Nelson, K.E.; Bowman, S.; Paulsen, I.T.; James, K.; Eisen, J.A.; Rutherford, K.; Salzberg, S.L. *et al*. *Nature*. **2002**, *419*, 498-511.
8. Barry, A.E. *J. Mol. Genet. Med*. **2005**, *1*, 76-86.
9. http://www.who.int/malaria/travellers/en/
10. *World Malaria Report, 2011*; World Health Organisation: Geneva, **2011**.
11. Hartman, T.K.; Rogerson, S.J.; Fischer, P.R. *Ann. Trop. Paediatr*. **2010**, *30*, 271–82.
12. Taylor, W.R.; Hanson, J.; Turner, G.D.; White, N.J.; Dondorp, A.M. *Chest.* **2012**, *142*, 492–505.
13. Kajfasz, P. *International Maritime Health*. **2009**, *60*, 67–70.
14. Bell, D.; Wongsrichanalai, C.; Barnwell, J.W. *Nat. Rev. Micro*. **2006**, *4*, 682-695.
15. Jamieson, A.; Toovey, S.; Maurel, M. *Struik*. **2006**, 30.
16. http://www.malaria.com/overview/malaria-countries-map
17. Cui, L.; Yan, G.; Sattabongkot, J.; Cao, Y.; Chen, B.; Chen, X.; Fan, Q.; Fang, Q.; Jongwutiwes, S.; Parker, D.; Sirichaisinthop, J.; Kyaw, M.P.; Su, X.Z.; Yang, H.; Yang, Z.; Wang, B.; Xu, J.; Zheng, B.; Zhong, D.; Zhou, G. *Acta. Tropica*. **2012**, *121*, 227–239.
18. Machault, V.; Vignolles, C.; Borchi, F.; Vounatsou, P.; Pages, F.; Briolant, S.; Lacaux, J.P.; Rogier, C. *Geospatial Health*. **2011**, *5*, 151-168.
19. Howitt, P.; Darzi, A.; Yang, G.Z.; Ashrafian, H.; Atun, R.; Barlow, J.; Blakemore, A.; Bull, A.M.; Car, J.; Conteh, L.; Cooke, G.S.; Ford, N.; Gregson, S.A.; Kerr, K.; King,

D.; Kulendran, M.; Malkin, R.A.; Majeed, A.; Matlin, S.; Merrifield, R.; Penfold, H.A.; Reid, S.D.; Smith, P.C.; Stevens, M.M.; Templeton, M.R.; Vincent, C.; Wilson, E. *The Lancet*. **2012**, *380*, 507–535.

20. http://www.who.int/mediacentre/factsheets/fs094/en/ (Accessed on July 17, 2013).
21. *The Biology of the Malaria Parasites, 1987*; World Health Organisation: Geneva, **1987**.
22. Trager, W.; Jensen, J.B. *Science*, **1976**, *193*, 673-675.
23. http://www.cdc.gov/malaria/about/biology/ (Accessed on July 18, 2013).
24. http://www.niaid.nih.gov/topics/malaria/pages/lifecycle.aspx (Accessed on July 20, 2013).

25a. http://www.tulane.edu/~wiser/malaria/fv.html (Accessed on July 23, 2013).

25b. Russo, I.; Babbitt, S.; Muralidharan, V.; Butler, T.; Oksman, A.; Goldberg, D.E. *Nature*. **2010**, *463*, 632-636.

26c. Maier, A.G.; Cooke, B.M.; Cowman, A.F.; Tilley, L. *Nat. Rev. Microbiol*. **2009**, *7*, 341–354.

25d. Klemba, M.; Goldberg, D.E. *Mol. Biochem. Parasitol*. **2005**, *143*, 183-191.

25e. Boddey, J.A.; Hodder, A.N.; Gunther, S.; Gilson, P.R.; Patsiouras, H.; Kapp, E.A.; Pearce, J.A.; de Koning-Ward, T.F.; Simpson, R.J.; Crabb, B.S.; Cowman, A.F. *Nature*, **2010**, *463*, 627–631.

26. Rosenthal, P.J.; Miller, L.H. In Antimalarial Chemotherapy. Mechanisms of Action, Resistance and New Directions in Drug Discovery. Rosenthal, P. J. Ed.; *Humana Press*: *Totowa*, New Jersey. **2001**, 3-13.
27. Bannister, L.H.; Hopkins, J.M.; Fowler, R.E.; Krishna, S.; Mitchell, G.H. *Parasitology Today*. **2000**, *16*, 427- 433.
28. Ting, I.P.; Sherman, I.W. *Comp. Biochem. Physiol*. **1966**, *19*, 855-869.
29. Sherman, I.W. *Bull. WHO.* **1977**, *55*, 265-276.
30. Pollet, H.; Conrad, M.E. *Proc. Soc. Exp Biol. Med.* **1968**, *127*, 251-253.
31. Sherman, I.W.; Tanigoshi, L. *Int. J. Biochem.* **1970**, *1*, 635-637.
32. Zarchin, S.; Krughak, M.; Ginsburg, H. *Biochem. Pharmacol.* **1986**, *35,* 2435-2442.
33. Ginsburg, H.; Famin, O.; Zhang, F.; Krugliak, M. *Biochem. Pharmacol.* **1998**, *56,* 1305-1313.
34. Loria, P.; Miller, S.; Foley, M.; Tilley, L. *Biochem. J.* **1999**, *339,* 363-370.
35. Egan, T.J.; Combrinck, J.M.; Egan, J.; Hearne, G.R.; Marques, H.M.; Ntenteni, S.; Sewell,

B.T.; Smith, P.J.; Taylor, D.; van Schalkwyk, D.A.; Walden, J.C. *Biochem. J.* **2002**, *365,* 343-347.

36. Krugliak, M.; Zhang, F.; Ginsburg, H. *Mol. Biochem. Parasitol.* **2002**, *119,* 249-256.
37. Ginsburg, H. *Blood Cells.* **1990**, *16,* 225-235.
38. Lew, V.L.; Tiffert, T.; Ginsburg, H. *Blood*, **2003**, *101,* 4189-4194.
39. Krogstad, D.J.; Schlesinger, P.H.; Gluzman, I.Y. *J. Cell Biol,* **1985**, *101,* 2302-2309.
40. Yayon, A.; Cabantchik, Z.I.; Ginsburg, H. *Proc. Natl. Acad. Sci.USA.* **1985**, *82,* 2784-2788.
41. Dzekunov, S.M.; Ursos, L.M.B.; Roepe, P.D. *Mol. Biochem. Parasitol.* **2000**, *110,* 107-124.
42. Bray, P.G.; Saliba, K.J.; Davies, J.D.; Spiller, D.G.; White, M.R.; Kirk, K.; Ward, S.A. *Mol. Biochem. Parasitol.* **2002**, *119,* 301-304.
43. Hempelmann, E.; Motta, C.; Hughes, R.; Ward, S.A.; Bray, P.G. *Trends Parasitol.* **2002**, *19,* 23-26.
44. Banerjee, R.; Liu, J.; Beatty, W.; Pelosof, L.; Klemba, M.; Goldberg, D.E. *Proc. Natl. Acad. Sci. USA.* **2002**, *99,* 990-995.
45. Shenai, B.R.; Sijwali, P.S.; Singh, A.; Rosenthal, P.J. *J. Biol. Chem.* **2000**, *275,* 29000-29010.
46. Egan, T.J.; *Drug Design Reviews Online*. **2004**, *1*, 93-110.
47. Rosenthal, P.J.; Sijwali, P.S.; Singh, A.; Shenai, B.R. *Curr. Pharm. Des.* **2002**, *8,* 1659-1672.
48. Eggleson, K.K.; Duffin, K.L.; Goldberg, D.E. *J. Biol. Chem.* **1999**, *274,* 32411-32417.

49a. Goldberg, D.E. *Curr Top Microbiol Immunol.* **2005**, *295*, 275-291.

49b. Kumar, A.; Kumar, K.; Korde, R.; Puri, K.; Malhotra, P.; Chauhan, V.S. *Infect. Immun.* **2007**, *75*, **2026-2034**.

50. Sijwali, P.S.; Shenai, B.R.; Gut, J.; Singh, A.; Rosenthal, P.J. *Biochem. J.* **2001**, *360*, 481-489.
51. Dalal, S.; Klemba, M. *J Biol Chem*. **2007**, *282*, 35978-35987.
52. Curley, G.P.; O'Donovan, S.M.; McNally, J.; Mullally, M.; O'Hara, H.; Troy, A.; O'Callaghan, S.A.; Dalton, J.P. *J. Euk. Microbiol*. **1994**, *41*, 119-123.
53. Florent, I.; Derhy, Z.; Allary, M.; Monsigny, M.; Mayer, R.; Schrével, J. *Mol. Biochem. Parasitol.* **1998**, 97, 149-160.
54. Kolakovich, K.A.; Gluzman, I.Y.; Duffin, K.L.; Goldberg, D.E. *Mol. Biochem. Parasitol.* **1997**, *87,* 123-135.
55. http://omlc.ogi.edu/spectra/hemoglobin/hemestruct/ (Accessed on August 16, 2013).
56. Ladan, H.; Nitzan, Y.; Malik, Z. *FEMS Microbiol. Lett.* **1993**, *112,* 173-177.
57. Baker, H.M.; Anderson, B.F.; Baker, E.N. *Proc. Natl. Acad. Sci. USA.* **2003**, *100,* 3579-

3583.
58. Brown, W. *J. Exp. Med.* **1911**, *13,* 290-299.
59. Atamna, H.; Ginsburg, H. *J. Biol. Chem.* **1995**, *270,* 24876-24883.
60. Egan, T.J.; Combrinck, J.M.; Egan, J.; Hearne, G.R.; Marques, H.M.; Ntenteni, S.; Sewell, B. T.; Smith, P.J.; Taylor, D.; van Schalkwyk, D. A.; Walden, J. C. *Biochem. J.* **2002**, *365,* 343-347.
61. http://www.eac.int/health/index.php?option=com_content&id=95%3Aclassification system&Itemid=32 (Accessed on August 03, 2013).
62. http://www.uptodate.com/contents/epidemiology-prevention-and-control-of-malaria-in-endemic-areas (Accessed on August 03, 2013).
63. http://www.malariavaccine.org/pr2013Oct8-RTSS.php (Accessed on November 06, 2013).
64. http://www.who.int/heli/risks/vectors/malariacontrol/en/index3.html (Accessed on August 07, 2013).
65. http://www.cdc.gov/malaria/malaria_worldwide/reduction/ (Accessed on August 07, 2013).
66. Butler, A.R.; Khan, S.; Ferguson, E. *J R Coll Physicians Edinb.* **2010**, *40*, 172–177.
67. Kumar, A.; Katiyar, S.B.; Agarwal, A.; Chauhan, P.M. *Curr Med Chem.* **2003**, *10,* 1137-1150.
68. http://www.kit.nl/kit/Malaria-treatment-and-drug-resistance (Accessed on August 08, 2013).
69. White, N.J. *Science.* **2008**, *320,* 330–334.
70. Wongsrichanalai, C.; Meshnick, S.R. *Emerging Infect. Dis.* **2008**, *14,* 716–719.
71. Vijaykadga, S.; Rojanawatsirivej, C.; Cholpol, S.; Phoungmanee, D.; Nakavej, A.; Wongsrichanalai, C. *Trop Med Int Health.* **2005**, 11, 211–219.
72. Aultman, K.S.; Gottlieb, M.; Giovanni, M.Y.; Fauci, A.S. *Science*. **2002**, 298, 13.
73. Winzeler, E.A. *Nature.* **2008**, 455, 751–756.
74. Sahu, N.K.; Sahu, S.; Kohli, D.V. *Chem Biol Drug Des.* **2008**, *71*, 287–297.
75. Kun, J.F.; de Carvalho, E.G. *Expert Opin Ther Targets.* **2009**, *13*, 385-394.
76. Parker, M.D.; Hyde, R.J.; Yao, S.Y.; McRobert, L.; Cass, C.E.; Young, J.D.; McConkey, G.A.; Baldwin. S.A. *Biochem. J.* **2000**, *349*, 67-75.
77. http://nobleboss.awardspace.com/mednotes/pharmanotes/chapter_set1/antimalarial.htm
78. Rudrapal, M. *et al*. *CPR*. **2011**, *1*, 286-292.
79. Bruce-Chwatt, L.J. *Bull World Health Organ*. **1962**, *27,* 287–290.

CHAPTER 2

THIAZOLES AND RELATED DERIVATIVES AS ANTIMALARIAL AND ANTIPLASMODIAL AGENTS

2.1 Introduction

The main objective of this MSc research project was to expand structure activity relationship (SAR) studies of aminomethylthiazole analogues as antiplasmodial agents. SAR studies around the lead compound **MMV010539** (Figure 2.1) would also serve to identify other analogues with improved potencies and devoid of the liabilities (moderate potential to inhibit cytochrome P450 1A2 (CYP1A2) and cytochrome P450 2D6 (CYP2D6) and potential human ***E**ther-à-go-go-***R**elated **G**ene (hERG) liability)[1] of the aforementioned lead compound. In this chapter, the antiplasmodial and antimalarial activity of **MMV010539** and other thiazole derivatives, in general, is discussed.

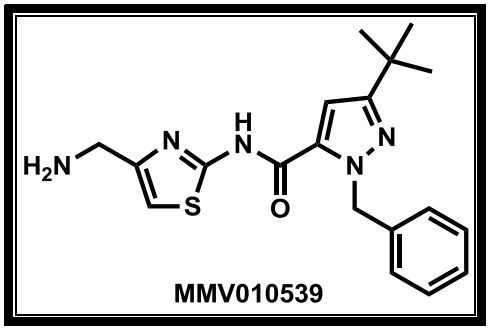

Figure 2.1 Chemical structure of **MMV010539**[1]

2.2 Introduction to Thiazoles

Many biologically potent molecules have been found to contain a thiazole moiety, including Sulfathiazole (antimicrobial drug), Abafungin (antifungal drug), Ritonavir (antiretroviral drug), and Tiazofurin (antineoplastic drug) (Figure 2.2) to name a few.[2,3] Recent drug development in various therapeutic areas, such as treatment of allergies,[4] hypertension,[5] inflammation,[6] schizophrenia,[7] bacterial infection,[8] HIV infection,[9] and hypnotics,[10] has utilised thiazole derivatives. More recently, thiazole derivatives have found application as new bacterial DNA gyrase B inhibitors and as antagonists of fibrinogen receptor (antithrombotic activity).[11,12] Moreover, thiazole derivatives have shown promise as potential antimalarial agents.[13-15]

Thiazoles, therefore, represent an important class of heterocyclic compounds in many therapeutic areas.

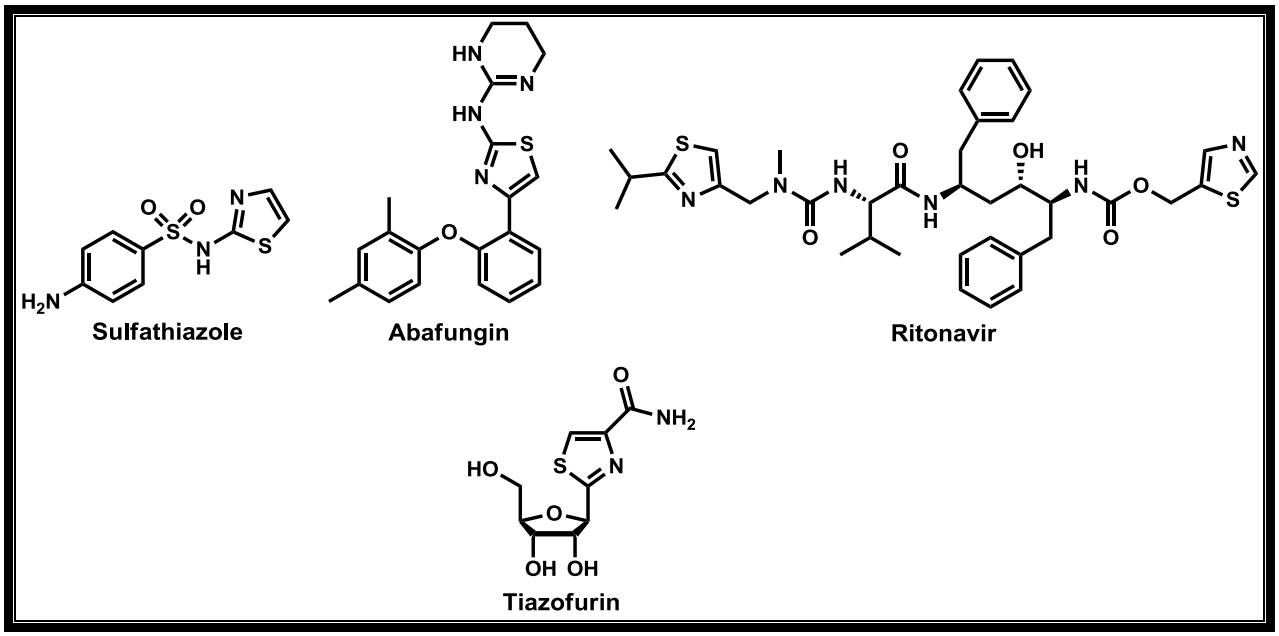

Figure 2.2 Chemical structures of drugs with a thiazole moiety

2.3 Thiazole Derivatives as Antimalarial and Antiplasmodial Agents

2.3.1 Thiazole Derivatives Inhibiting *P. falciparum* Cysteine Proteases

The understanding of the biochemistry of the most virulent causative agent of malaria, *P. falciparum,* has led to the identification of various novel potential therapeutic targets.[16,17] Among the well established chemotherapeutic targets are falcipain-II and falcipain-III, which are plasmodial cysteine proteases implicated in Hb digestion in *P. falciparum*.[18-20] Based on the reported model structures of falcipain-II[21] and falcipain-III[22], Goud *et al*. have employed *de novo* drug design approaches to design and synthesise several trisubstituted thiazole analogues.[13] Through *in vitro* enzyme inhibition studies, analogue **14**, possessing dual activity against both falcipain-II and falcipain-III, was identified (Figure 2.3).

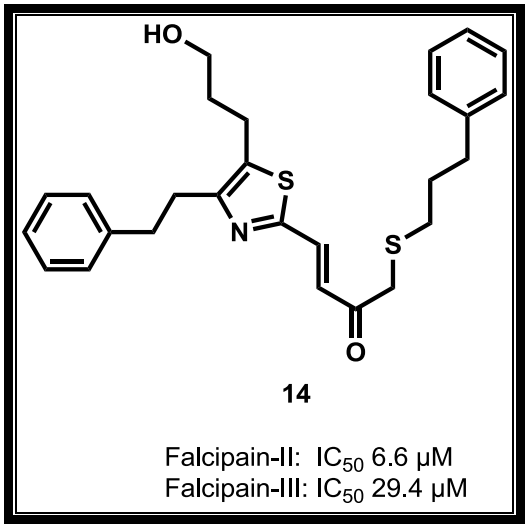

Figure 2.3 Trisubstituted thiazole analogue inhibiting falcipain-II and falcipain-III[13]

Owing to its dual inhibition of the key enzymes of *P. falciparum*, analogue **14** represents a chemical scaffold which could potentially possess antimalarial activity.

2.3.2 Thiazole-derived Amino Acids: Plasmepsin Inhibitors

The reported drug resistance of the malaria parasites to all classes of antimalarial drugs currently in clinical use has given impetus to research efforts aimed at the design and development of antimalarials with novel modes of action.[23] Because plasmepsins in the parasite FV are crucial to Hb degradation in the human erythrocyte,[24-26] these enzymes have been the central focus of various target based drug design efforts.[27-33]

Recently, Karade *et al*. have reported the design, synthesis and antiplasmodial evaluation of thiazole-derived amino acids (Figure 2.4).[14] Of all the derivatives evaluated, **3f** and **3g** (Figure 2.4) were the most potent against both chloroquine susceptible (CQS) and chloroquine resistant (CQR) strains of *P. falciparum.* The two derivatives were also found to dock to the active site of plasmepsin-II,[14] suggesting that they could be exerting their antiparasitic activity through inhibition of the plasmepsin-II enzyme.

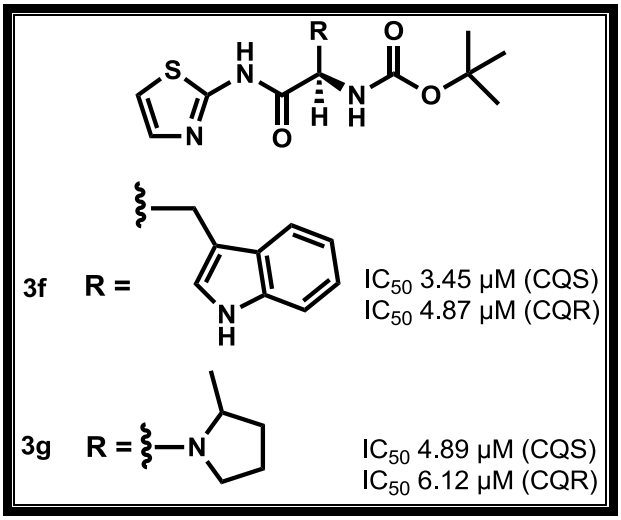

Figure 2.4 Thiazole-derived α-amino acids with antiplasmodial activity[14]

2.3.3 Other Thiazole Derivatives with Antiplasmodial and Antimalarial Activity

Thiazolium salts and their derivatives have shown potential as the next generation of effective antimalarials with novel mechanisms of action. Bisthiazolium compounds have recently been found to possess exceptionally high potencies and have been designed to inhibit phospholipid metabolism in a way that mimics choline.[34-38] **T3** (Figure 2.5) is one such bisthiazolium compound and is currently undergoing clinical trials.[15]

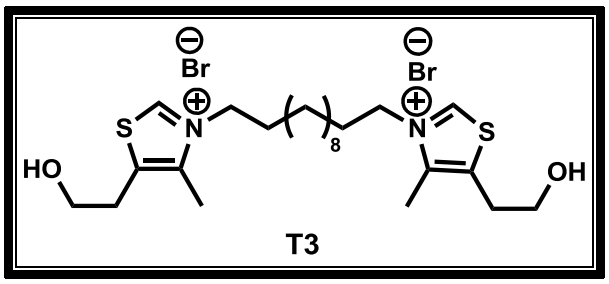

Figure 2.5 Chemical structure of bisthiazolium salt **T3** currently in clinical development[15]

However, bisthiazolium salt **T3** suffers the setback that because of the permanent cationic charges, it has limited capability to cross the gastrointestinal barrier and as a result, has low oral bioavailability.[15] Remedial measures aimed at improving oral bioavailability have been undertaken through the synthesis of bisalkylamidines as bioisosteric analogues.[39,40] Many other thiazole derivatives in the likes of 2,4-diarylthiazoles,[41] 2,5-bis[amidinoaryl]thiazoles[42] have been studied and found to possess antiplasmodial activity.

2.3.4 Aminomethylthiazoles as Antimalarials

Aminomethylthiazoles represent another novel class of thiazole derivatives with potential clean pharmacology and *in vitro* as well as *in vivo* antiplasmodial potency. Recent high throughput whole cell screening of a Biofocus SoftFocus kinase library containing over 36000 compounds led to the uncovering of an aminomethylthiazole pyrazole carboxamide lead **MMV010539** (Figure 2.6).

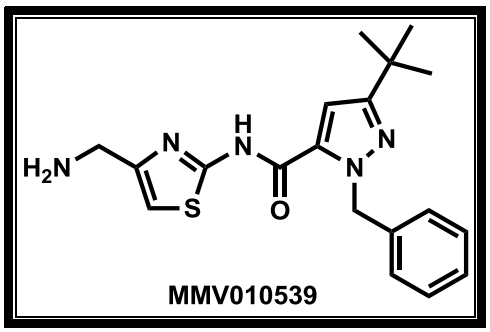

Figure 2.6 Chemical structure of an aminomethylthiazole pyrazole carboxamide **MMV010539**[1]

Owing to its good *in vitro* antiplasmodial activity against CQ and multidrug resistant strain K1 (IC_{50} = 0.08 μM) and CQS NF54 (IC_{50} = 0.07 μM) compared to CQ (K1 IC_{50} = 0.194 μM, NF54 IC_{50} = 0.016 μM), along with *in vivo* activity in the *P. berghei* mouse model, **MMV010539** has been further explored as a potential antimalarial lead.[1] Cytochrome P450 (CYP) profiling of the aforementioned lead compound has shown that it has moderate potential to inhibit CYP1A2 (IC_{50} = 1.5 μM) and CYP2D6 (IC_{50} = 0.4 μM). It has also been found to have a potential **h**uman ***E**ther-à-go-go-***R**elated **G**ene (hERG) liability (IC_{50} = 3.7 μM). Preliminary SAR studies around **MMV010539** have been undertaken to establish which groups of this lead molecule are essential for activity (Figure 2.7).

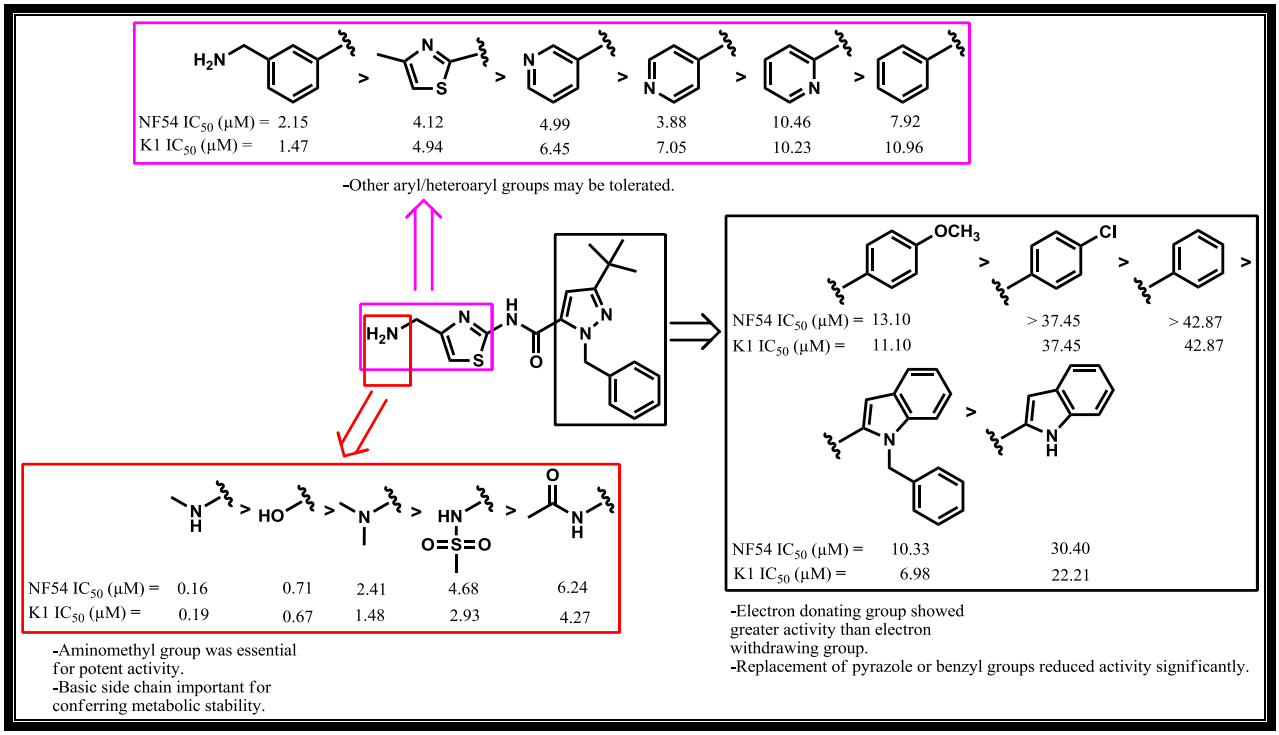

Figure 2.7 Preliminary SAR studies on **MMV010539**[1]

This SAR study revealed that functionalization or removal of the primary amine generally resulted in reduced or loss of antiplasmodial activity. The unsubstituted aminomethyl group was also found to be important for potent *in vitro* activity. Replacement of the pyrazole moiety by other aromatic and heteroaromatic groups was detrimental to activity. The scope of structural modification of **MMV010539**, therefore, seems very limited. However, it is clear that thiazoles and their derivatives represent an attractive and active area of research as antimalarial agents and further exploration is therefore warranted. This dissertation will focus on further exploration of SAR around **MMV010539**.

2.4 Justification of the Study of Thiazole Analogues

As discussed in the preceding sections 2.3.1-2.3.4, the thiazole moiety is an interesting scaffold in antimalarial research and further research is justified for a number of reasons.

Firstly, some thiazole derivatives have shown inhibition of key proteolytic enzymes of the *P. falciparum* FV and hence show potential as new antimalarials with a potential novel mode of action necessary to circumvent drug resistance. Secondly, thiazole derivatives have made great strides in antimalarial research as indicated by recent clinical development of **T3**. Thirdly, **MMV010539** (Figure 2.6), is a potent antimalarial lead upon which further SAR studies can be

based in order to circumvent off-target and cardio-toxicity risks as well as achieve desirable pharmacological profiles.

2.5 OBJECTIVE AND AIMS

The main objective of this MSc study was to expand SAR studies of aminomethylthiazole analogues as antiplasmodial agents (Figure 2.8). This investigation is based on synthesising analogues in which the main substructure motifs of **MMV010539**, such as the thiazole moiety (SAR 1), the *N*-benzyl group of the pyrazole moiety (SAR 2), *N*-benzylpyrazole (SAR 3), and the *tert*-butyl (SAR 4), have been replaced by other groups (Figure 2.8).

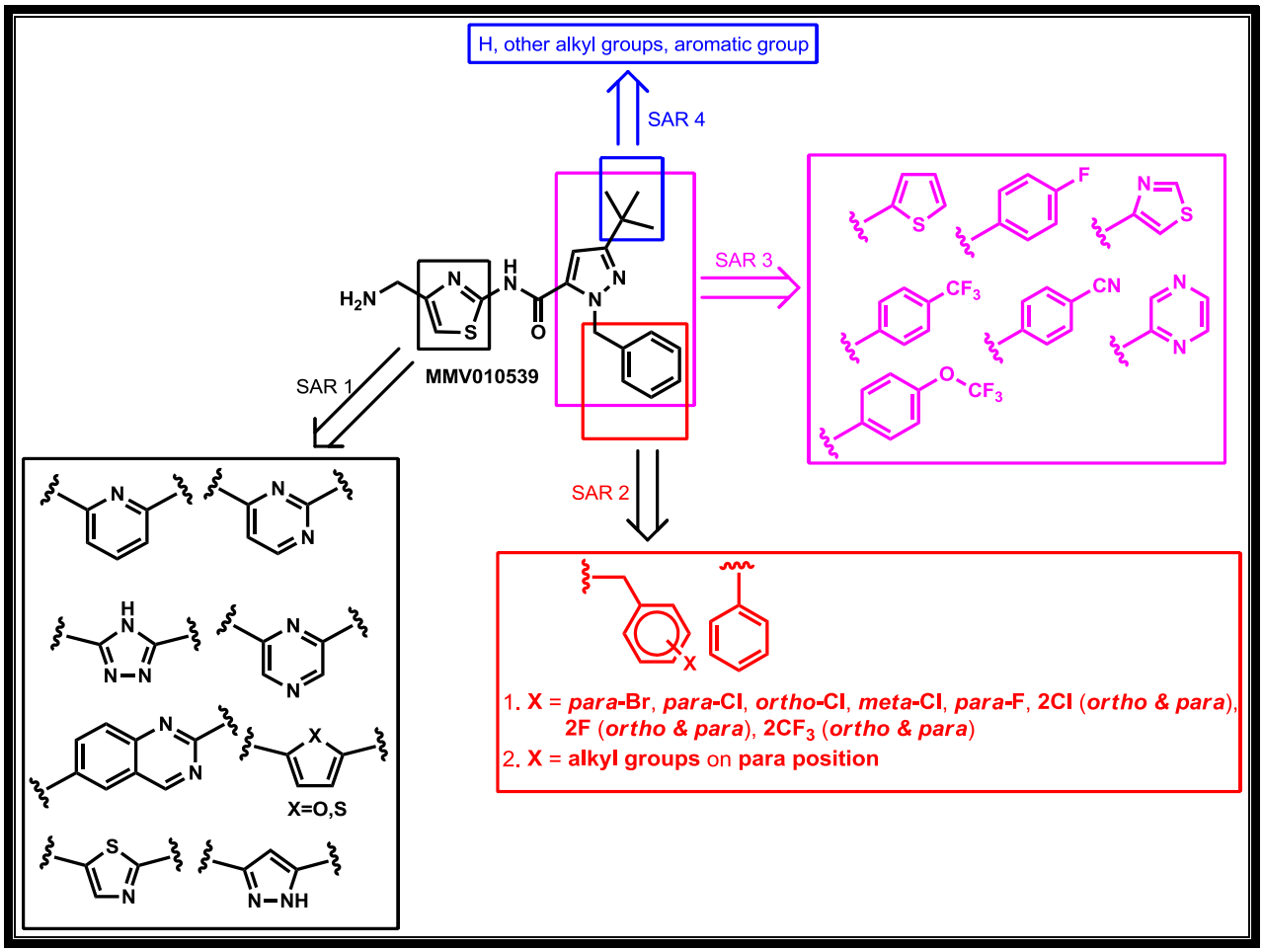

Figure 2.8 Proposed SAR summary on **MMV010539**

From the suggested SAR expansion, the following analogues were chosen as specific synthetic targets due to synthetic accessibility (Figure 2.9).

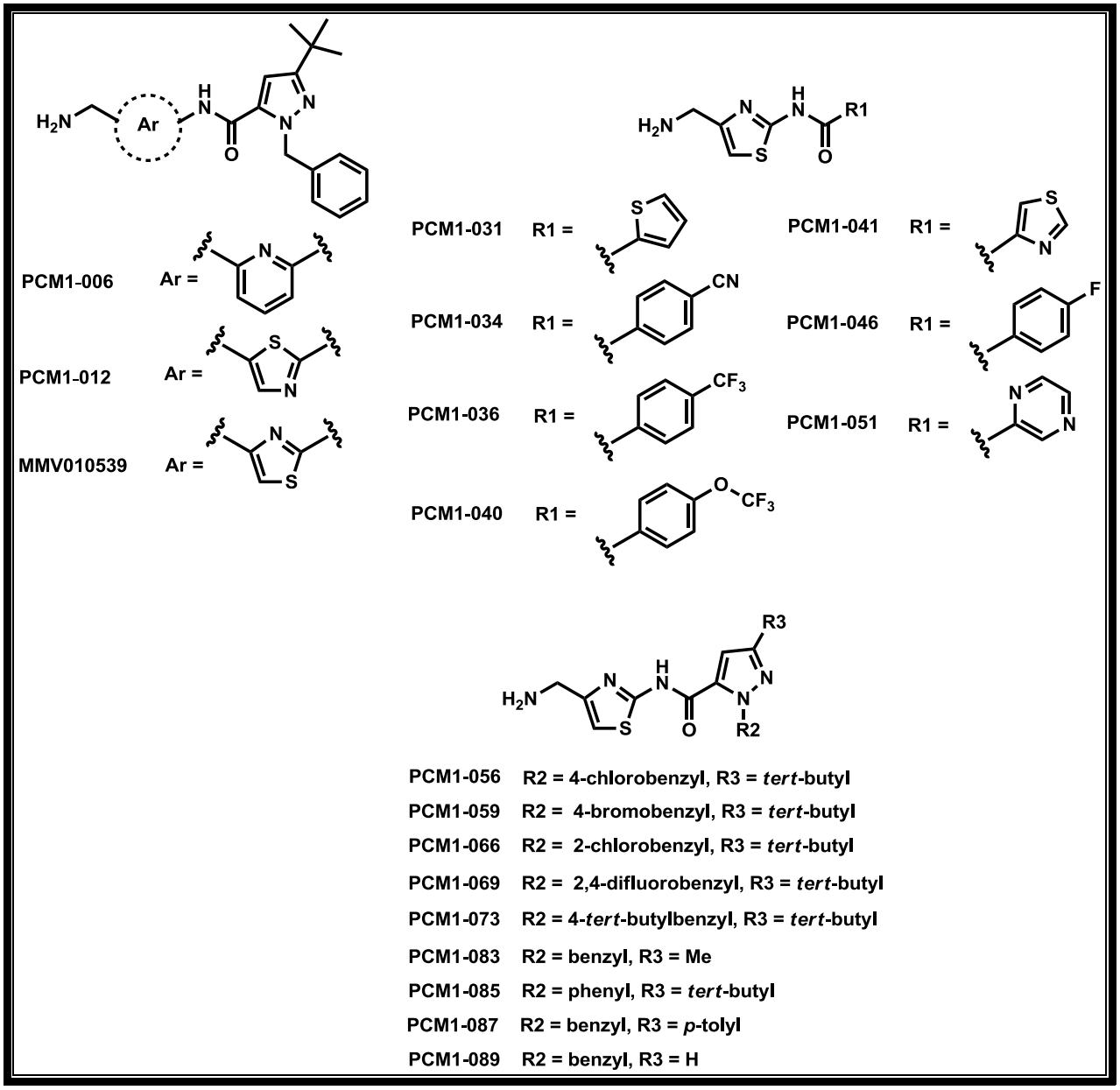

Figure 2.9 Chemical structures of target compounds.

Synthetic routes towards these targets were designed such that each SAR collection could readily be obtained.

To achieve the overall objective, this study focused on a number of specific aims:

Firstly, target compounds would be synthesised, characterised, and submitted for antiplasmodial evaluation. Secondly, solubility profiling of the target compounds would be done in parallel with antiplasmodial evaluation. Solubility is an important physicochemical parameter to establish as it impacts gastrointestinal absorption of oral drugs. Generally, low solubility of oral drugs can lead to suboptimal oral bioavailability, lack of efficacy, abnormal PK profiles, toxicity of vehicles (prodrug approach), expensive and prolonged drug development, and burdensome daily multiple

doses to patients.[43] Thirdly, the most potent analogues identified from pharmacological evaluation would be profiled for *in vitro* metabolic stability. Suboptimal PK parameters which may result in drug candidate failure in later clinical development are identified through metabolic characterisation.[44]

2.6 References

1. Cabrera Gonzalez, D.; Douelle, F.; Feng, T.J.; Nchinda, A.T.; Younis, Y.; White, K.L.; Wu, Q.; Ryan, E.; Burrows, J.N.; Waterson, D.; Witty, M.J.; Wittlin, S.; Charman, S.A.; Chibale, K. *J. Med. Chem.* **2011***, 54,* 7713-7719.
2. Quiroga, J.; Hernandez, P.; Insuasty, B.; Abonia, R.; Cobo, J.; Sanchez, A.; Nogueras, M.; Low, J.N. *J Chem Soc Perkin Trans*. **2002**, *4*, 555-559.
3. Hutchinson, I.; Jennings, S.A.; Vishnuvajjala, B.R.; Westwell, A.D.; Stevens, M.F.G. *J Med Chem.* **2002**, *45*, 744-747.
4. Hargrave, K.D.; Hess, F.K.; Oliver, J.T. *J Med Chem.* **1983**, *26*, 1158-1163.
5. Patt, W.C.; Hamilton, H.W.; Taylor, M.D.; Ryan, M.J.; Taylor Jr, D.G.; Connolly, C.J.C.; Doherty, A.M.; Klutchko, S.R.; Sircar, I.; Steinbaugh, B.A.; Batley, B.L.; Painchaud, C.A.; Rapundalo, S.T.; Michniewicz, B.M.; Olson, S.C.J. *J Med Chem.* **1992**, *35*, 2562-2572.
6. Sharma, R.N.; Xavier, F.P.; Vasu, K.K.; Chaturvedi, S.C.; Pancholi, S.S. *J Enz Inhib Med Chem.* **2009**, *24*, 890 – 897.
7. Jaen, J.C.; Wise, L.D.; Caprathe, B.W.; Tecle, H.; Bergmeier, S.; Humblet, C.C.; Heffner, T.G.; Meltzner, L.T.; Pugsley, T.A. *J Med Chem*. **1990**, *33*, 311-317.
8. Tsuji, K.; Ishikawa, H. *Bioorg Med Chem Lett.* **1994**, *4*, 1601-1606.
9. Bell, F.W.; Cantrell, A.S.; Hogberg, M.; Jaskunas, S.R.; Johansson, N.G.; Jordon, C.L.; Kinnick, M.D.; Lind, P.; Morin Jr, J.M.; Noreen, R.; Oberg, B.; Palkowitz, J.A.; Parrish, C.A.; Pranc, P.; Sahlberg, C.; Ternansky, R.J.; Vasileff, R.T.; Vrang, L.; West, S.J.; Zhang, H.; Zhou, X.X. *J Med Chem.* **1995**, *38*, 4929-4936.
10. Ergenc, N.; Capan, G.; Gunay, N.S.; Ozkirimli, S.; Gungor, M.; Ozbey, S.; Kendi, E. *Arch Pharm Med Chem.* **1999**, *332*, 343-347.
11. Rudolph, J.; Theis, H.; Hanke, R.; Endermann, R.; Johannsen, L.; Geschke, F.U. *J Med Chem.* **2001**, *44*, 619-626.
12. Badorc, A.; Bordes, M.F.; De Cointet, P.; Savi, P.; Bernat, A.; Lale, A.; Petitou, M.; Maffrand, J.P.; Herbert, J.M. *J Med Chem.* **1997**, *40*, 3393-3401.
13. Goud, P.M.; Sheri, A.; Desai, P.V.; Watkins, E.B.; Tekwani, B.; Sabnis, Y.; Gut, J.; Rosenthal, P.J.; Avery, M.A. *Med Chem Res.* **2005**, *14*, 74-105.
14. Karade, H.N.; Acharya, B.N.; Sathe, M.; Kaushik, M.P. *Med Chem Res.* **2008**, *17*, 19–29.
15. Ortial, S.; Denoyelle, S.; Wein, S.; Berger, O.; Durand, T.; Escale, R.; Pellet, A.; Vial, H.; Vo-Hoang, Y. *ChemMedChem.* **2010**, *5*, 52-55.

16. Kun, J.F.; de Carvalho, E.G. *Expert Opin Ther Targets.* **2009**, *13*, 385-394.
17. Parker, M.D.; Hyde, R.J.; Yao, S.Y.; McRobert, L.; Cass, C.E.; Young, J.D.; McConkey, G.A.; Baldwin. S.A. *Biochem. J.* **2000**, *349*, 67-75.
18. Shenai, B.R.; Lee, B.J.; Alvarez-Hernandez, A.; Chong, P.Y.; Emal, C.D.; Neitz, R.J.; Roush, W.R.; Rosenthal, P.J. *Antimicrob Agents Chemother.* **2003**, *47*, 154-160.
19. Shenai, B.R.; Sijwali, P.S.; Singh, A.; Rosenthal, P.J. *J Biol Chem.* **2000**, *15*, 275, 29000-29010.
20. Sijwali, P.S.; Shenai, B.R.; Gut, J.; Singh, A.; Rosenthal, P.J. *Biochem J.* **2001**, *360*, 481-489.
21. Sabnis, Y.; Rosenthal, P.J.; Desai, P.; Avery, M.A. *J Biomol Struct Dyn.* **2002**, *19*, 765-774.
22. Sabnis, Y.; Desai, P.V.; Rosenthal, P.J.; Avery, M.A. *Protein Sci*. **2003**, *12*, 501-509.
23. Gardiner, D.L.; Skinner-Adams, T.S.; Brown, C.L.; Andrews, K.T.; Stack, C.M.; McCarthy, J.S.; Dalton, J.P.; Trenholme, K.R. *Expert Rev Anti Infect Ther.* **2009**, *7*, 1087-1098.
24. Rosenthal, P.J.; McKerrow, J.H.; Aikawa, M.; Nagasawa, H.; Leech, J.H. *J Clin Invest.* **1988**, *82*, 1560–1566.
25. Eggleson, K.K.; Duffin, K.L.; Goldberg, D.E. *J. Biol. Chem.* **1999**, *274,* 32411-32417.
26. Francis, S.E.; Gluzman, I.Y.; Oksman, A.; Knickerbocker, A.; Mueller, R.; Bryant, M.; Sherman, D.R.; Russell, D.G.; Goldberg, D.E. *EMBO J.* **1994**, *13*, 306–317.
27. Coombs, G.H.; Goldberg, D.E.; Klemba, M.; Berry, C.; Kay, J.; Mottram, J.C. *Trends Parasitol.* **2001**, *17*, 532–537.
28. Silva, A.M.; Lee, A.Y.; Gulnik, S.V.; Majer, P.; Collins, J.; Bhat, T.N.; Collins, P.J.; Cachau, R.E.; Luker, K.E.; Gluzman, I.Y.; Francis, S.E.; Oksman, A.; Goldberg, D.E.; Erickson, J.W. *Proc Natl Acad Sci USA*. **1996**, *93*, 10034–10039.
29. Asojo, O.A.; Gulnik, S.V.; Afonina, E.; Yu, B.; Ellman, J.A.; Haque, T.S.; Silva, A.M. *J Mol Biol.* **2003**, *327*, 173–181.
30. Asojo, O.A.; Afonina, E.; Gulnik, S.V.; Yu, B.; Erickson, J.W.; Randad, R.; Medjahed, D.; Silva, A.M. *Acta cryst D*. **2002**, *58*, 2001–2008.
31. Prade, L.; Jones, A.F.; Boss, C.; Richard-Bildstein, S.; Meyer, S.; Binkert, C.; Bur, D. *J Biol Chem.* **2005**, *280*, 23837–23843.
32. Jiang, S.; Prigge, S.T.; Wei, L.; Gao, Y.E.; Hudson, T.H.; Gerena, L.; Dame, J.B.; Kyle, D.E. *Antimicrob Agents Chemother*. **2001**, *45*, 2577–2584.
33. Ersmark, K.; Feierberg, I.; Bjelic, S.; Hamelink, E.; Hackett, F.; Blackman, M.J.; Hulten, J.; Samuelsson, B.; Aqvist, J.; Hallberg, A. *J Med Chem.* **2004**, *47*, 110–122.
34. Vial, H.J.; Eldin, P.; Tielens, A.G.M.; Van Hellemond, J.J. *Mol. Biochem. Parasitol.* **2003**,

126, 143-154.

35. Calas, M.; Cordina, G.; Bompart, J.; Bari, M.B.; Jei, T.; Ancelin, M.L.; Vial, H.J. *J. Med. Chem.* **1997**, *40*, 3557-3566.
36. Calas, M.; Ancelin, M.L.; Cordina, G.; Portefaix, P.; Piquet, G.; Vidal-Sailhan, V.; Vial, H.J. *J. Med. Chem.* **2000**, *43*, 505-516.
37. Ancelin, M.L.; Calas, M.; Bompart, J.; Cordina, G.; Martin, D.; Ben Bari, M.; Jei, T.; Druilhe, P.; Vial, H.J. *Blood*. **1998**, *91*, 1426-1437.
38. Ancelin, M.L.; Calas, M.; Vidal-Sailhan, V.; Herbute, S.; Ringwald, P.; Vial, H.J. *Antimicrob. Agents Chemother.* **2003**, *47*, 2598-2605.
39. Calas, M.; Ouattara, M.; Piquet, G.; Ziora, Z.; Bordat, Y.; Ancelin, M.L.; Escale, R.; Vial, H.J. *J. Med. Chem.* **2007**, *50*, 6307-6315.
40. Vial, H.J.; Calas, M.; Ancelin, M.L.; Escale, R.; Vidal, V.; Bressolle, F. WO Patent WO 04/009068, **2004**.
41. Thompson, M.J.; Louth, J.C.; Little, S.M.; Chen, B.; Coldham, I. *Bioorg Med Chem Lett.* **2011**, *21*, 3644-3647.
42. Branowska, D.; Farahat, A.A.; Kumar, A.; Wenzler, T.; Brun, R.; Liu, Y.; Wilson, W.D.; Boykin, D.W. *Bioorg Med Chem*. **2010**, *18*, 3551-3558.
43. Kerns, E.H.; Di, L. **2008**, Drug-like properties: Concepts, structure design and methods. Burlington, MA: Academic Press.
44. Wu, X.; Wang, J.; Tan, L.; Bui, J.; Gjerstad, E.; McMillan, K.; Zhang, W. *J. Biomol. Screen.* **2012**, *17*, 761-772.

CHAPTER 3

SYNTHESIS AND CHARACTERISATION OF TARGET COMPOUNDS

3.1 Rationale for Design of Target Compounds

Aminomethylthiazoles and their analogues have well documented antimalarial properties as outlined in the previous chapter. Thus, the design, synthesis, and pharmacological evaluation of more analogues presented in this dissertation are based on the antimalarial properties observed initially. The rationale behind the synthesis of more aminomethylthiazole analogues was to expand the SAR studies of this class of compounds. In addition, the synthesis of more analogues was envisaged to potentially fine-tune the pharmacological and physicochemical properties of the lead compound. In this light, the goal was also to identify analogues with comparable or superior pharmacological activity and physicochemical properties to the lead compound. Identified analogues would then be profiled extensively in future to evaluate if they are devoid of the liabilities (hERG and CYPs 1A2 and 2D6 inhibition)[1] reported to be associated with the lead compound. Figure 3.1 summarises the rationale for the design and synthesis of the analogues.

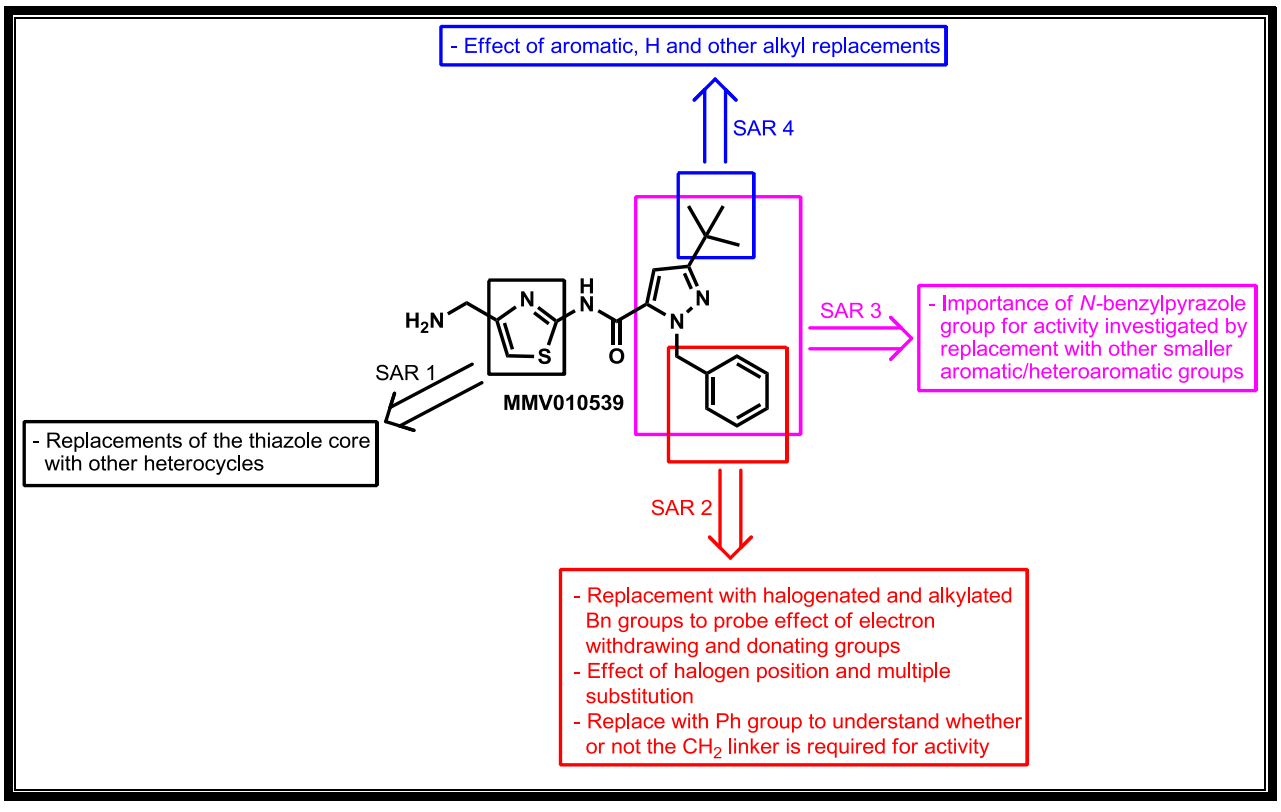

Figure 3.1 Rationale for design of target compounds.

Preliminary SAR studies around **MMV010539** have previously been reported in the literature (Figure 2.5).[1] As stated in the previous chapter, these studies have revealed the importance of the different substructural motifs, such as aminomethyl, basic side chain, aminomethylthiazole, and *N*-benzylpyrazole groups. Replacement of any of these groups was found generally detrimental to potency (Chapter 2. Section 2.3.4)[1]

The two target compounds **PCM1-006** and **PCM1-012** (Figure 3.2) were designed and synthesised to obtain analogues in which the thiazole core (2,4-thiazolyl) of **MMV010539** is replaced by the pyridyl and reversed thiazole (2,5-thiazolyl) moieties. This was done to potentially identify other heterocycles with superior or comparable activity to the lead compound. Moreover, the design of **PCM1-012** sought to understand whether or not the relative positions of nitrogen and sulfur atoms on the thiazole ring were important for antiplasmodial activity. **MMV010539** was re-synthesised in order to compare its activity to the new analogues.

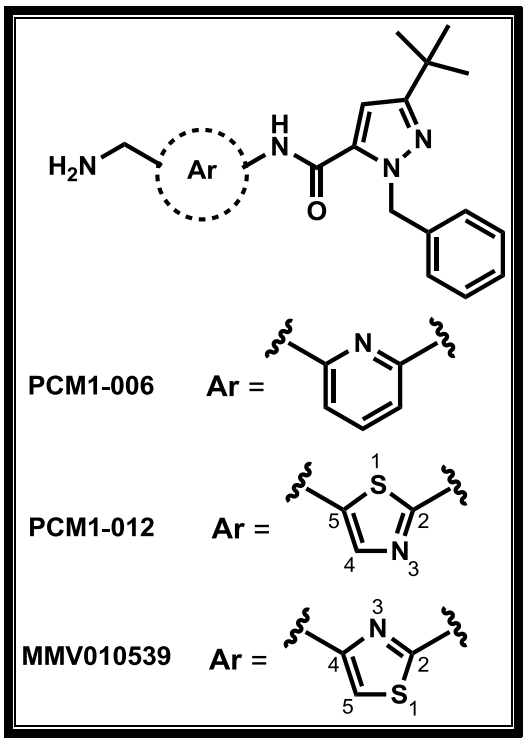

Figure 3.2 Chemical structures of target compounds **PCM1-006**, **PCM1-012**, and **MMV010539**.

In the preliminary SAR[1], it was found that replacement of the *N*-benzylpyrazole moiety with other aromatic and heteroaromatic groups resulted in a significant reduction of antiplasmodial

activity (Figure 2.5). In this MSc dissertation, we further explored this portion of SAR, i.e. substitution of the *N*-benzylpyrazole moiety with various aromatic and heteroaromatic substituents SAR 3 (Figure 3.3). This was done in order to potentially identify other simpler and favourable replacements for the *N*-benzylpyrazole moiety. In this regard, analogues **PCM1-031** - **PCM1-051** were designed and synthesised (Figure 3.3).

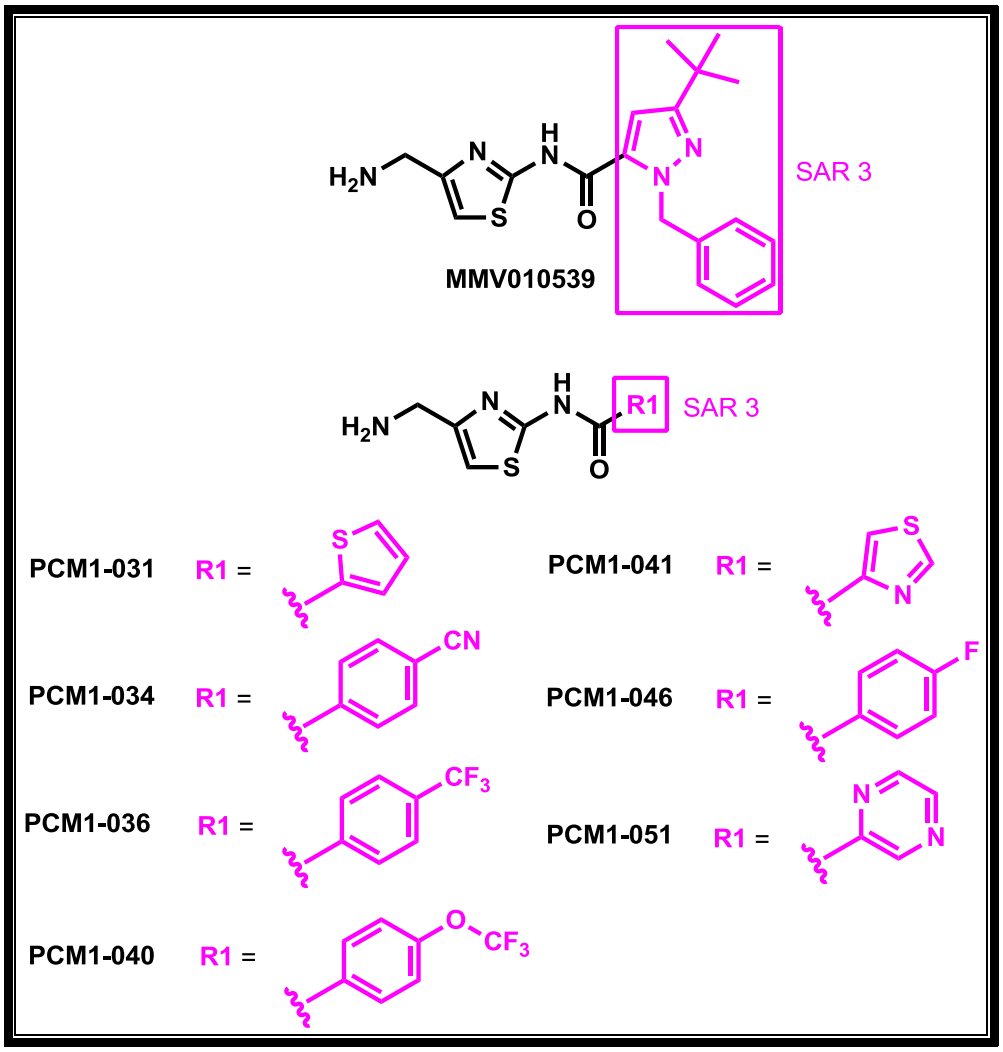

Figure 3.3 Chemical structures of target compounds **PCM1-031 - PCM1-051**.

Another important aspect of this MSc study was the exploration of SAR 2, which involved the generation of analogues bearing substituents on the aromatic portion of the benzyl group (Figure 3.4). This SAR exploration was lacking in the preliminary SAR studies reported in literature.[1] In this benzyl portion of the compound, the effect of electron withdrawing groups (halogens) and an alkyl (*tert*-butyl) group on activity was investigated. The effect of the relative position of the halogen group on the benzyl ring on activity was further explored in an attempt to establish if a

more favourable position on the ring exists. Target compounds **PCM1-056**, **PCM1-059**, **PCM1-066**, **PCM1-069**, and **PCM1-073** were thus designed and synthesised (Figure 3.4).

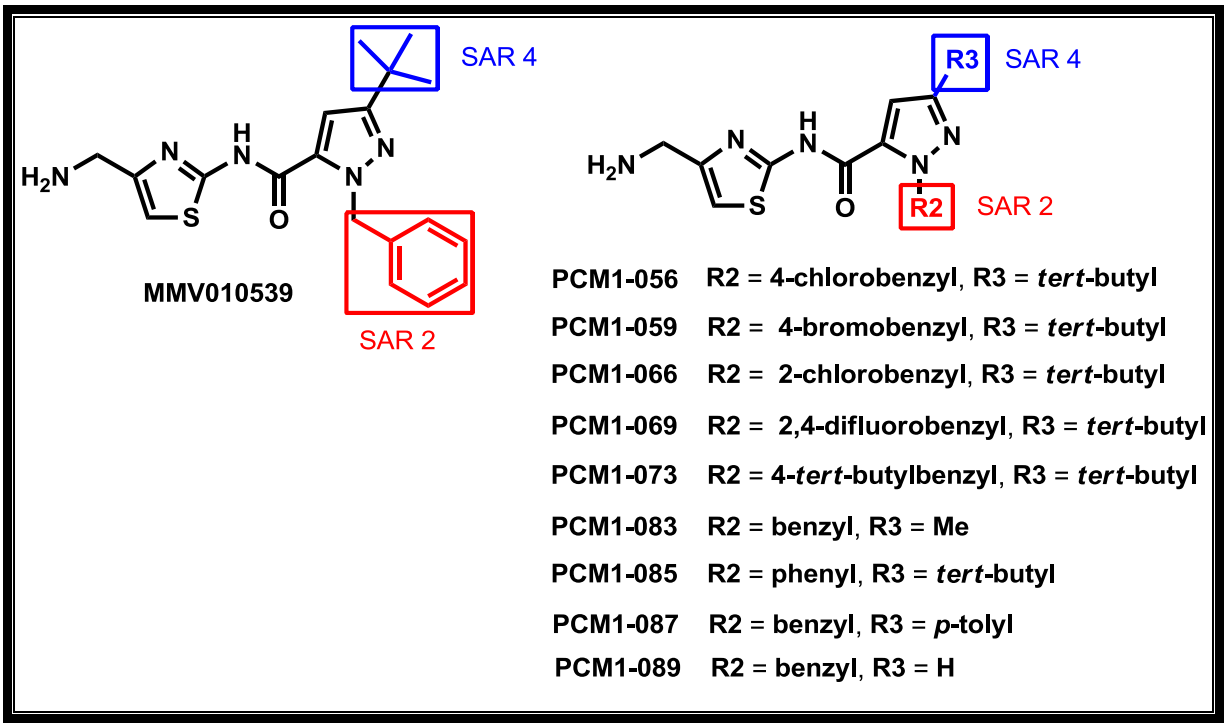

Figure 3.4 Chemical structures of target compounds **PCM1-056 - PCM1-089**.

In order to establish whether the benzyl methylene (CH_2) linker in the lead **MMV010539** is critical for activity, **PCM1-085** (Figure 3.4) was also designed. Finally SAR 4 (Figure 3.4), in which the *tert*-butyl group was replaced by other substituents, was explored in an effort to establish if variations at this position are tolerable with respect to activity. This gave rise to analogues **PCM1-083**, **PCM1-087**, and **PCM1-089** with methyl (Me), *p*-tolyl and hydrogen (H) substituents respectively. These analogues were also expected to shed some light on the size of substituents tolerable at that position.

3.2 Synthesis and Characterisation of Aminomethylheteroaryl Pyrazole Carboxamides (PCM1-012, PCM1-006 and MMV010539)

3.2.1 Retrosynthetic Analysis (PCM1-012, PCM1-006 and MMV010539)

Scheme 3.1 shows the retrosynthetic analysis of target molecules **PCM1-012**, **PCM1-006**, and **MMV010539**. For target molecules **PCM1-012** and **PCM1-006**, an amine protection step leads to *N*-boc-protected intermediates **PCM1-011** and **PCM1-005**. A C-N bond disconnection of the

boc-protected amine and functional group interconversion (FGI) further breaks down these intermediates to nitrile precursors **PCM1-009** and **PCM1-004**. Amide bond dissociation of precursors **PCM1-009** and **PCM1-004** then leads back to appropriate commercially available aromatic amino cyano analogues and pyrazole carboxylic acid.

The retrosynthetic strategy for **MMV010539** was somewhat different with the first step involving a FGI to an azide precursor **PCM1-008**, which was obtained via nucleophilic substitution of the corresponding chloro intermediate **PCM1-007**. The chloro intermediate **PCM1-007** was in turn obtained via amide bond formation between the commercially available pyrazole carboxylic acid and the amine hydrochloride salt **PCM1-032**. Further disconnections of C-N and C-S bonds of the amine hydrochloride salt **PCM1-032** finally lead to commercially available thiourea and 1,3-dichloroacetone.

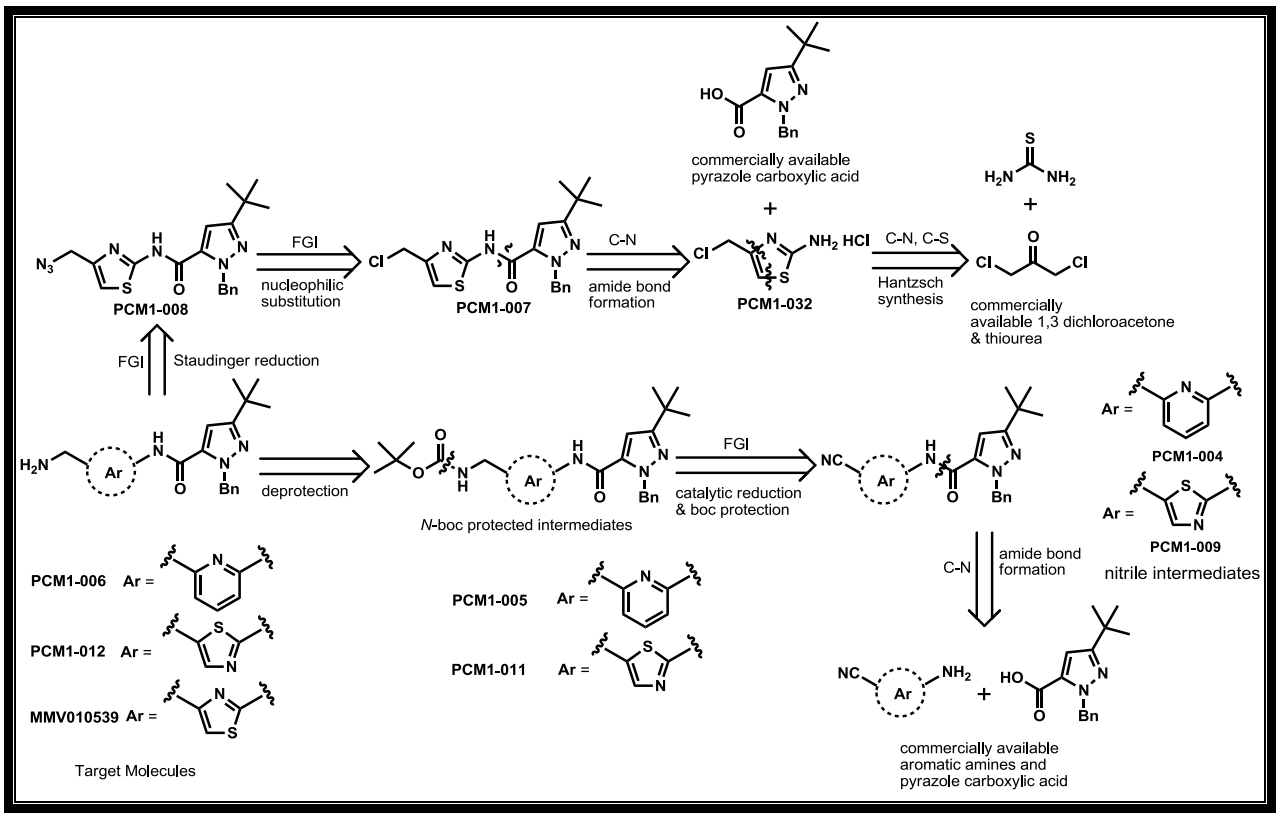

Scheme 3.1 Retrosynthetic scheme for carboxamides **PCM1-012**, **PCM1-006**, and **MMV010539**

3.2.2 Synthesis of Cyanoheteroaryl Pyrazole Carboxamides PCM1-004 and PCM1-009

Preparation of the cyanoheteroaryl pyrazole carboxamides **PCM1-004** and **PCM1-009** was achieved following a modified literature procedure described by Cabrera Gonzalez *et al.* (Scheme 3.2).[1]

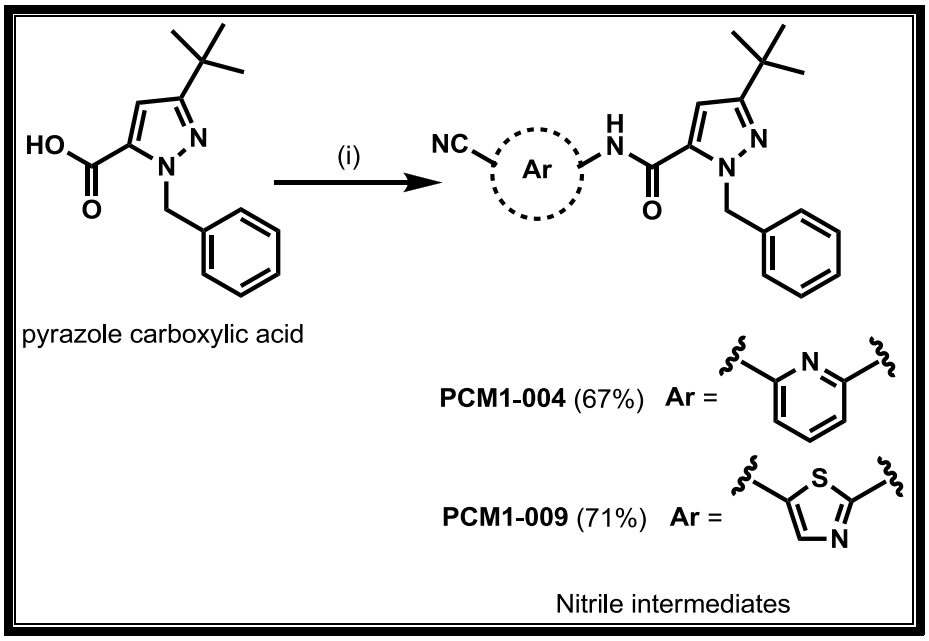

Scheme 3.2 General synthetic approach for cyanoheteroaryl pyrazole carboxamides **PCM1-004** and **PCM1-009**. *Reagents and conditions:* (i) appropriate aminonitrile, EDCI, DMAP, CH_2Cl_2, rt, 4-20 h

These cyano intermediates were synthesised via amidation of the commercially available pyrazole carboxylic acid in the presence of an appropriate commercially available amino cyano analogue. This was achieved by stirring a mixture of the benzyl pyrazole carboxylic acid and an appropriate amino cyano starting material in the presence of 1-ethyl-3-(3-dimethylaminopropyl) carbodiimide (EDCI) hydrochloride and 4-dimethylaminopyridine (DMAP) in dichloromethane (DCM). The reaction leading to the formation of **PCM1-004** was complete in 20 h while that for the formation of **PCM1-009** required only 4 h to go to completion. Good yields of 1-benzyl-3-*tert*-butyl-*N*-*(*6-cyanopyridin-2-yl)-1*H*-pyrazole-5-carboxamide (**PCM1-004**) and 1-benzyl-3-*tert*-butyl-*N*-(5-cyanothiazol-2-yl)-1*H*-pyrazole-5-carboxamide (**PCM1-009**) were obtained, 67% and 71% respectively. Confirmation of the structures of these two intermediates was achieved using ^{1}H NMR.

3.2.2.1 General Reaction Mechanism

The formation of the amide bond in the reaction of scheme 3.2 proceeds via the mechanism outlined below (Scheme 3.3).[2-5] Nucleophilic addition of the deprotonated carboxylic acid (carboxylate ion) to EDCI forms the *O*-acylisourea mixed ester making the carbonyl carbon more prone to nucleophilic attack. EDCI, therefore, serves as an activating agent for the carboxylic acid. Reaction of the amine with the activated intermediate leads to the desired amide and a urea by-product. The formation of the stable urea by-product is the driving force for this reaction.[6] However, a rearrangement of the unstable *O*-acylisourea mixed ester, via an acetyl transfer, to an unreactive *N*-acylurea often occurs. This side reaction compromises yields during amide bond formation.[6] Nevertheless, it can be circumvented to a large extent by carrying out the coupling reaction in the presence of a nucleophile like DMAP, whose reaction with the reactive *O*-acylisourea mixed ester is faster than the acetyl transfer side reaction. This produces an intermediate still reactive enough to react with the amine.

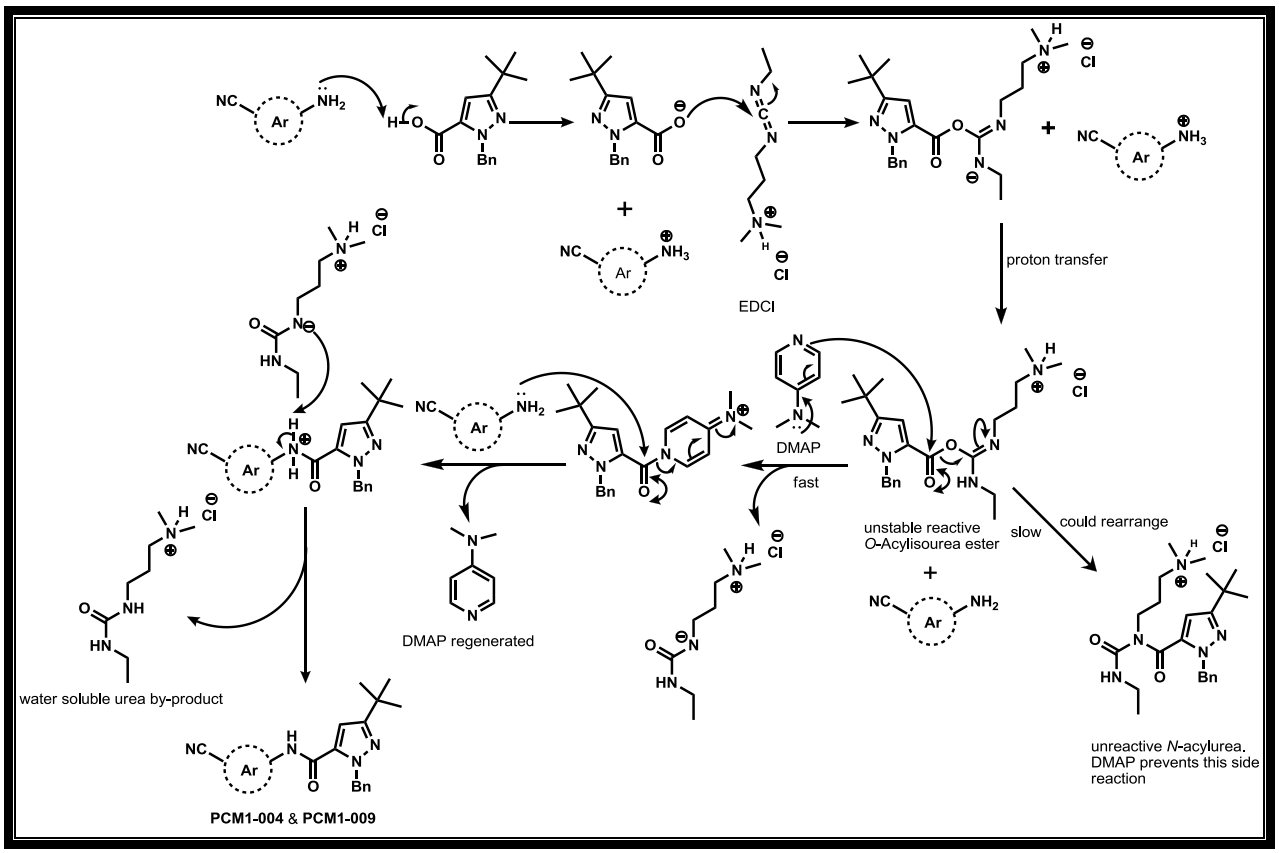

Scheme 3.3 Reaction mechanism for amide bond formation

3.2.3 Synthesis of Methylcarbamates PCM1-005 and PCM1-011

The synthesis of *N*-boc protected intermediates **PCM1-005** and **PCM1-011** exploited a modified literature procedure reported by Caddick *et al*.[7] This involved the catalytic reduction of the cyano groups and *in situ* boc-protection of the resulting primary amines (scheme 3.4). The reaction was carried out by adding an excess of sodium borohydride ($NaBH_4$) to a mixture of the nitrile compound (**PCM1-004** or **PCM1-009**), di-*tert*-butyl dicarbonate (Boc_2O), and nickel(II) chloride ($NiCl_2$) catalyst in methanol at 0 °C. The reactions proceeded at room temperature and as indicated by thin layer chromatography (TLC), were complete in 3-12 h. The nickel catalyst was sequestered from the reaction mixtures by treatment with excess ethylenediamine. The reactions afforded *tert*-butyl [6-(1-benzyl-3-*tert*-butyl-1*H*-pyrazole-5-carboxamido)pyridin-2-yl]methylcarbamate (**PCM1-005**) and *tert*-butyl [2-(1-benzyl-3-*tert*-butyl-1*H*-pyrazole-5-carboxamido)thiazol-5-yl]methylcarbamate (**PCM1-011**) in 45% and 28% yield respectively (scheme 3.4). The diagnostic appearance of a peak around δ 4.27 ppm on the ^{1}H NMR spectra corresponding to the methylene (CH_2) protons of the reduced cyano group confirmed the successful reaction. Successful *in situ* boc-protection of the resulting primary amine was confirmed by a ^{1}H NMR signal around δ 1.35 ppm corresponding to 9 protons of the *tert*-butyl group of the boc functionality.

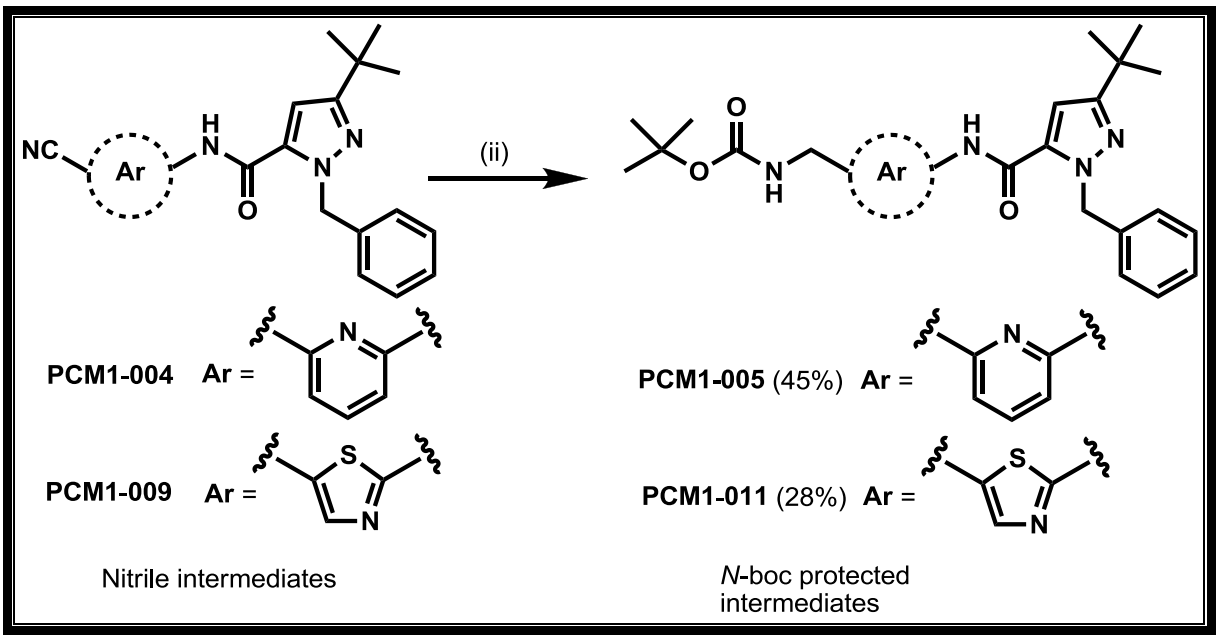

Scheme 3.4 General synthetic approach for methylcarbamates **PCM1-005** and **PCM1-011**. *Reagents and conditions:* (ii) Boc_2O, $NiCl_2$, $NaBH_4$, 0 °C to rt, 3-12 h, then 1,2-ethylenediamine

3.2.3.1 General Reaction Mechanism

To date, reaction mechanisms involving "transition-metal-assisted" hydride reductions remain poorly understood and the nature of the actual reducing species and catalyst generated *in situ* remains a subject of controversy.[8] However, a probable mechanism is proposed below (scheme 3.5) based on the mechanistic studies done on cobalt(II)-mediated reductions by Osby *et al.*[8] From their findings, they concluded that the cyano group is first activated by complexation to cobalt(II) boride (Co_2B) surface which is generated *in situ*. This is followed by the rate determining hydride addition to the activated cyano group with dissolved uncoordinated $NaBH_4$ acting as the donor of hydride ions. Repeated additions of hydride ions lead to the formation of the primary amine. Nickel(II) boride (Ni_2B) can as well be formed *in situ* from the reaction of $NiCl_2$ and $NaBH_4$ in methanol.[9,10] The Ni_2B generated *in situ*, therefore, acts as a catalytic surface in the same fashion Co_2B does. The Boc_2O present in the reaction mixture serves to circumvent the undesirable formation of dimers by reacting with the formed primary amine to yield boc-protected analogues.[7,11]

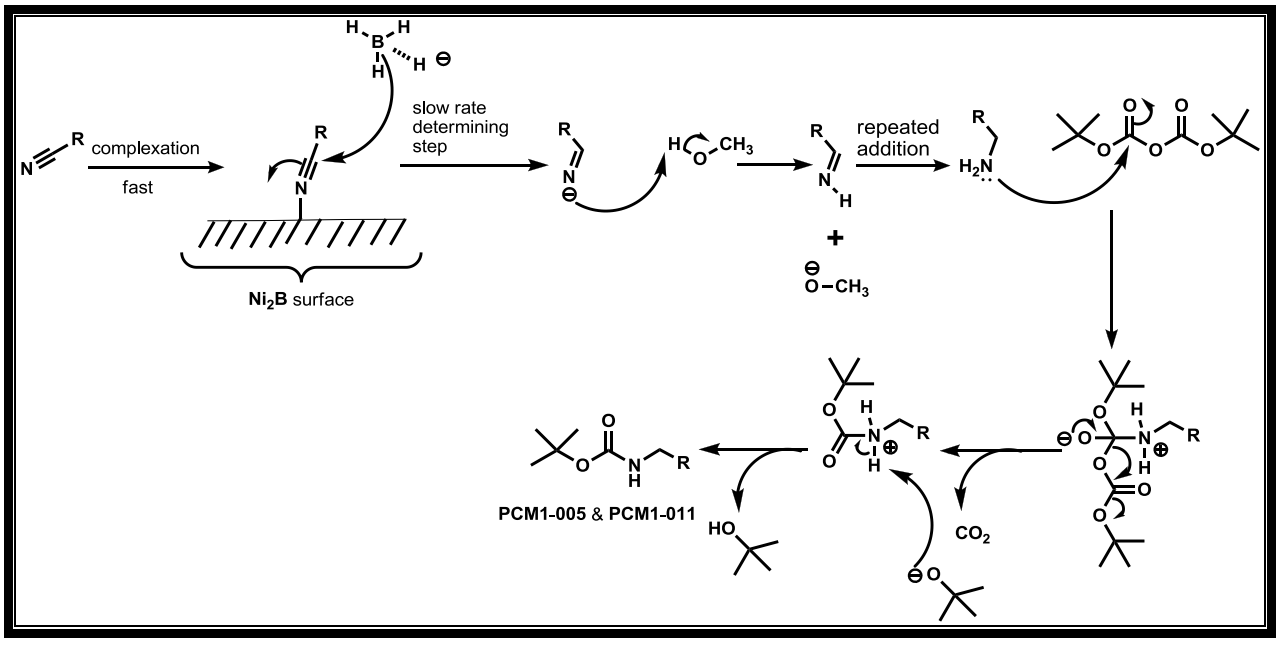

Scheme 3.5 General reaction mechanism for nitrile reduction and *N*-boc-protection

3.2.4 Synthesis of Aminomethylheteroaryl Pyrazole Carboxamides PCM1-006 and PCM1-012

The final step in the synthesis of carboxamides **PCM1-006** and **PCM1-012** was a simple deprotection of the boc-protected amines to give free amines (Scheme 3.6). With slight modifications, the procedure described by Cabrera Gonzalez *et al.*[1] was followed.

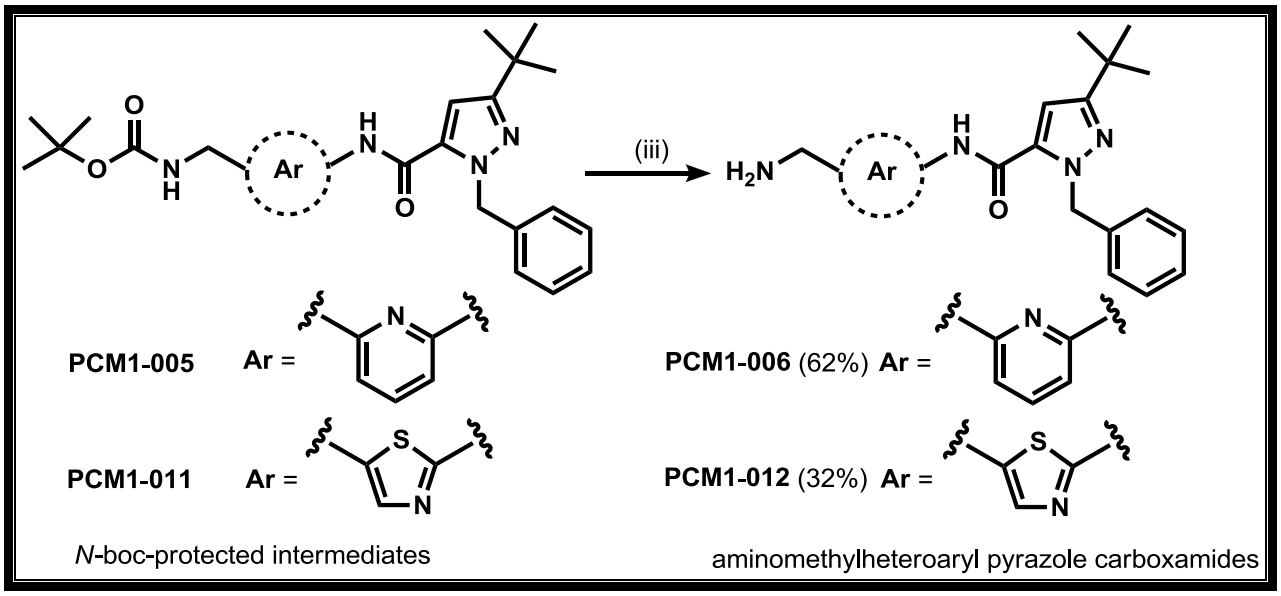

Scheme 3.6 General synthetic scheme for aminomethylheteroaryl pyrazole carboxamides **PCM1-006** and **PCM1-012**. *Reagents and conditions:* (iii) TFA, CH_2Cl_2, rt, 15-24 h, then Amberlyst A-21, CH_2Cl_2/CH_3OH, 1 h

Excess trifluoroacetic acid (TFA) was added to a solution of the *N*-boc-protected compound (**PCM1-005** or **PCM1-011**) in DCM and reaction mixtures stirred at room temperature for 15-24 h. Treatment with Amberlyst A-21 weak base ion exchange resin afforded the carboxamides **PCM1-006** (62% yield) and **PCM1-012** (32% yield). With the removal of the boc functionality in the deprotection reaction, there was a corresponding disappearance of its 9 proton ^{1}H NMR signal. The final target compounds were further characterised by ^{13}C NMR, infrared (IR) spectroscopy, mass spectrometry (MS), high performance liquid chromatography (HPLC), TLC, and melting point (m.p.) measurements.

3.2.4.1 General Reaction Mechanism

The boc-deprotection reaction mechanism (Scheme 3.7) starts with the protonation of the *tert*-butyl carbamate and the subsequent loss of the *tert*-butyl cation leads to the formation of the carbamic acid. The carbamic acid then undergoes decarboxylation to form the amine, which is obtained as a salt due to protonation from excess TFA. Deprotonation of the *tert*-butyl cation results in isobutylene gas which escapes from the reaction mixture together with carbon dioxide (CO_2).[12] The ammonium salt is finally converted to the free amine by the action of Amberlyst A-21 weak base ion exchange resin.

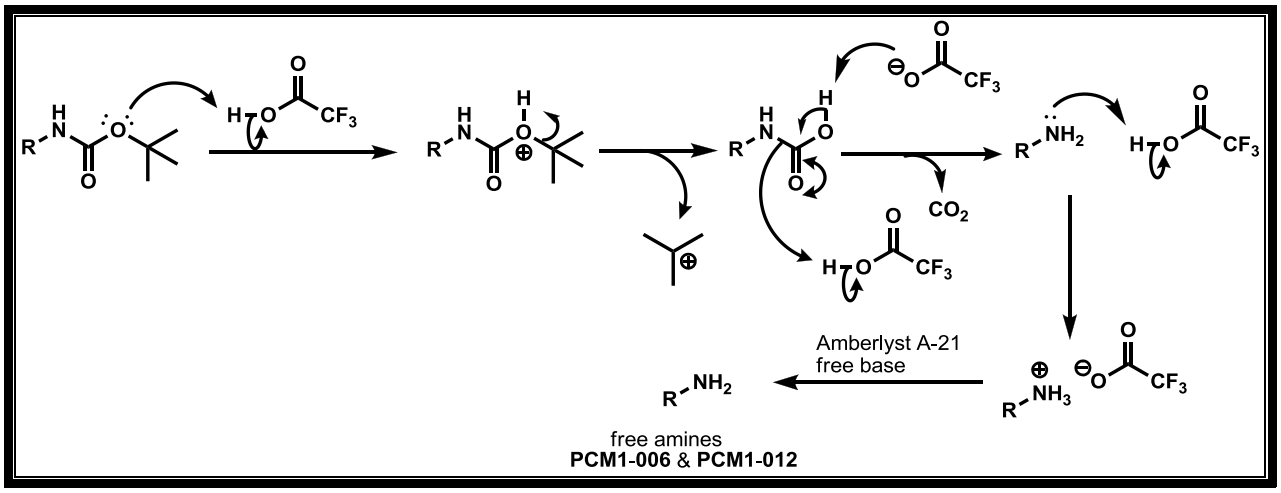

Scheme 3.7 General reaction mechanism for boc-deprotection

3.2.5 Synthesis of Chloromethylthiazole Amine Hydrochloride PCM1-032

The chloromethylthiazole amine hydrochloride salt **PCM1-032** was prepared via a modified version of the Hantzsch thiazole synthesis[13] detailed by Cabrera Gonzalez *et al.*[1] (Scheme 3.8).

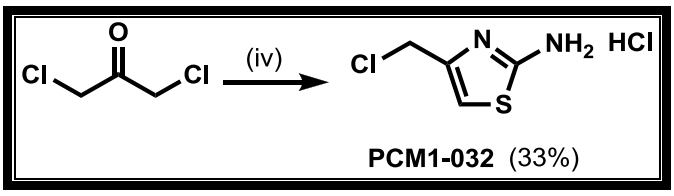

Scheme 3.8 Synthetic scheme for chloromethylthiazole amine hydrochloride **PCM1-032**. *Reagents and conditions:* (iv) $CS(NH_2)_2$, acetone, rt, 48 h, then Ethanol, rt, 6 h

The synthesis involved the condensation of 1,3-dichloroacetone and thiourea $CS(NH_2)_2$ in equimolar amounts to afford **PCM1-032** as a white hydrochloride salt in 33% yield. A molecular

ion ($[M+H]^+$) peak at mass to charge ratio (*m/z*) of 149.8571 ($C_4H_6ClN_2S$ requires M 148.9935) was observed on the mass spectrum which partly confirmed the identity of this thiazole intermediate.

3.2.5.1 Reaction Mechanism

Formation of the thiazole ring starts with bimolecular nucleophilic substitution (S_N2) followed by intramolecular nucleophilic addition of the imine nitrogen to the carbonyl carbon (Scheme 3.9). The resulting hydroxyl intermediate undergoes unimolecular elimination (E1) forming chloromethylthiazole amine **PCM1-032** as a hydrochloride salt.[14,15]

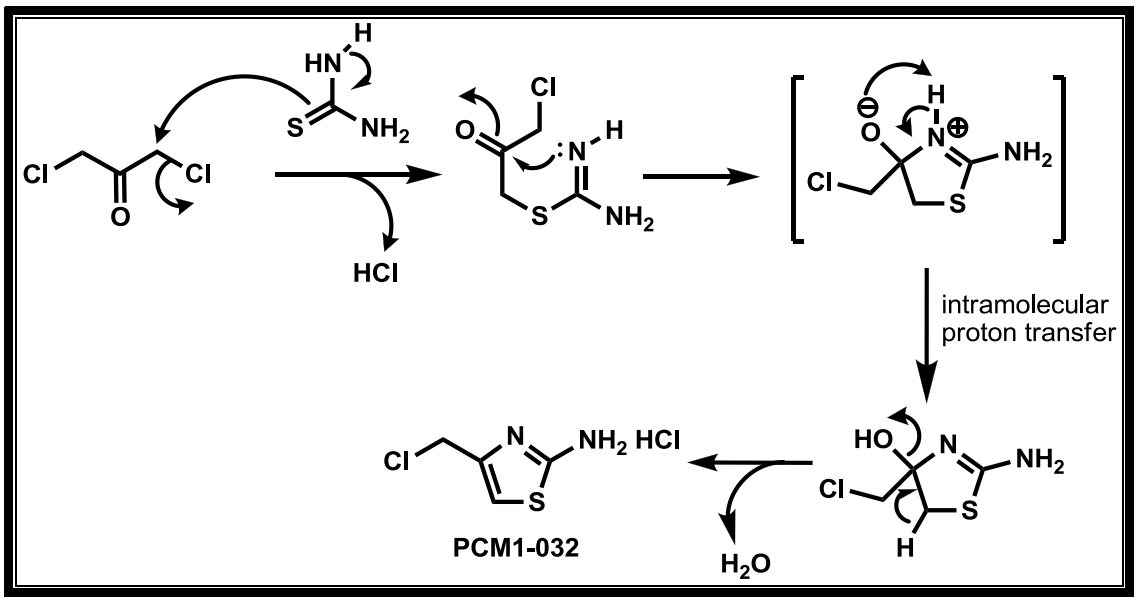

Scheme 3.9 Reaction mechanism for Hantzsch thiazole formation.

3.2.6 Synthesis of Chloromethylthiazole Pyrazole Carboxamide PCM1-007

An acid-amine coupling protocol detailed in section 3.2.2 was followed with minor modifications. Since the amine in this instance was in the form of a hydrochloride salt (**PCM1-032**), it was treated with *N*,*N*-diisopropylethylamine (DIPEA) to generate a free basic amine before addition to a mixture of pyrazole carboxylic acid, 1-hydroxybenzotriazole (HOBt), and EDCI in DCM (Scheme 3.10). HOBt was used in place of DMAP in order to circumvent the rearrangement side reaction. The reaction mixture was stirred for 15 h to afford chloromethylthiazole pyrazole carboxamide (**PCM1-007**) in 50% yield. ^{1}H NMR was used to confirm the structure of **PCM1-007.** The reaction proceeds via the same mechanism as detailed in section 3.2.2.1.

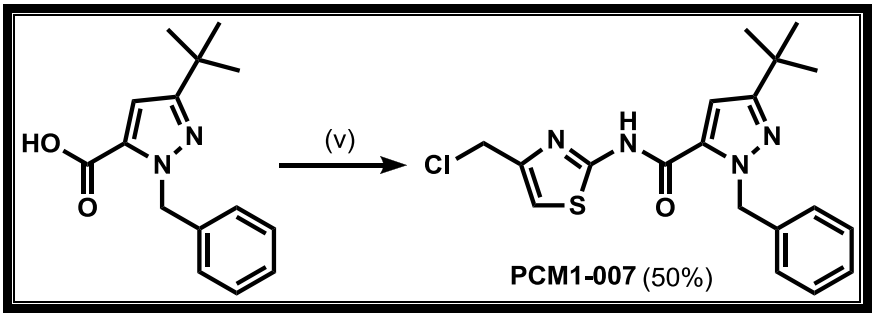

Scheme 3.10 Synthetic scheme to chloromethylthiazole pyrazole carboxamide **PCM1-007**. *Reagents and conditions:* (v) 4-(chloromethyl)thiazol-2-amine hydrochloride (**PCM1-032**), *N,N*-diisopropylethylamine, EDCI, HOBt, CH_2Cl_2, 15 h.

3.2.7 Synthesis of Azidomethylthiazole Pyrazole Carboxamide PCM1-008

Synthesis of the azide intermediate **PCM1-008** was accomplished via a simple nucleophilic substitution reaction, by stirring a mixture of 1-benzyl-3-*tert*-butyl-*N*-(4-(chloromethyl)thiazol-2-yl)-1*H*-pyrazole-5-carboxamide **PCM1-007** and excess sodium azide (NaN_3) in *N,N*-dimethylformamide (DMF) solvent at 80 °C for 26 h. This afforded the azide precursor **PCM1-008** in good yield (90%) (Scheme 3.11).[1] The azide precursor was subjected to electron ionisation mass spectrometry (EI-MS) analysis. A molecular ion at *m/z* 395.0193 ($C_{19}H_{21}N_7OS$ requires M 395.1528) was observed. The reaction mechanism for this reaction involves an S_N2 pathway described in section 3.2.5.1.[16]

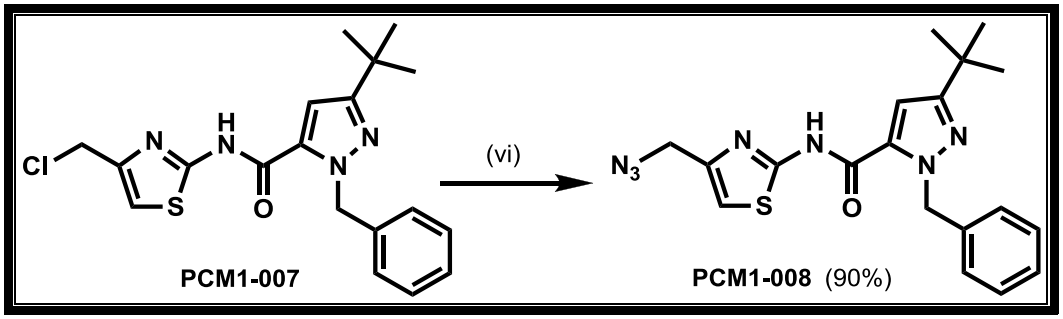

Scheme 3.11 Synthetic scheme to the azide precursor **PCM1-008**. *Reagents and conditions:* (vi) NaN_3, DMF, 80 °C, 26 h.

3.2.8 Synthesis of Aminomethylthiazole Pyrazole Carboxamide MMV010539

The final target compound **MMV010539**, bearing a free primary amine, was synthesised via the Staudinger reduction[17] of the azide group of precursor **PCM1-008**. The azide precursor **PCM1-008** was stirred with triphenylphosphine (PPh_3) and water in tetrahydrofuran (THF) (Scheme

3.12) to furnish the title compound in 68% yield. Characterisation of the target compound was performed by ^{1}H NMR, and HPLC.

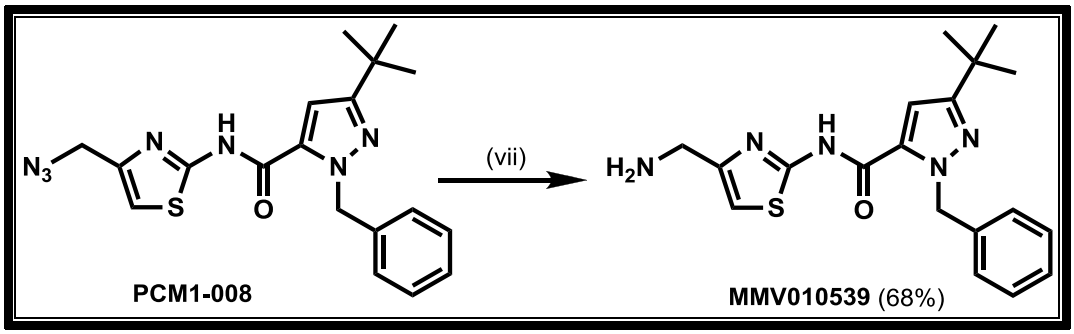

Scheme 3.12 Synthetic scheme to an aminomethylthiazole pyrazole carboxamide **MMV010539**. *Reagents and conditions:* (vii) H_2O, PPh_3, THF, rt, 24 h.

3.2.8.1 Reaction Mechanism

In the first step, the terminal nitrogen of the organic azide is attacked by the nucleophilic phosphorous atom of triphenylphosphine (Scheme 3.13). The phosphazide intermediate generated undergoes rearrangement to release nitrogen gas and form a N-P ylide, which is resonance stabilised. A water molecule then adds to the phosphorous atom. A series of proton transfer steps then leads to the formation of the primary amine, along with the triphenylphosphine oxide by-product.[18]

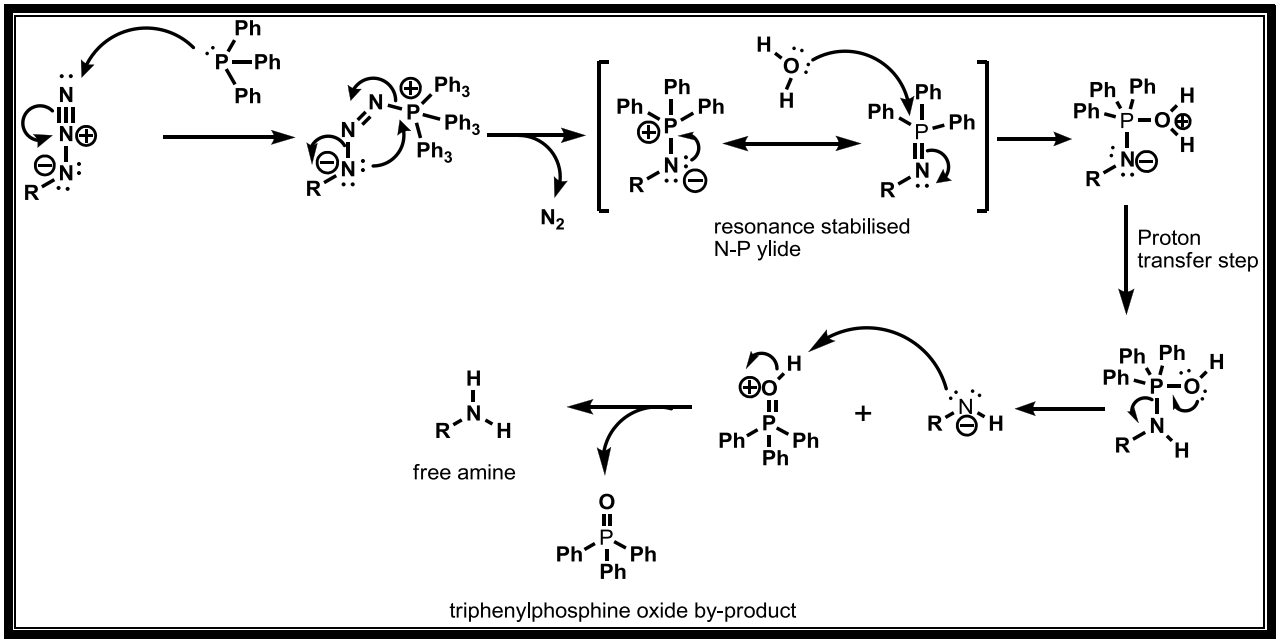

Scheme 3.13 Reaction mechanism of Staudinger reduction.[17,18]

Table 1 summarises the final target compounds with their respective percentage yields and melting points. Compound **MMV010539** was originally synthesised and reported by Cabrera Gonzalez *et al.*[1] and, therefore, the literature melting point is recorded.

Table 1. Aminomethylheteroaryl pyrazole carboxamides **PCM1-006**, **PCM1-012** and **MMV010539** with their respective yields and melting points.

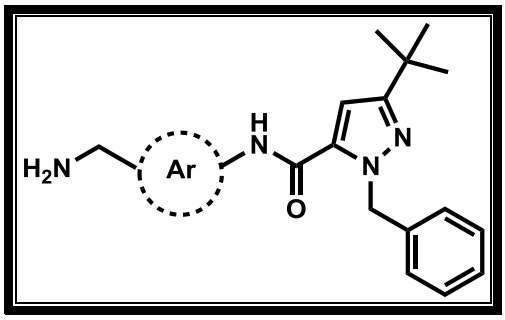

Ar	Code	% Yield	Mp (°C)
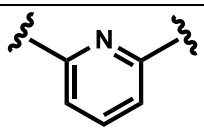	**PCM1-006**	62	137-140
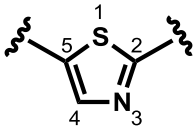	**PCM1-012**	32	83-85
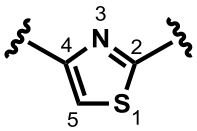	**MMV010539**	68	163-165*

*Literature value[1]

3.3 Synthesis and Characterisation of Aminomethylthiazole Carboxamides (PCM1-031, PCM1-041, PCM1-051, PCM1-083, PCM1-085 and PCM1-087) and Aminomethylthiazole Benzamides (PCM1-034, PCM1-036, PCM1-040 and PCM1-046)

3.3.1 Retrosynthetic Analysis for Aminomethylthiazole Carboxamides (PCM1-031, PCM1-041, PCM1-051, PCM1-083, PCM1-085 and PCM1-087) and Aminomethylthiazole Benzamides (PCM1-034, PCM1-036, PCM1-040 and PCM1-046)

A retrosynthetic approach shown in scheme 3.14 was followed to generate the aforementioned carboxamides and benzamides.

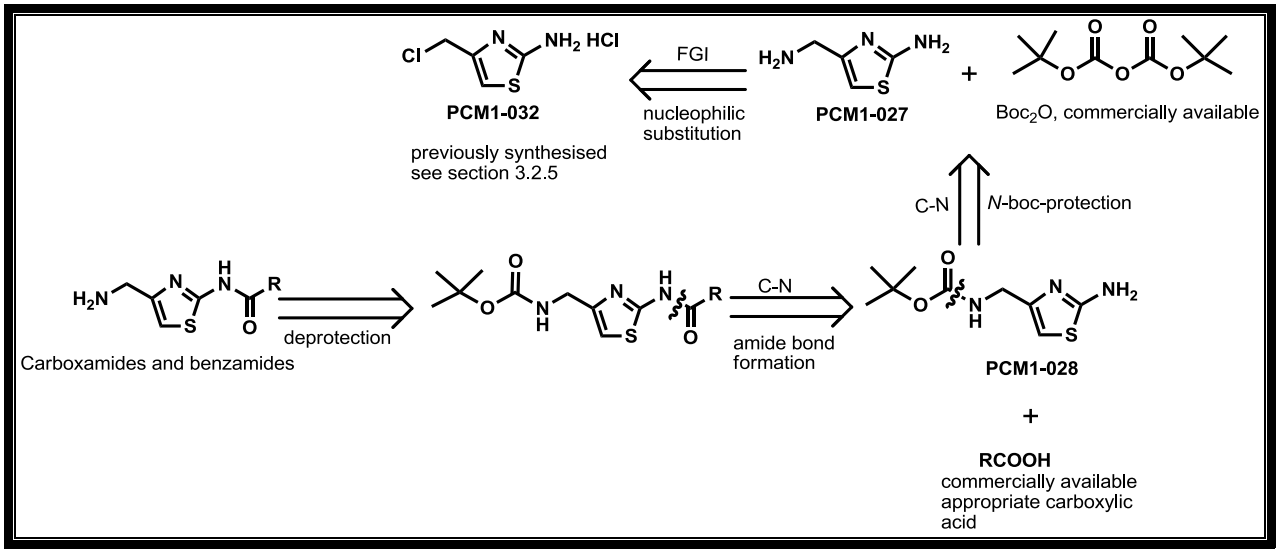

Scheme 3.14 Retrosynthetic approach to carboxamides (**PCM1-031**, **PCM1-041**, **PCM1-051**, **PCM1-083**, **PCM1-085** and **PCM1-087**) and benzamides (**PCM1-034**, **PCM1-036**, **PCM1-040**, and **PCM1-046**).

The retrosynthetic approach (Scheme 3.14) towards the aforementioned benzamides and carboxamides indicates an *N*-boc-protection step and a C-N disconnection to lead back to the amino intermediate **PCM1-028** and appropriate commercially available carboxylic acids. Further analysis suggests *N*-boc-deprotection to an aminomethylthiazole intermediate **PCM1-027**. The *N*-boc-protection step is necessary to ensure regioselective amidation of the amino group at position 2 of the thiazole intermediate **PCM1-027**. An FGI step converts the aminomethyl functionality of **PCM1-027** to the chloromethyl group of the previously synthesised (see section 3.2.5) starting material **PCM1-032**.

3.3.2 Synthesis of the Aminothiazole Methylcarbamate PCM1-028

Aminothiazole methylcarbamate **PCM1-028** was synthesised following scheme 3.15 outlined below. This involved a nucleophilic substitution followed by the *N*-boc protection of the resulting primary amine **PCM1-027**. The amine alkylation, or amino-de-halogenation (nucleophilic substitution), reaction was carried out following a modified literature procedure detailed by Cabrera Gonzalez *et al.*[1] The 4-(chloromethyl)thiazol-2-amine hydrochloride salt **PCM1-032** was stirred in excess 7 *N* ammonia in methanol for 72 h at rt. The alkylation of ammonia to give primary amines is usually problematic and characterised by poor yields. This is due to the primary amine, $\mathbf{RNH_2}$, formed being highly nucleophilic and will, therefore, also react with the alkyl halide in the reaction mixture, resulting in a mixture containing primary amines,

secondary amines, tertiary amines and quaternary ammonium salts. To circumvent the formation of other undesirable amines, a large excess of ammonia (33 eq) was used.[19a] The bright yellow solution was concentrated *in vacuo* to afford 4-(aminomethyl)thiazol-2-amine (**PCM1-027**) as a yellow solid which was used without further purification. The reaction mechanism involved is a simple S_N2 pathway as discussed in section 3.2.5.1.

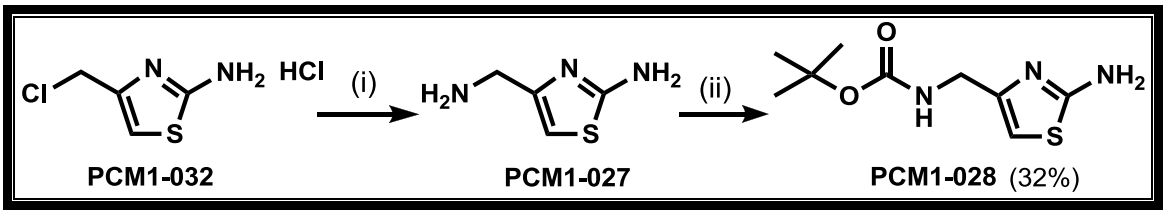

Scheme 3.15 Synthetic approach to an aminothiazole methylcarbamate **PCM1-028**. *Reagents and conditions:* (i) methanolic ammonia (7 *N*), sealed tube, rt, 72 h; (ii) triethylamine, di-*tert*-butyl dicarbonate, 0 °C to rt, 20 h.

Selective *N*-boc protection of the primary amine was achieved by reacting equimolar amounts of Boc_2O and 4-(aminomethyl)thiazol-2-amine **PCM1-027** in the presence of a slightly excess amount of triethylamine (TEA) in DMF (Scheme 3.15). This afforded *tert*-butyl (2-aminothiazol-4-yl)methylcarbamate (**PCM1-028)** as a yellow solid in 32% yield. The appearance of a ^1H NMR signal around δ 1.43 ppm integrating for the relatively shielded 9 protons confirmed the successful incorporation of the boc functionality.

The reaction proceeds via a nucleophilic addition of the primary amine to Boc_2O (see scheme 3.5). In this specific case, TEA serves to scavenge acid formed after nucleophilic addition.[19b]

3.3.3 Synthesis of Thiazole Methylcarbamates PCM1-081, PCM1-084, PCM1-086 and PCM1-029 - PCM1-049

The thiazole methylcarbamates, **PCM1-081**, **PCM1-084**, **PCM1-086** and **PCM1-029** - **PCM1-049** were synthesised via amidation of the appropriate commercially available carboxylic acids in the presence of *tert*-butyl(2-aminothiazol-4-yl)methylcarbamate **PCM1-028**. The protocol is as described in section 3.2.2 with minor modifications in some instances (Scheme 3.16). All the acid-amine coupling reactions exploited the presence of EDCI and DMAP and required 3 – 48 h to go to completion. Progress of the reactions was monitored by TLC. The crude reaction mixtures of intermediates **PCM1-029** - **PCM1-049** were not subjected to aqueous work up. Instead, they were directly concentrated *in vacuo* and purified by column chromatography. The

thiazole methylcarbamate intermediates **PCM1-081**, **PCM1-084**, **PCM1-086** and **PCM1-029 - PCM1-049** were obtained in low to excellent yields (32 – 95%).

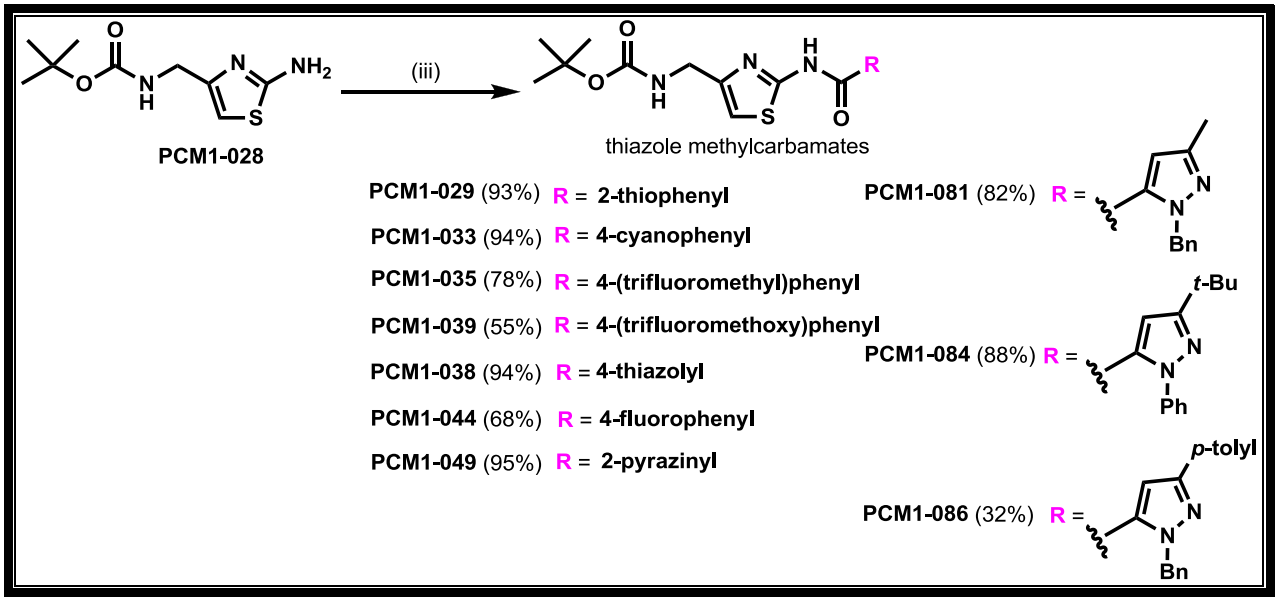

Scheme 3.16 Synthetic approach to thiazole methylcarbamates **PCM1-081**, **PCM1-084**, **PCM1-086** and **PCM1-029 - PCM1-049**. *Reagents and conditions:* (iii) Appropriate carboxylic acid, EDCI, DMAP, CH_2Cl_2, 3 - 48 h.

During the acid-amine coupling, the carboxylic acid is activated by a nucleophilic reaction with EDCI. This is followed by nucleophilic addition of the amine to the activated carboxylic acid-EDCI adduct to form the amide bond. As described in section 3.2.2.1, DMAP serves to circumvent the rearrangement side reaction by forming a carboxylic acid-DMAP adduct which is still reactive enough to react with the amine (see section 3.2.2.1 for detailed description of reaction mechanism).

3.3.4 Synthesis of Aminomethylthiazole Carboxamides and Aminomethylthiazole Benzamides PCM1-083, PCM1-085, PCM1-087 and PCM1-031-PCM1-051

The final step in the synthesis of aminomethylthiazole carboxamides and aminomethylthiazole benzamides (**PCM1-083**, **PCM1-085**, **PCM1-087** and **PCM1-031-PCM1-051**) involved the *N*-boc-deprotection reaction using TFA to give the free amines (Scheme 3.17). The procedure described in section 3.2.4 was followed to obtain the title compounds in poor to good yields (13 – 84%). The disappearance of the ^{1}H NMR signal around δ 1.47 ppm integrating for 9 protons of the boc group confirmed the successful *N*-boc-deprotection of the amino functionality. The target

compounds were further subjected to ^{13}C NMR, IR, EI-MS, HPLC, TLC, and m.p measurements for full characterisation.

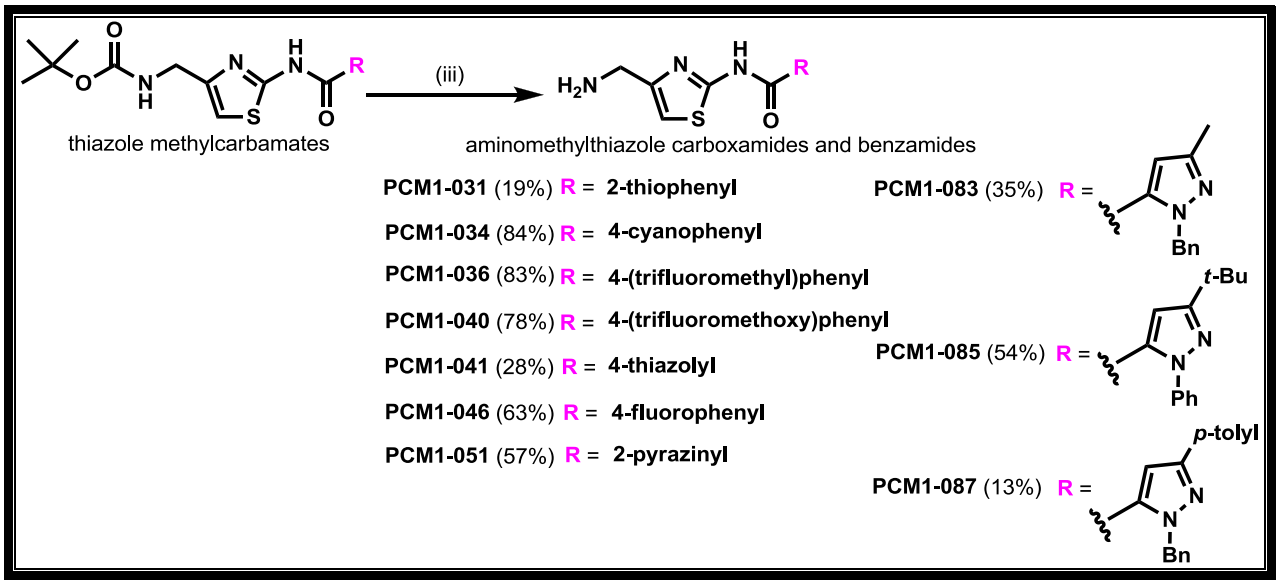

Scheme 3.17 Synthetic approach to aminomethylthiazole carboxamides and aminomethylthiazole benzamides **PCM1-083**, **PCM1-085**, **PCM1-087** and **PCM1-031 - PCM1-051**. *Reagents and conditions:* (iii) TFA, CH_2Cl_2, rt, 4 - 42 h, then Amberlyst A-21, CH_2Cl_2/CH_3OH, 1 h.

The isolated yields, melting points, and chemical structures of the aminomethylthiazole carboxamides and aminomethylthiazole benzamides **PCM1-083**, **PCM1-085**, **PCM1-087** and **PCM1-031 - PCM1-051** are summarised in table 2.

Table 2. Isolated yields, melting points and chemical structures of analogues **PCM1-083**, **PCM1-085**, **PCM1-087**, and **PCM1-031 - PCM1-051**.

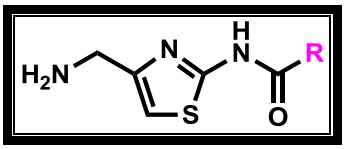

R	Code	% Yield	Mp (°C)
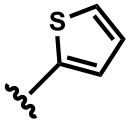	**PCM1-031**	19	174-176

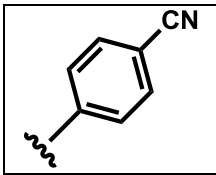	**PCM1-034**	84	214-216
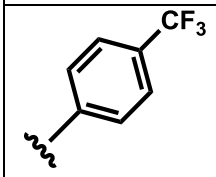	**PCM1-036**	83	213-214
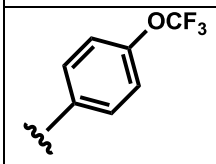	**PCM1-040**	78	182-186
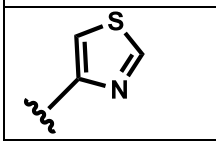	**PCM1-041**	28	151-153
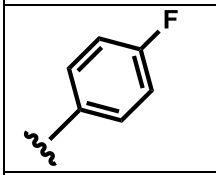	**PCM1-046**	63	209-210
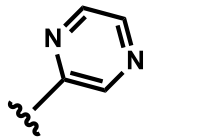	**PCM1-051**	57	176-180
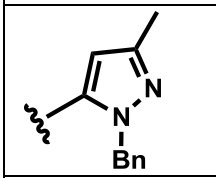	**PCM1-083**	35	158-160
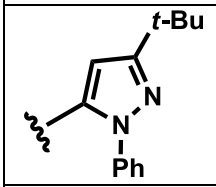	**PCM1-085**	54	85-88
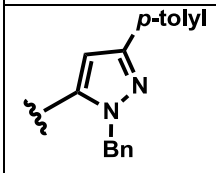	**PCM1-087**	13	85-87

3.4 Synthesis and Characterisation of Aminomethylthiazole Pyrazole Carboxamides (PCM1-056 - PCM1-073 and PCM1-089)

3.4.1 Retrosynthetic Analysis (PCM1-056 - PCM1-073 and PCM1-089)

Aminomethylthiazole pyrazole carboxamides, **PCM1-056 - PCM1-073** and **PCM1-089** were obtained following a retrosynthetic plan shown in scheme 3.18. Protection of the amino group yields *N*-boc-protected intermediates, which upon a C-N disconnection, lead to a variety of commercially available benzyl bromides and the basic pyrazole intermediate. A further amide disconnection then leads to the crucial amino intermediate **PCM1-028**, of which the synthesis has been discussed (See section 3.3.1), and commercially available pyrazole carboxylic acids. Keeping the amine boc-protected in the synthetic steps 1 and 2 is necessary to avoid its coupling to the carboxylic acid and *N*-benzylation respectively. Once steps 1 and 2 are executed, the amine could be deprotected to afford the target compounds.

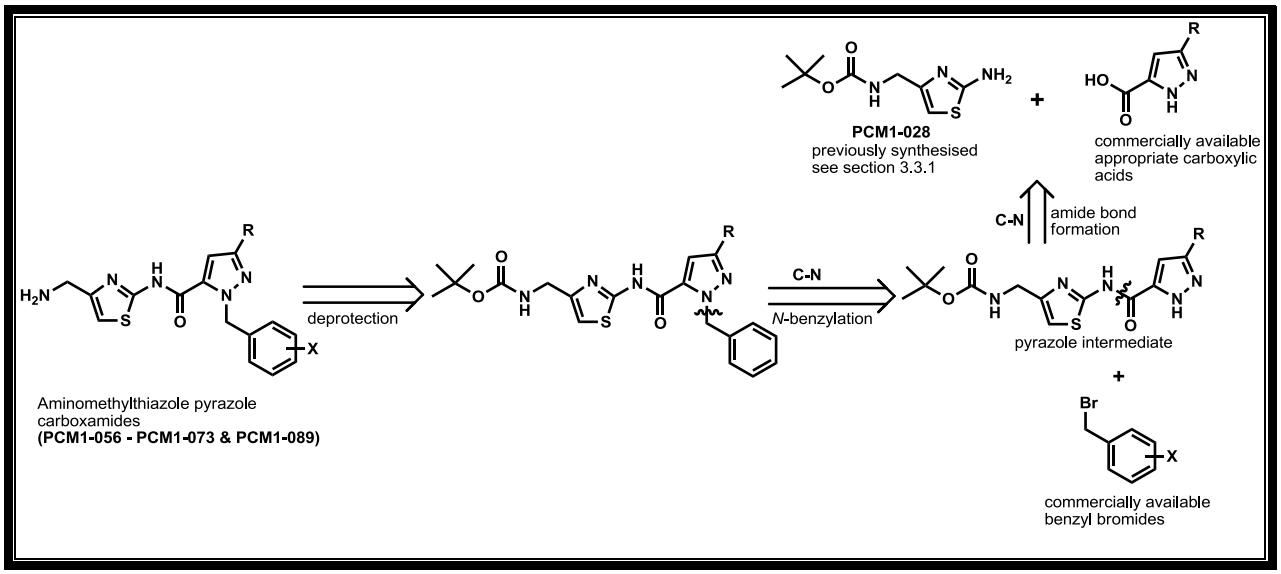

Scheme 3.18 Retrosynthetic approach to aminomethylthiazole pyrazole carboxamides, **PCM1-056 - PCM1-073** and **PCM1-089**

3.4.2 Synthesis of Pyrazole Thiazole Methylcarbamates PCM1-054 and PCM1-082

The preparation of the pyrazole intermediates **PCM1-054** and **PCM1-082** exploited an acid-amine coupling reaction (Scheme 3.19) mediated by EDCI and DMAP as discussed previously (see section 3.2.2) albeit minor modifications were made. To obtain the pyrazole intermediate **PCM1-082**, the reaction was carried out in DMF due to the poor solubility of the carboxylic acid starting material in DCM. After stirring for 48 h, the **PCM1-054** reaction mixture was concentrated *in vacuo* and directly subjected to column chromatography without any aqueous work up. This afforded *tert*-butyl (2-(3-*tert*-butyl-1*H*-pyrazole-5-carboxamido)thiazol-4-yl)methylcarbamate (**PCM1-054**) as a white solid in 42% yield. The reaction mixture for

PCM1-082 was stirred for 20 h, after which water was added to precipitate the product out of solution. The resulting precipitate was filtered, sequentially washed with water, hexane, and a minimal amount of ethyl acetate to furnish *tert*-butyl (2-(1*H*-pyrazole-5-carboxamido)thiazol-4-yl)methylcarbamate (**PCM1-082**) as a brown solid in 55% yield.

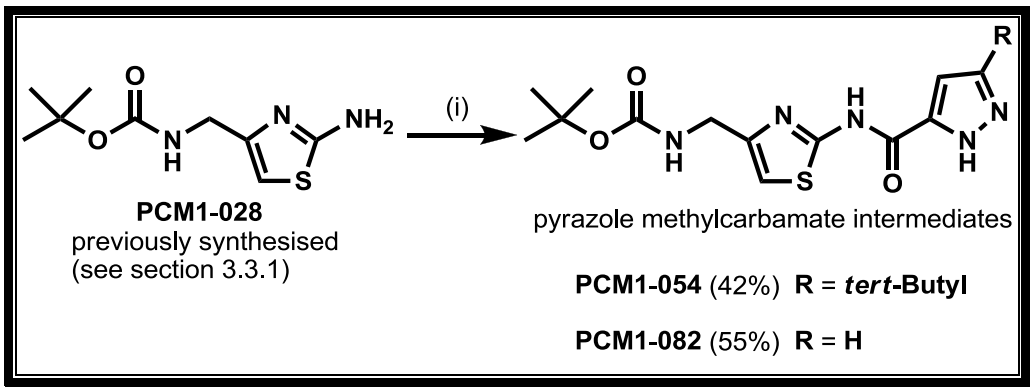

Scheme 3.19 Synthetic approach to pyrazole thiazole methylcarbamates **PCM1-054** and **PCM1-082**. *Reagents and conditions:* (iii) Appropriate pyrazole carboxylic acid, EDCI, DMAP, CH_2Cl_2 (**PCM1-054**), DMF (**PCM1-082**), 20 - 48 h.

The pyrazole intermediates were confirmed by ^{1}H NMR. Additional peaks in the aromatic region at approximately δ 7.24 ppm and δ 7.02 ppm, integrating for a proton each, correspond to the two CH protons on the pyrazole moiety of **PCM1-082**. The appearance of an extra peak at δ 6.80 ppm and δ 1.34 ppm integrating to 1 aromatic CH proton and comparatively shielded 9 *tert*-butyl protons respectively confirmed the successful synthesis of **PCM1-054**.
The two coupling reactions proceed via the mechanism outlined in section 3.2.2.1 (see scheme 3.3).

3.4.3 Synthesis of Benzyl Pyrazole Thiazole Methylcarbamates PCM1-055, PCM1-057 PCM1-064, PCM1-067, PCM1-071, and PCM1-088

The benzyl pyrazole thiazole methylcarbamates **PCM1-055**, **PCM1-057**, **PCM1-064**, **PCM1-067** and **PCM1-071** were synthesised via a common pyrazole intermediate **PCM1-054**. Analogue **PCM1-088** on the contrary, was synthesised from the pyrazole intermediate **PCM1-082** (Scheme 3.20).

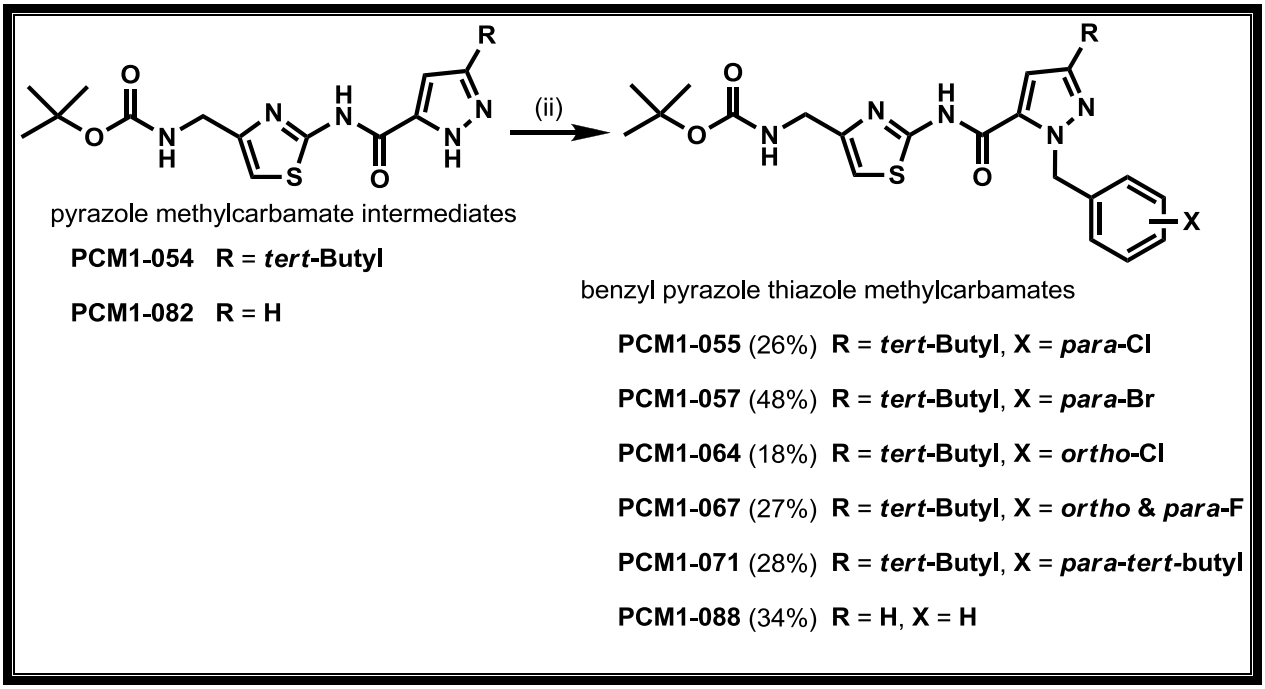

Scheme 3.20 Synthetic approach to benzyl pyrazole thiazole methylcarbamates. *Reagents and conditions:* (iii) Appropriate benzyl bromide, K_2CO_3, DMF or acetonitrile, rt, 21 - 48 h

A protocol described by Andrés *et al.*[20], with a few modifications made in some reactions, was followed to carry out benzylation of the NH group of the pyrazole moiety. Analogues **PCM1-055** - **PCM1-071** and **PCM1-088** were synthesised by respectively benzylating the pyrazoles **PCM1-054** and **PCM1-082** with appropriate benzyl bromides in the presence of potassium carbonate (K_2CO_3) base in DMF or acetonitrile at room temperature. The majority of the reactions were performed in DMF due to poor solubility of the starting materials in acetonitrile. Analogue **PCM1-071** was purified by preparative-TLC after failed column chromatographic separation. For analogues **PCM1-055** and **PCM1-057**, acetonitrile was used as the solvent. All the analogues were obtained in 26 – 48 % yield and confirmed by ^{1}H NMR.

3.4.3.1 General Reaction Mechanism

The mechanism for the formation of *N*-benzylated pyrazoles involves attack of the benzyl carbon by the nucleophilic pyrazole nitrogen in an S_N2 fashion. K_2CO_3 base then scavenges the proton on the positively charged intermediate (Scheme 3.21).[21]

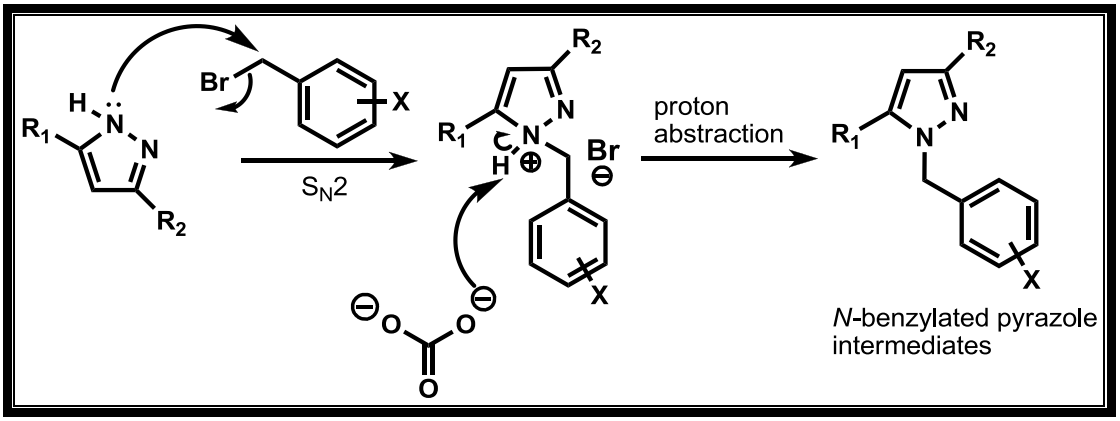

Scheme 3.21 Reaction mechanism for *N*-benzylation.[21]

3.4.4 Synthesis of Aminomethylthiazole Pyrazole Carboxamides PCM1-056 - PCM1-073 and PCM1-089

The aminomethylthiazole pyrazole carboxamides, **PCM1-056** - **PCM1-073** and **PCM1-089** were obtained from the corresponding benzyl pyrazole thiazole methylcarbamate precursors by an *N*-boc-deprotection reaction (Scheme 3.22) through treatment with TFA, similar to that discussed in section 3.2.4.

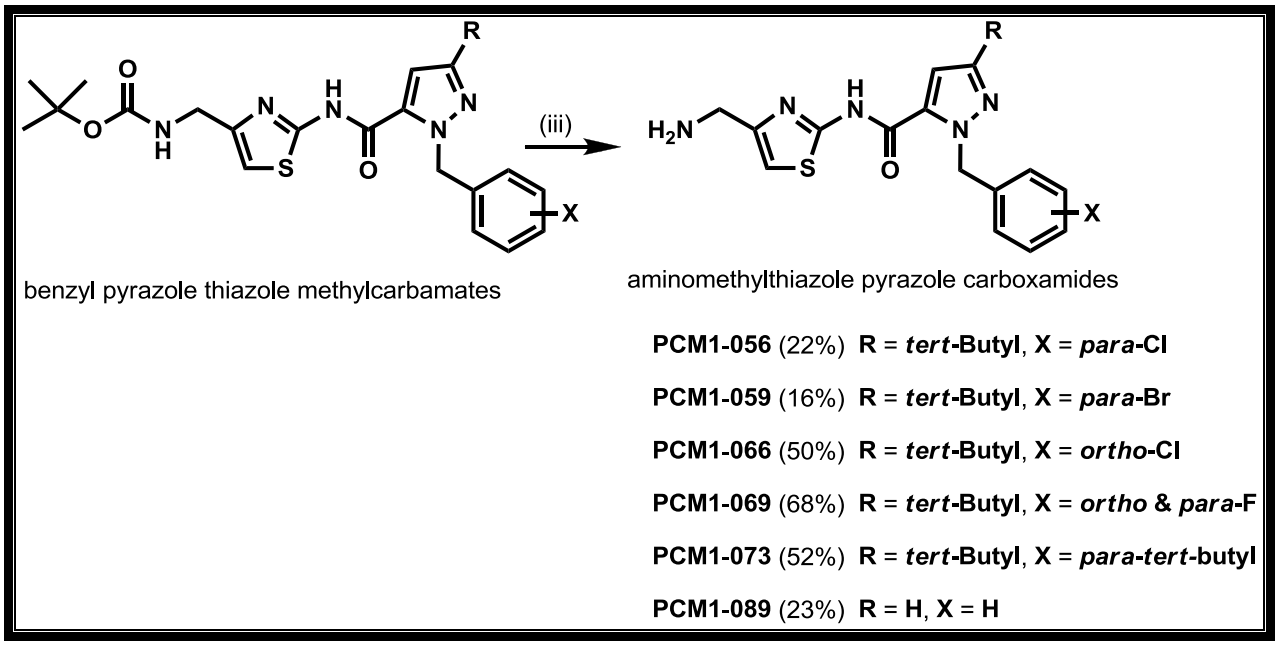

Scheme 3.22 Synthetic scheme to aminomethylthiazole pyrazole carboxamides **PCM1-056** - **PCM1-073** and **PCM1-089**. *Reagents and conditions:* (iii) TFA, CH_2Cl_2, rt, 12 - 72 h, then Amberlyst A-21, CH_2Cl_2/CH_3OH, 1 h.

The aminomethylthiazole pyrazole carboxamides were obtained in low to moderate yields and characterised by ^{1}H NMR, ^{13}C NMR, IR, EI-MS, HPLC, TLC, and melting point measurements. ^{1}H NMR spectra for all the analogues showed a disappearance of a 9 proton signal around δ 1.45 ppm that corresponded to the relatively shielded *tert*-butyl protons of the boc group. This confirmed the successful amine-boc-deprotection.

The final target compounds with their yields and melting points are tabulated below (Table 3)

Table 3. Isolated yields, melting points and chemical structures of Aminomethylthiazole Pyrazole Carboxamides **PCM1-056** - **PCM1-073** and **PCM1-089**.

Product Structure	Code	% Yield	Mp (°C)
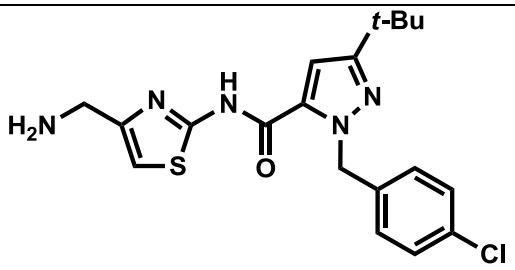	**PCM1-056**	22	115-117
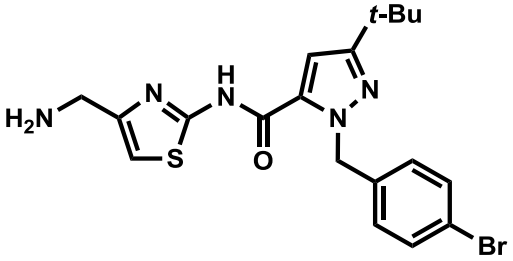	**PCM1-059**	16	92-94
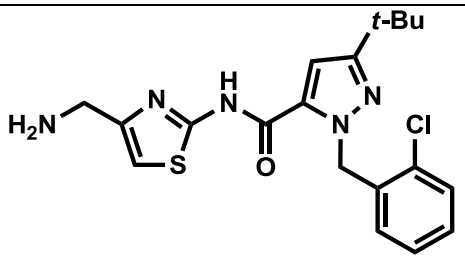	**PCM1-066**	50	143-145
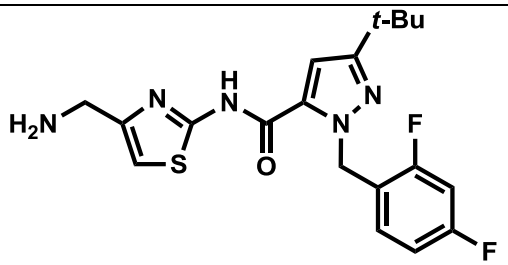	**PCM1-069**	68	149-153

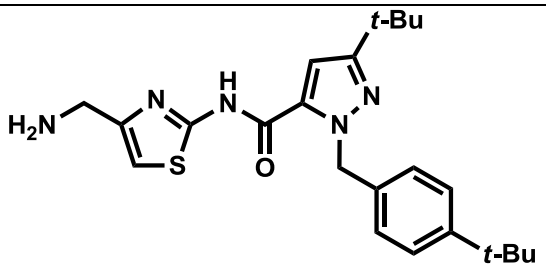	**PCM1-073**	52	118-120
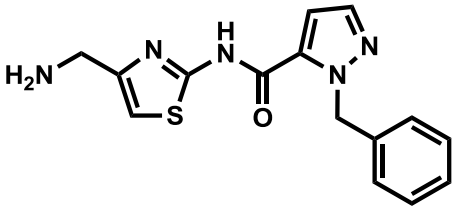	**PCM1-089**	23	166-169

3.5 Characterisation of Target Compounds

All the resulting analogues displayed a characteristic singlet ^{1}H NMR peak around δ 4 ppm integrating for 2 protons. This signal corresponds to the 2 methylene (CH_2) protons of the aminomethyl motif, which is common in all the final target compounds. Except for **PCM1-031** - **PCM1-051**, and **PCM1-085** (Table 2), which lacked a benzyl group, a characteristic singlet ^{1}H NMR peak around δ 5.8 ppm integrating for 2 benzyl CH_2 protons was observed in the ^{1}H NMR spectra of all the final compounds. A common ^{1}H NMR peak at around δ 1.30 ppm integrating for 9 protons of the *tert*-butyl group was also observed for final compounds bearing the *tert*-butyl group on the pyrazole ring. For example **MMV010539**, **PCM1-006**, **PCM1-012** (Table 1), **PCM1-056**, **PCM1-059**, **PCM1-066**, **PCM1-069**, **PCM1-073** (Table 3), and **PCM1-085** (Table 2), exhibited this common ^{1}H NMR peak. A characteristic ^{13}C NMR peak at around δ 39 ppm was evident in the ^{13}C NMR spectra of all the final target compounds. This common peak corresponds to the aminomethyl methylene (CH$_2$NH$_2$) carbon that is present in all the compounds. A relatively shielded benzyl carbon present in analogues **PCM1-089**, **PCM1-073**, **PCM1-069**, **PCM1-066**, **PCM1-059**, **PCM1-056** (Table 3), **PCM1-087**, **PCM1-083** (Table 2), **MMV010539**, **PCM1-012**, and **PCM1-006** (Table 1), gave rise to a ^{13}C NMR peak at around δ 55 ppm. For all the analogues bearing a *tert*-butyl group on the pyrazole ring such as **MMV010539**, **PCM1-006**, **PCM1-012** (Table 1), **PCM1-056**, **PCM1-059**, **PCM1-066**, **PCM1-069**, **PCM1-073** (Table 3), and **PCM1-085** (Table 2), a corresponding peak appeared relatively upfield at around δ 30 ppm in all their ^{13}C NMR spectra. In addition, a ^{13}C NMR signal at around the same chemical shift (δ 30.5 ppm) corresponding to the highly shielded *tertiary* carbon of the *tert*-butyl group was observed for such compounds. Also notable and common to all ^{13}C NMR spectra of all the target compounds was the signal of the carbonyl carbon of the amide bond.

This, as expected from the structures of the compounds, was observed relatively downfield at approximately δ 160 ppm. This further confirms the authenticity of the target compounds.

For the aminomethylheteroaryl pyrazole carboxamides **PCM1-006**, **PCM1-012** and **MMV010539** (Table 1), a representative ^{1}H NMR spectrum for **PCM1-012** is shown (Figure 3.5). A representative ^{1}H NMR spectrum for **PCM1-036** (Figure 3.6) from the aminomethylthiazole benzamides and aminomethylthiazole carboxamides **PCM1-083**, **PCM1-085**, **PCM1-087** and **PCM1-031 - PCM1-051** (Table 2) is also shown. The aminomethylthiazole pyrazole carboxamides **PCM1-056** - **PCM1-073** and **PCM1-089** of Table 3 are represented by the ^{1}H NMR spectrum of **PCM1-056** (Figure 3.7).

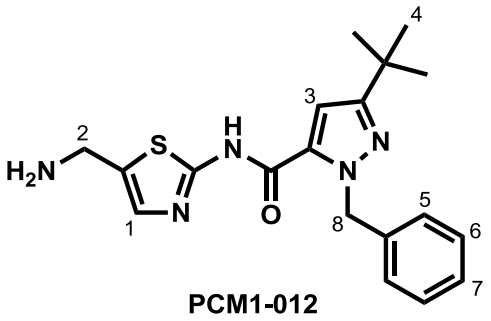

PCM1-012

δ/ppm	Multiplicity	J/Hz	H
7.22-7.11	m	-	H5, H6, H7
6.96	s	-	H1
6.64	s	-	H3
5.71	s	-	H8
3.91	s	-	H2
1.24	s	-	H4

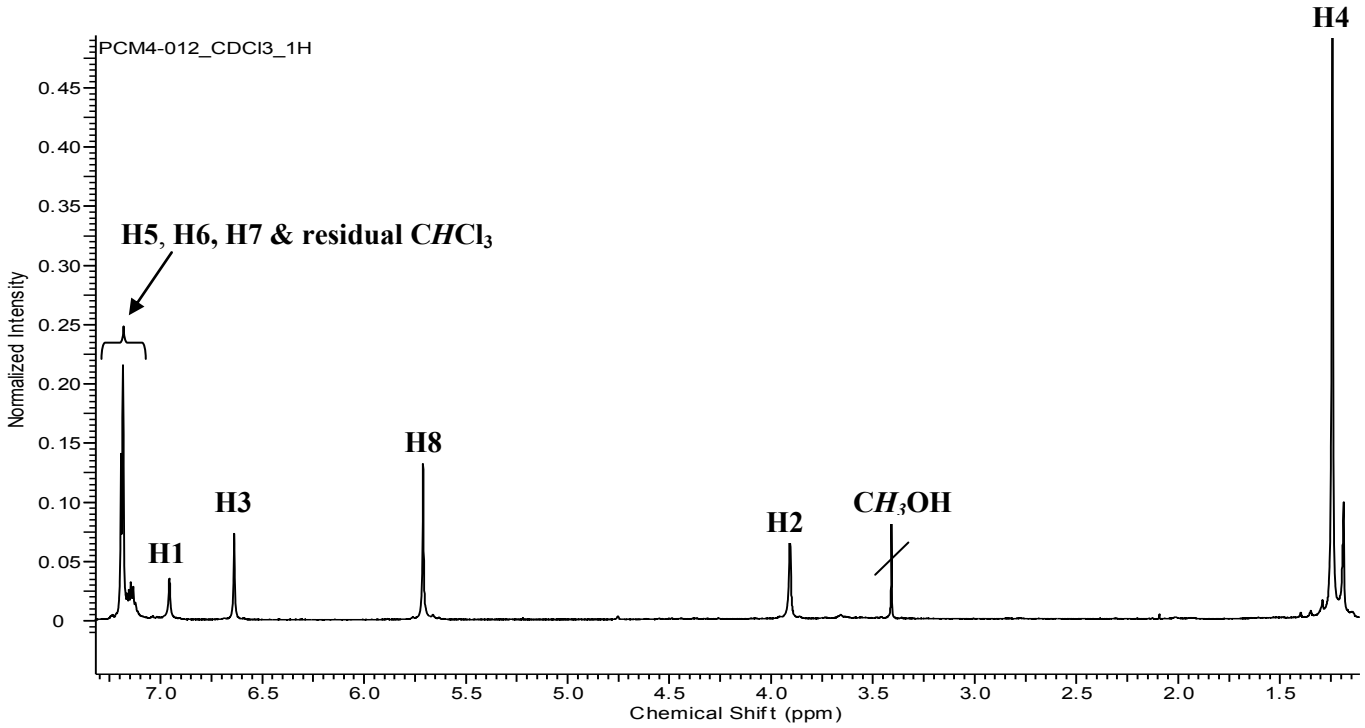

Figure 3.5 ^{1}H NMR spectrum of **PCM1-012** at 400 MHz in $CDCl_3$.

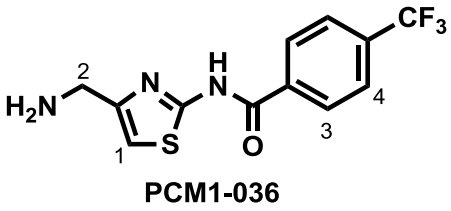

PCM1-036

δ/ppm	Multiplicity	J/Hz	H
8.17	d	8.2	H3
7.87	d	8.1	H4
7.18	s	-	H1
4.12	s	-	H2

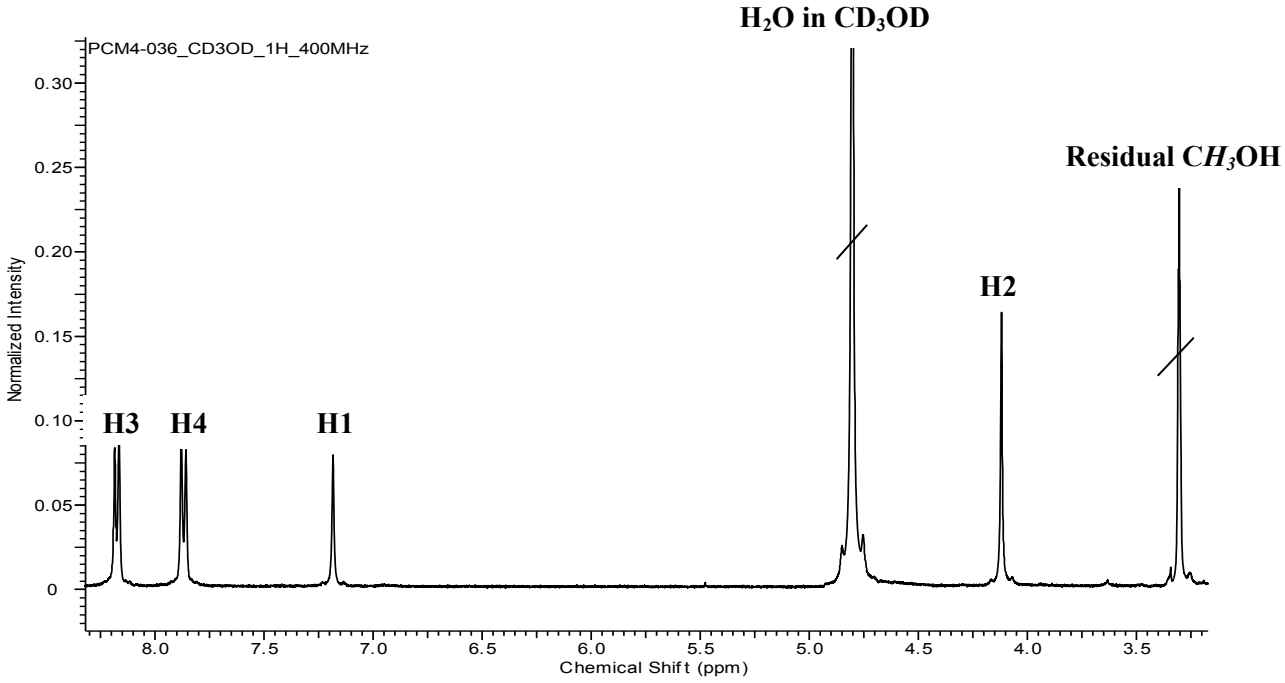

Figure 3.6 ^{1}H NMR spectrum of **PCM1-036** at 400 MHz in CD_3OD.

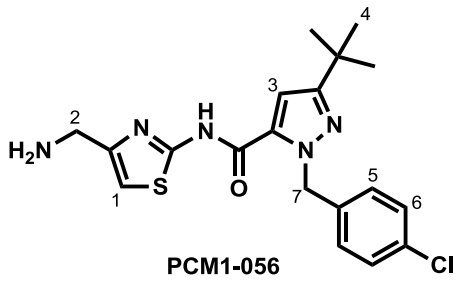

δ/ppm	Multiplicity	J/Hz	H
7.22	d	8.7	H6
7.20	s	-	H1
7.14	d	8.6	H5
6.50	s	-	H3
6.09	s	-	H7
4.06	s	-	H2
1.32	s	-	H4

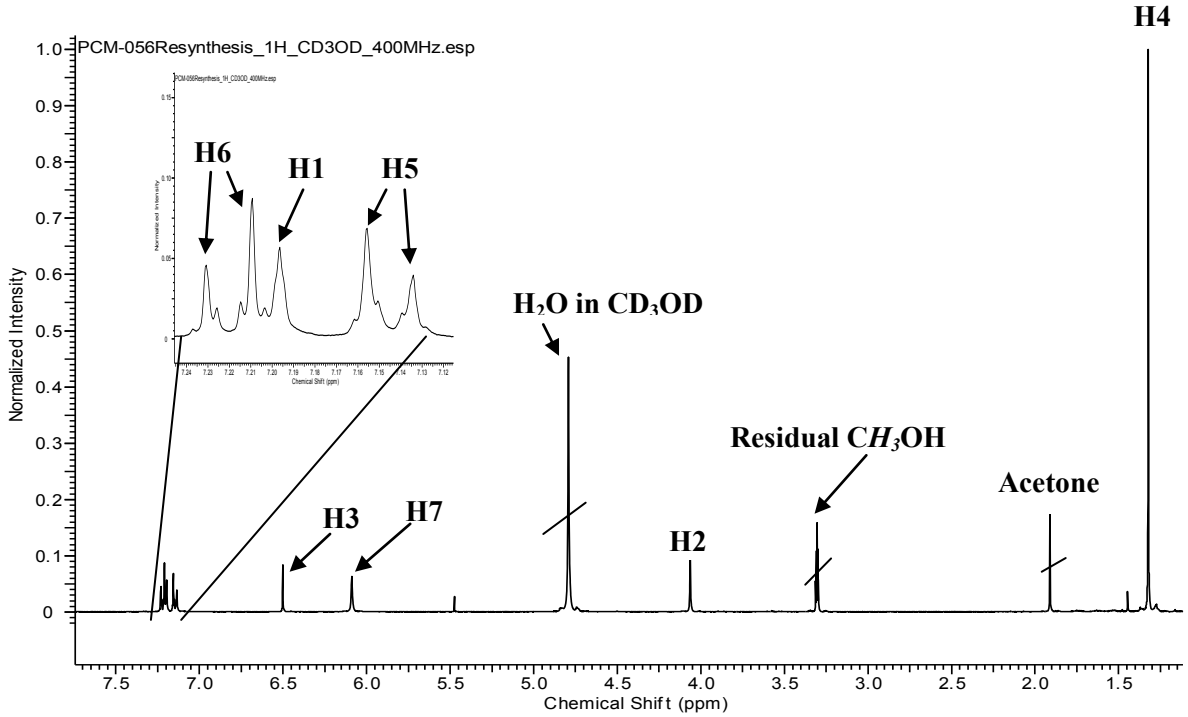

Figure 3.7 ^{1}H NMR spectrum of **PCM1-056** at 400 MHz in CD_3OD

IR analysis of all target compounds revealed common characteristic IR bands at around 1700 cm^{-1} and 3400 cm^{-1} corresponding to the carbonyl (C=O), and primary amine (N-H) stretches respectively. A relatively strong absorption band corresponding to a C-H stretch of the aminomethyl methylene (CH_2) group was as well observed at around 2900 cm^{-1} for all the analogues. Analogue **PCM1-034** (Table 2) notably showed a distinct and sharp absorption band at 2228.44 cm^{-1} corresponding to the cyano (CN) stretch. Other notable functionalities like the aromatics also displayed absorption bands at approximately 1550 cm^{-1} and 3100 cm^{-1} which correspond to aromatic C=C and Ar-H stretches respectively. Mass spectrometry (EI-MS) analysis was used to confirm the molecular weights of the target compounds. HPLC was used to

check the purity of the target compounds. This was to ensure the target compounds had acceptable purity (≥ 95%) for biological evaluation.

3.6 References

1. Cabrera Gonzalez, D.; Douelle, F.; Feng, T.J.; Nchinda, A.T.; Younis, Y.; White, K.L.; Wu, Q.; Ryan, E.; Burrows, J.N.; Waterson, D.; Witty, M.J.; Wittlin, S.; Charman, S.A.; Chibale, K. *J. Med. Chem.* **2011***, 54,* 7713-7719.
2. Rebek, J.; Feitler, D. *J. Am. Chem. Soc.* **1973**, *95*, 4052–4053.
3. Smith, M.B.; March, J. In March's Advanced Organic Chemistry, Reactions, Mechanisms, And Structure, 5th ed.; Wiley-Interscience: New York, **2001**.
4. Schuessler, H.; Zahn, H. *Chem. Ber.* **1962**, *95*, 1076–1080.
5. Rebek, J.; Feitler, D. *J. Am. Chem. Soc.* **1974**, *96*, 1606–1607.
6. Montalbetti, C.A.G.N.; Falque, V. *Tetrahedron*. **2005**, *61*, 10827–10852.
7. Caddick, S.; Judd, D.B.; Lewis, A.K.de K.; Reicha, M.T.; Williams, M.R.V. *Tetrahedron*. **2003**, *59*, 5417–5423.
8. Osby, J.O.; Heinzman, S.W.; Ganem, B. *J. Am. Chem. Soc.* **1986**, *108,* 67-72.
9. Schlesinger, H.I.; Brown, H.C.; Finholt, E.; Gilbreath, J.R.; Hoekstra, H.R.; Hyde, E.K. *J. Am. Chem. Soc.* **1953**, *75*, 215-219.
10. Schlesinger, H.I.; Brown, H.C. *USP.* **1949**, 2461661.
11. http://www.umich.edu/~chemh215/W09HTML/SSG2/ssg5/boc.html (Accessed on September 06, 2013).
12. http://www.commonorganicchemistry.com/Rxn_Pages/Boc_Protection/Boc_Protection_TFA_Mech.htm (Accessed on September 06, 2013).
13. Hantzsch, A. *Ann. Chem*. **1889**, *250*, 257-273.
14. http://www.chemtube3d.com/HetThiazole_formation.html (Accessed on September 09, 2013).
15. http://www.chem.ox.ac.uk/vrchemistry/NOR/flashequation.asp?id=18 (Accessed on September 09, 2013).
16. http://orgchem.chem.uconn.edu/2443s2012/2443-041612.pdf (Accessed on September 11, 2013).
17. Staudinger, H.; Meyer, J. *Helv. Chim. Acta.* **1919**, *2*, 635–646.
18. http://www.name-reaction.com/staudinger-reaction (Accessed on September 12, 2013).

19a. http://www.mhhe.com/physsci/chemistry/carey/student/olc/ch22alkylationammonia.html (Accessed on September 26, 2013).

19b. http://www.commonorganicchemistry.com/Rxn_Pages/Boc_Protection/Boc_Protection/Boc2O_Base_Mech.htm (Accessed on November 17, 2013).

20. Andrés, M.; Bravo, M.; Buil, M.A.; Calbet, M.; Castro, J.; Domènech, T.; Eichhorn, P.; Ferrer, M.; Gómez, E.; Lehner, M.D.; Moreno, I.; Roberts, R.S.; Sevilla, S. *Bioorg. Med. Chem. Lett*. **2013**, *23*, 3349-3353.
21. http://web.mnstate.edu/jasperse/Chem360/Handouts/Ch%2019%20Reactions%20(p%201-6).pdf (Accessed on November 18, 2013).

CHAPTER 4

PHARMACOLOGICAL EVALUATION, SOLUBILITY, AND DISCUSSION

4.1 Chapter Overview

The pharmacological evaluation and aqueous solubility results of the synthesised target compounds are covered in this chapter. A number of analogues of the lead compound **MMV010539** were synthesised. Some analogues resulted from the changes made on the periphery of the lead molecule such us the introduction of substituents on the aromatic portion of the benzyl group and replacement of the *tert*-butyl group with other groups. The SAR, with respect to *in vitro* antiplasmodial activity, resulting from such peripheral modifications is discussed. Further drastic modifications to the skeleton of the aforementioned lead molecule were made. Such modifications included completely replacing the bulky benzyl pyrazole motif with smaller aromatic and heteroaromatic groups. Such a simplification resulted in another set of analogues whose SAR data is also discussed. In addition, the chapter discusses the SAR of the two analogues derived from replacements of the thiazole core. A more subtle change – eliminating the benzylic CH_2 in the lead molecule, was made. The importance of such a linker with respect to *in vitro* antiplasmodial activity is also discussed in this chapter. As pointed out earlier in section 2.5 of this dissertation, the aqueous solubility of a drug is of paramount importance as poor solubility negatively impacts many other properties of the drug such as bioavailability, efficacy, and PK profiles.[1] This chapter therefore further endeavours to discuss the solubility results of the analogues. The *in vitro* antiplasmodial activity for each compound is expressed as an IC_{50} value which represents a concentration of the test compound which produces a 50% inhibition of the parasite growth.[2] It is extremely important for drugs to exert their therapeutic action at a low concentration to minimise undesirable side effects.[3] Therefore, a low IC_{50} value for each analogue was of paramount importance in this project. Unless otherwise stated, all the IC_{50} values are averages of experiments done in triplicate and are presented and discussed in μM although corresponding values in μg/mL are also given in brackets in the tables. The drug-sensitive strain of *P. falciparum*, NF54, was employed in all the assays to test the compounds for activity. The full details for the biological assays used are presented in the experimental section.

Solubility determination was performed using the turbidimetric (kinetic) method.[4] Solubility values are classified as follows: < 20 μM = poorly soluble, 20 – 80 μM = moderately soluble, 80 - 200 μM = good solubility, > 200 μM = highly soluble.

4.2 *In Vitro* Antiplasmodial Activity and Solubility of Aminomethylheteroaryl Pyrazole Carboxamides (PCM1-012, PCM1-006 and MMV010539)

The lead compound **MMV010539** and analogue **PCM1-006** were evaluated for *in vitro* antiplasmodial activity in the same assay while a different assay was used for analogue **PCM1-012** albeit the same method was employed. The *in vitro* antiplasmodial evaluation for these compounds and all the others in this MSc dissertation was undertaken at University of Cape Town Division of Pharmacology in Professor Peter Smith's laboratory. The lead compound **MMV010539** was synthesised and tested for comparison purposes. Chloroquine diphosphate and artesunate were used as reference drugs. Aqueous solubility profiling of the compounds was performed at pH 7.4 to mimic physiological pH,[5] using the turbidimetric assay in which hydrocortisone and reserpine served as controls. The *in vitro* antiplasmodial activity and solubility results are tabulated below (Table 4).

Table 4. *In vitro* antiplasmodial activity and aqueous solubility for **PCM1-006**, **PCM1-012** and **MMV010539**

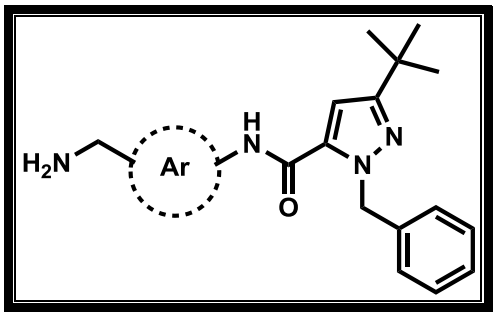

Ar	Code	IC_{50} µM (µg/mL), NF54	Solubility µM, pH 7.4
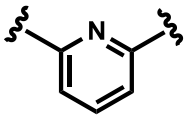	**PCM1-006**	0.125 (0.0453)	40
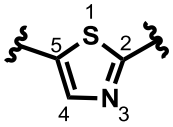	**PCM1-012**	9.09 (0.336)[a]	80
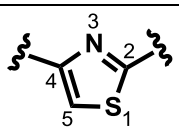	**MMV010539**	0.0203 (0.0075)	> 200
_	**Chloroquine**	0.014 (0.0072)*	_
_	**Artesunate**	0.0109 (0.0042)*	_

*Mean from n = 4 experiments

[a]Tested in the same assay as analogues of table 5

The lead compound **MMV010539** exhibited comparable activity (IC_{50} = 0.0203 μM) to chloroquine (IC_{50} = 0.014 μM) but was relatively less active than artesunate (IC_{50} = 0.0109 μM). Neither of the two analogues, **PCM1-006** and **PCM1-012**, possessed potency comparable or superior to that of the lead compound. Although replacement of the thiazole nucleus with the two heterocycles reduced the activity, analogue **PCM1-006** was the most active of all the analogues investigated in this project. **PCM1-006** retained sub-μM activity (IC_{50} = 0.125 μM) and this result points to the fact that changes on this portion of the molecule may be the most favourable. Noteworthy is the activity of **PCM1-012** (IC_{50} = 9.09 μM) which is significantly lower than that of the lead compound **MMV010539** (IC_{50} = 0.0203 μM). A relatively subtle change – interchanging the positions of nitrogen and sulfur atoms on the thiazole nucleus, dramatically reduces the activity. This change is also equivalent to changing the position of the aminomethyl group from 4 to 5.

The lead compound **MMV010539** also possessed higher solubility (> 200 μM) than its counterparts **PCM1-006** (40 μM) and **PCM1-012** (80 μM). The relatively low solubility of **PCM1-006** compared to **MMV010539** and **PCM1-012** is expected since its pyridyl core makes it more lipophilic and hence less soluble in the aqueous medium at physiological pH. **MMV010539** and **PCM1-012**, however, have a more polar thiazole core with twice the number of hydrogen bond acceptors (nitrogen and sulfur atoms) as **PCM1-006** (nitrogen atom only). The relatively low solubility of analogue **PCM1-12** (80 μM) compared to **MMV010539** (> 200 μM) could be due to disruption of the intermolecular interactions that favour maximum solubility in the aqueous medium as the nitrogen and sulphur atoms are interchanged.

4.3 *In Vitro* Antiplasmodial Activity and Solubility of Aminomethylthiazole Carboxamides and Aminomethylthiazole Benzamides (PCM1-031 - PCM1-051)

Analogues **PCM1-031 - PCM1-051** were tested as a single batch with analogue **PCM1-012** of table 4 in the same assay. This series (**PCM1-031 - PCM1-051**) of analogues was generated by replacement of the benzyl pyrazole moiety of the lead molecule **MMV010539** with other simpler aromatic and heteroaromatic groups. The *in vitro* antiplasmodial activity of the lead compound is included for comparison purposes. The *in vitro* antiplasmodial activities and aqueous solubility data are summarised in table 5.

Table 5. *In vitro* antiplasmodial activity and aqueous solubility for analogues **PCM1-031 - PCM1-051**, and **MMV010539**

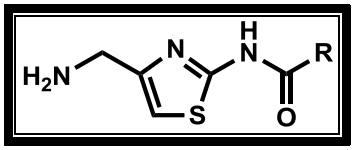

R	Code	IC_{50} µM (µg/ml), NF54	Solubility µM, pH 7.4
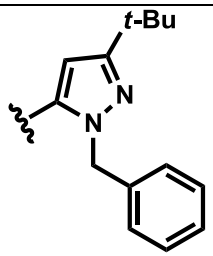	**MMV010539**	0.0203 (0.0075)[a]	> 200
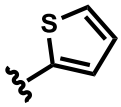	**PCM1-031**	91.7 (22.0)	80
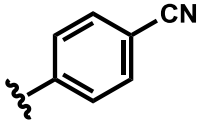	**PCM1-034**	146 (37.7)	20
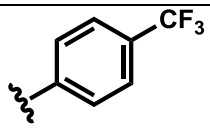	**PCM1-036**	40.2 (12.1)	40
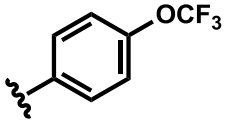	**PCM1-040**	43.9 (13.9)	40
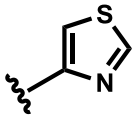	**PCM1-041**	149 (35.7)	80
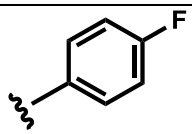	**PCM1-046**	123 (30.9)	80
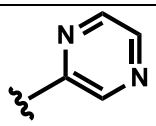	**PCM1-051**	173 (40.7)	> 200
–	**Chloroquine**	0.0119 (0.00613)	–
–	**Artesunate**	0.00663 (0.00255)*	–

*Mean from n = 2 experiments

[a]Tested in the same assay as analogue **PCM1-006** of table 4

From the antiplasmodial activities of all the analogues of this series (**PCM1-031 - PCM1-051**), we can generally conclude that drastic modifications to the skeleton of the lead molecule

MMV010539 appears detrimental to potent activity. Activity was on average most negatively affected in this series compared to other series of analogues resulting from other modifications made around the lead compound. Cabrera Gonzalez *et al.*[6], have reported significant reduction in *in vitro* antiplasmodial activity with the replacement of the benzyl pyrazole motif with other aromatic and heteroaromatic substituents. *In vitro* antiplasmodial activity results for this series of compounds **PCM1-031 - PCM1-051** is, therefore, not surprising at all. From these findings, it is clear that the benzyl pyrazole motif is the most critical portion of the lead molecule.

With the exception of **PCM1-051**, all the analogues in this series had moderate to good aqueous solubilities (20 - 80 μM), but much lower than that of the lead compound **MMV010539** (> 200 μM). The good solubility of analogue **PCM1-051** could be due to the two hydrogen bond acceptors (two nitrogen atoms) present in its pyrazinyl moiety. These nitrogen centres could be facilitating hydrogen bonding interactions with water in the aqueous medium of the assay and hence enhancing its solubility.

4.4 *In Vitro* Antiplasmodial Activity and Solubility of Aminomethylthiazole Pyrazole Carboxamides (PCM1-056 - PCM1-073 and PCM1-085)

This series of compounds resulted from much more subtle modifications made to the lead compound **MMV010539**, which included introducing substituents on the aromatic portion of the benzyl group as well as replacing the benzyl group with a phenyl ring. All the resulting analogues including the lead molecule were evaluated in the same assay and their IC_{50} and solubility values are presented in table 6. The solubility of the lead compound **MMV010539** was only determined once from the previous experiments and is only listed here for comparison purposes.

Table 6. *In vitro* antiplasmodial activity and aqueous solubility for analogues **PCM1-056 - PCM1-073**, **PCM1-085** and **MMV010539**

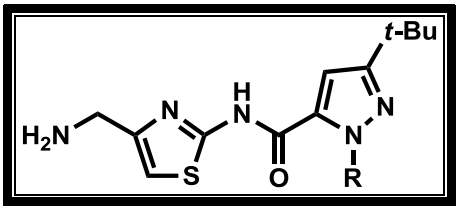

R	Code	IC_{50} μM (μg/ml), NF54	Solubility μM, pH 7.4

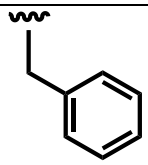	**MMV010539**	0.0218 (0.00804)	> 200
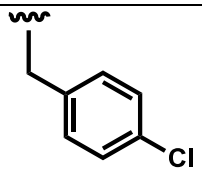	**PCM1-056**	12.1 (4.88)	> 200
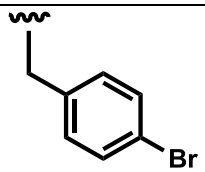	**PCM1-059**	12.8 (5.76)	80
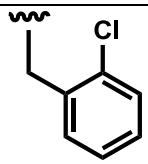	**PCM1-066**	1.84 (0.743)	> 200
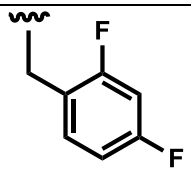	**PCM1-069**	4.70 (1.90)	ND*
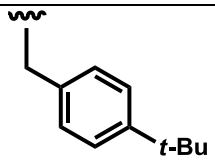	**PCM1-073**	2.58 (1.10)	10
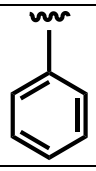	**PCM1-085**	67.5 (24.0)	160
–	**Chloroquine**	0.0106 (0.00548)	–
–	**Artesunate**	0.00520 (< 0.002)	–

*ND = Not determined

A few conclusions can be drawn from the *in vitro* antiplasmodial data obtained for this limited series (**PCM1-056 - PCM1-073** and **PCM1-085**) of analogues. It is clear that generally, the modifications resulting in the analogues of this series appear tolerable compared to replacements of the benzyl pyrazole motif. Although the introduction of substituents on the aromatic portion of the benzyl group (analogues **PCM1-056 - PCM1-073**), generally reduced the activity (IC_{50} = 1.84 – 12.8 μM), it does not however, dramatically reduce it compared to activities of analogues resulting from benzyl pyrazole replacements. The lead compound **MMV010539** still retained superior activity (IC_{50} = 0.0218 μM) relative to all the analogues. Interestingly, analogue **PCM1-**

066 with the chloro substituent in the *ortho* position of the benzyl ring, had approximately 7 fold higher activity (IC_{50} = 1.84 μM) than its *para* regioisomer **PCM1-056** (IC_{50} = 12.1 μM). It is also noteworthy that, of all the benzyl substituted analogues, **PCM1-066** had the highest activity, which suggests that substitutions at this position may be much more favourable. Another interesting result is the poor activity of analogue **PCM1-085** (IC_{50} = 67.5 μM) in which the benzyl group was replaced by a phenyl ring which suggests that the benzyl methylene linker is important for activity.

All the analogues, save for **PCM1-073**, generally exhibited good to high aqueous solubility (80 - > 200 μM) – a result which was generally expected due to the fact that this series of analogues resulted from minor peripheral changes to the lead molecule. The poor solubility observed for analogue **PCM1-073** (10 μM) is not surprising at all since this compound contains the highly lipophilic *tert*-butyl substituent on the benzyl ring.

4.5 *In Vitro* Antiplasmodial Activity and Solubility of Aminomethylthiazole Pyrazole Carboxamides (PCM1-083, PCM1-087 and PCM1-089)

The three carboxamides **PCM1-083, PCM1-087 and PCM1-089** had methyl, *para*-tolyl, and hydrogen substituents respectively in place of the *tert*-butyl group on the pyrazole heterocycle (Table 7). This was an attempt to identify other favourable groups besides the *tert*-butyl on this position of the pyrazole. The IC_{50} value of the lead compound **MMV010539** and those of the control drugs, chloroquine and artesunate, are listed in table 7 for comparison purposes.

Table 7. *In vitro* antiplasmodial activity and aqueous solubility for analogues **PCM1-083**, **PCM1-087**, **PCM1-089**, and **MMV010539**

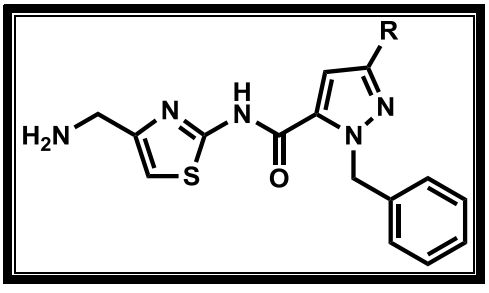

R	Code	IC_{50} μM (μg/ml), NF54	Solubility μM, pH 7.4
	**MMV010539**	0.0218 (0.00804)	> 200

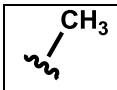	**PCM1-083**	19.8 (6.47)	160
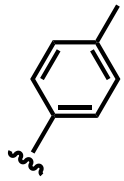	**PCM1-087**	2.03 (0.818)	40
	**PCM1-089**	43.7 (13.7)	> 200
–	**Chloroquine**	0.0106 (0.00548)	–
–	**Artesunate**	0.00520 (< 0.002)	–

A decrease in activity with decrease in size of the substituent was observed for this small series of analogues (Figure 4.1).

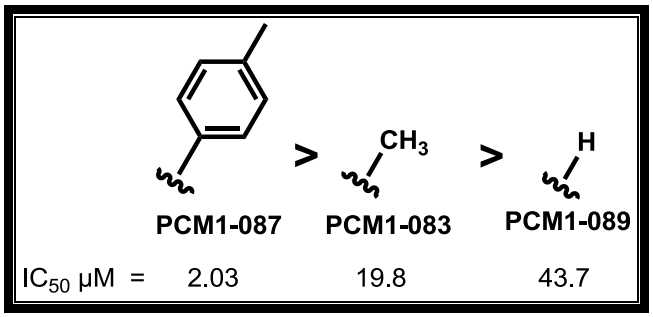

Figure 4.1 Decrease in activity with size of substituent

It appears, therefore, that although the activity is reduced as the *tert*-butyl is replaced with the groups in figure 4.1, bulky groups are much more tolerated.

The trend in the aqueous solubility of the three analogues was expected with analogue **PCM1-087** having the lowest solubility (40 µM), probably due to the bulky and lipophilic *para*-tolyl group on its pyrazole carboxylic acid residue. Analogue **PCM1-089** possessed the highest solubility (> 200 µM) probably due to its relatively less lipophilic nature (absence of an alkyl group on pyrazole motif) compared to the lead compound **MMV010539** as well as the other two analogues **PCM1-083** and **PCM1-087**. The relatively poor solubility of analogues **PCM1-087** and **PCM1-083** compared to **MMV010539** could also be explained from another perspective. Being a bulky group and extending above and below the planar aromatic system of the lead compound **MMV010539**, it (*tert*-butyl group) disrupts potential pi-pi stacking making the lead compound highly soluble. On the other hand, introduction of more confined groups like the

para-tolyl and methyl groups on analogues **PCM1-087** and **PCM1-083** respectively enhance pi-pi stacking which results in relatively poor solubility of these two analogues. However, this line of thought fails to explain the excellent solubility of analogue **PCM1-089** which on account of maximum pi-pi stacking expected, should be the least soluble.

4.6 Conclusion

Based on the preliminary SAR exploration executed around **MMV010539** by Cabrera Gonzalez *et al.*[5], we have successfully further broadened the SAR study around this lead compound. With respect to *in vitro* antiplasmodial activity, all the modifications made thus far resulted in reduced activity. For the majority of peripheral modifications on the skeleton of the lead compound such as the introduction of substituents on the benzyl ring as well as replacement of the *tert*-butyl group with other groups, activity was reduced but not significantly. This phenomenon is reflected in analogues **PCM1-056**, **PCM1-059**, **PCM1-066**, **PCM1-069**, **PCM1-073** (Table 6) and **PCM1-087** (Table 7) which retained some potency (IC_{50} = 1.84 – 12.8 μM). The benzylic CH_2 linker was found to be critically important for potent activity as is reflected in the poor activity (IC_{50} = 67.5 μM) of analogue **PCM1-085** (Table 6) in which it is absent. For analogues **PCM1-083**, **PCM1-087**, and **PCM1-089**, a positive correlation between the size of the substituent and *in vitro* antiplasmodial activity was observed as pointed out in figure 4.1. Replacement of the thiazole core was another portion of SAR that was explored in this MSc study. Although SAR investigation into this portion of the molecule was not extensive, it gave rise to the most potent analogue **PCM1-006** (Table 4) of all the analogues synthesised in this study. This pyridyl analogue retained sub-μM activity (IC_{50} = 0.125 μM) and, therefore, this result warrants further extensive SAR investigation into this portion of the molecule. The other analogue resulting from this portion of SAR **PCM1-012** (IC_{50} = 9.09 μM) uncovered the importance of the position of the aminomethyl group on the thiazole ring. As the aminomethyl moiety was shifted from position 4 to 5, activity was reduced approximately 400 fold though not completely eliminated. Apart from such thiazole replacements, other more drastic modifications to the skeleton of the lead compound **MMV010539** were made, which included replacing the bulky benzyl pyrazole moiety with other smaller and simpler aromatic/heteroaromatic groups (**PCM1-031** – **PCM1-051**) (Table 5). With such drastic modifications, activity was compromised the most and was significantly reduced in the majority of the resulting analogues (IC_{50} = 40.2 - 173 μM). The benzyl pyrazole motif, therefore, seems critical for activity and as

such, drastic modifications on this portion of the molecule should perhaps be avoided in future SAR explorations.

All the synthesised compounds were obtained in poor to good yields (13 – 84%). The poor yields of some analogues could be attributed to the difficulty associated with their isolation. For instance, chromatographic separation was particularly challenging for some complex crude mixtures.

4.7 Recommendations for Future Work

Further work recommended based on results obtained in this study is summarised in Figure 4.2. In light of retention of sub-μM activity (IC_{50} = 0.125 μM) of the pyridyl analogue **PCM1-006** (Table 4), there is need to generate more analogues with other aromatic heterocycles for more extensive investigation into SAR 1. We further found out that analogues resulting from replacement of the benzyl pyrazole motif on average had the poorest activity (IC_{50} = 40.2 - 173 μM) (Table 5). Future SAR 3 refinements on this portion of the lead compound, should, perhaps, focus on making more subtle modifications rather than drastic replacements of the benzyl pyrazole moiety. The poor activity (IC_{50} = 67.5 μM) of analogue **PCM1-085** (Table 6) highlighted the importance of the benzyl methylene (CH_2) linker. However, further SAR 5 investigations with respect to variations in the length of this linker (i.e. replacement with $(CH_2)_n$, n > 1) is necessary. Such a drug extension strategy would reveal which linker length is associated with optimal pharmacological activity and/or physicochemical parameters. Furthermore, additional analogues with other alkyl substituents (propyl, isopropyl, cyclopropyl cyclohexyl and others) replacing the *tert*-butyl group (SAR 4), need investigation. Finally, there is need to further replace the benzyl ring of the benzyl group with other five and six membered aromatic heterocycles (SAR 2) to potentially identify other groups which can be tolerated.

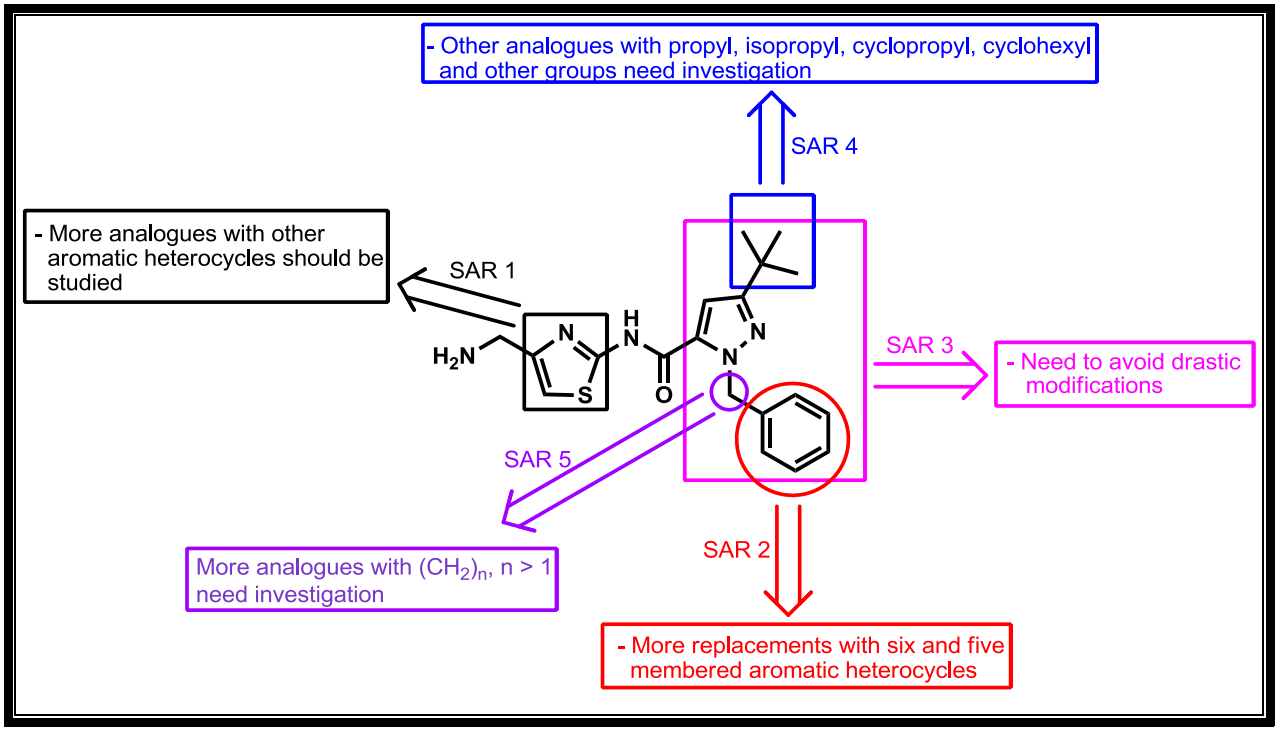

Figure 4.2 Recommendations for future work

4.8 References

1. Kerns, E.H.; Di, L. **2008**, Drug-like properties: Concepts, structure design and methods. Burlington, MA: Academic Press.
2. http://www.fda.gov/ohrms/dockets/ac/00/slides/3621s1d/sld036.htm (Accessed on November 02, 2013).
3. https://www.worstpills.org/public/page.cfm?op_id=48 (Accessed on November 02, 2013).
4. Lipinski, C.A.; Lombardo, F.; Dominy, B.W.; Feeney, P.J. *Adv.Drug Deliv.Rev*. **2001**, *46*, 1–3, 3-26.
5. http://www.nlm.nih.gov/medlineplus/ency/article/003855.htm (Accessed on November 02, 2013).
6. Cabrera Gonzalez, D.; Douelle, F.; Feng, T.J.; Nchinda, A.T.; Younis, Y.; White, K.L.; Wu, Q.; Ryan, E.; Burrows, J.N.; Waterson, D.; Witty, M.J.; Wittlin, S.; Charman, S.A.; Chibale, K. *J. Med. Chem.* **2011***, 54,* 7713-7719.

CHAPTER 5

EXPERIMENTAL

5.1 General Comments on Experimental Data

Solvents used for the majority of experiments were generally distilled and analytical reagent (AR) grade in some cases, with the exception of methanol (CH_3OH) and absolute ethanol (CH_3CH_2OH) which were exclusively AR grade. Dimethyl sulfoxide (DMSO) used in solubility assays was HPLC grade while *N,N*-dimethylformamide (DMF) used in reactions was anhydrous and AR grade. Unless otherwise stated, all the other reagents and starting materials were obtained commercially and used without further purification. Analytical thin layer chromatographic plates (Merck TLC Silica gel 60 F_{254} coated on aluminium sheets) were used to monitor reaction progress and visualised under ultraviolet (UV 254 and 366 nm) light and in cases of final amine compounds, with ninhydrin (2,2-dihydroxyindane-1,3-dione) spray. In column chromatographic separations, both on the Biotage isolera one automated flush machine, and manual glass tube columns, silica gel (*Fluka* high purity grade, pore size 60 Å, 70 – 230 mesh, 63 – 200 μm) was used.

^{1}H NMR and ^{13}C NMR experiments were performed on either a Bruker AV 400 (^{1}H 400.0, ^{13}C 100.6 MHz) or Varian Mercury 300 (^{1}H 300.1, ^{13}C 75.5 MHz) instrument housed in the Department of Chemistry University of Cape Town. All the spectra were acquired at room temperature. Deuterated solvents ($CDCl_3$, CD_3OD, and [D_6]DMSO) were used as solvents both for ^{1}H NMR and ^{13}C NMR experiments. Chemical shifts are reported from low field to high field in parts per million (ppm). Multiplicity in all the spectra is expressed using the following abbreviations: br s = broad singlet, d = doublet, t = triplet, q = quartet, m = multiplet. Coupling constants, *J* values, are given in Hz. Mass spectra were recorded on a JEOL GCmateII mass spectrometer under direct probe conditions and electron impact (EI) ionisation in the positive ionisation mode. Infrared (IR) absorption measurements were carried out on the PerkinElmer Spectrum 100 FT-IR Spectrometer in the wave number range 450 – 4000 cm^{-1}. All the samples were mixed and homogenised with potassium bromide (KBr) and analysed as circular pellets.

Melting point measurements were done on a Reichert-Jung Thermovar hot stage microscope and are not corrected. Purity of the compounds was determined using HPLC and all the compounds were found to have acceptable purity (> 95%).

Compounds **PCM1-069** and **PCM1-089** (Sub-section 5.24 of experimental section) are lacking ^{13}C NMR and IR data respectively due to insufficient material to undertake such analyses.

5.2 General procedure for the synthesis of cyanoheteroaryl pyrazole carboxamides (PCM1-004 and PCM1-009)

EDCI (2.0 eq) was added to a solution of 1-benzyl-3-(*tert*-butyl)-1*H*-pyrazole-5-carboxylic acid (1.0 eq) and DMAP (2.0 eq) in dichloromethane. The reaction mixture was stirred for 10 - 15 minutes, after which the appropriate amino cyano analogue (1.2 eq) was added. The resulting reaction mixture was stirred for 4 - 20 h before being washed with saturated aqueous solutions of $NaHCO_3$ (3 ×), NH_4Cl (2 ×), and NaCl (2 ×). The organic layer was dried ($MgSO_4$), filtered and concentrated *in vacuo*. The crude mixture was chromatographed (SiO_2, EtOAc-hexane, 10:90) to give the desired nitrile compound.

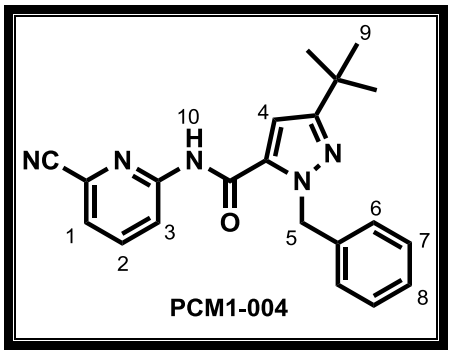

1-Benzyl-3-*tert*-butyl-*N*-(6-cyanopyridin-2-yl)-1*H*-pyrazole-5-carboxamide (PCM1-004)

White solid (0.4700 g, 67%), δ_H (400 MHz; $CDCl_3$) 8.83 (1H, br s, H_{10}), 8.40 (1H, d, J = 8.3 Hz, H_3), 7.93 (1H, t, J = 7.9 Hz, H_2), 7.33 (1H, d, J = 7.9 Hz, H_1), 7.28-7.03 (5H, m, H_6, H_7, H_8), 6.55 (1H, s, H_4), 5.62 (2H, s, H_5), 1.27 (9H, s, H_9).

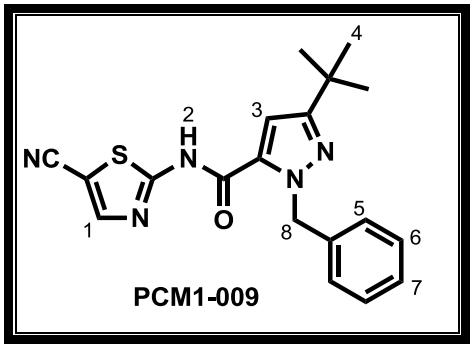

1-Benzyl-3-*tert*-butyl-*N*-(5-cyanothiazol-2-yl)-1*H*-pyrazole-5-carboxamide (PCM1-009)

White solid (0.4018 g, 71%), δ_H (400 MHz; $CDCl_3$) 10.27 (1H, br s, H_2), 7.88 (1H, s, H_1), 7.35-7.20 (5H, m, H_5, H_6, H_7), 6.66 (1H, s, H_3), 5.78 (2H, s, H_8), 1.34 (9H, s, H_4).

5.3 General procedure for the synthesis of benzyl pyrazole methylcarbamates (PCM1-005 and PCM1-011)

Boc_2O (2.0 eq) and $NiCl_2$ (1.0 eq) were added to a solution of the nitrile compound (**PCM1-004** or **PCM1-009**) (1.0 eq) in methanol and the mixture was cooled to 0 ^oC. $NaBH_4$ (12.0 eq) was added in small portions over approximately 1 h, where after the reaction mixture was warmed to room temperature and stirred for 3 - 12 h. Ethylenediamine (20.0 eq) was added and reaction mixture stirred for 30 min before the solvent was removed *in vacuo*. The resulting pink residue was taken up in EtOAc and washed with saturated aqueous solution of $NaHCO_3$ (3 ×). The organic layer was dried ($MgSO_4$), filtered, concentrated *in vacuo* and the crude product purified by column chromatography (SiO_2, 10 – 15% EtOAc/Hexane) to give the *N*-Boc protected intermediates **PCM1-005** and **PCM1-011**.

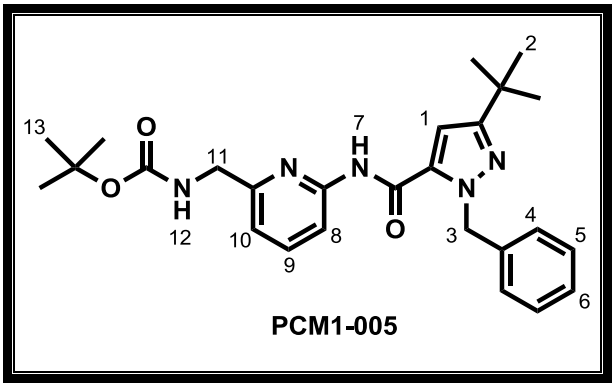

***tert*-Butyl (6-(1-benzyl-3-*tert*-butyl-1*H*-pyrazole-5-carboxamido)pyridin-2-yl)methylcarbamate (PCM1-005)**

White solid (0.1200 g, 45%), δ_H (400 MHz; $CDCl_3$) 8.18 (1H, br s, H_7), 8.04 (1H, d, J = 8.2, H_8), 7.61 (1H, t, J = 7.9, H_9), 7.26-7.11 (5H, m, H_4, H_5, H_6), 6.94 (1H, d, J = 7.4, H_{10}), 6.57 (1H, s, H_1), 5.70 (2H, s, H_3,), 4.43 (1H, br s, H_{12}), 4.27 (2H, s, H_{11}), 1.40 (9H, s, H_{13}), 1.29 (9H, s, H_2).

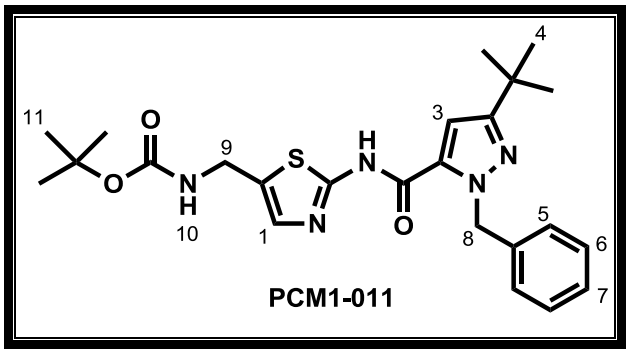

***tert*-Butyl (2-(1-benzyl-3-*tert*-butyl-1*H*-pyrazole-5-carboxamido)thiazol-5-yl)methylcarbamate (PCM1-011)**

White solid (0.0183 g, 28%), δ_H (400 MHz; $CDCl_3$) 7.24-7.10 (5H, m, H_5, H_6, H_7), 7.00 (1H, s, H_1), 6.64 (1H, s, H_3), 5.71 (2H, s, H_8,), 4.76 (1H, br s, H_{10}), 4.31 (2H, s, H_9), 1.38 (9H, s, H_{11},), 1.24 (9H, s, H_4).

5.4 General procedure for the synthesis of aminomethylheteroaryl pyrazole carboxamides (PCM1-006 and PCM1-012)

TFA (10.0 eq) was added to a stirred solution of *N*-Boc protected intermediate (**PCM1-005** or **PCM1-011**) (1.0 eq) in dichloromethane. The reaction mixture was stirred at room temperature for 15 - 24 h and concentrated *in vacuo*. The remaining residue was dissolved in 10% CH_3OH/DCM and Amberlyst A-21 weak base ion exchange resin was added where after mixture

was left to stir. After stirring for 1.5 h, the mixture was filtered and the Amberlyst washed with 50% CH_3OH/DCM. The filtrate was concentrated *in vacuo* and the resulting crude mixture further purified by column chromatography (SiO_2, CH_3OH-DCM, 5:95) to deliver the carboxamides **PCM1-006** and **PCM1-012**.

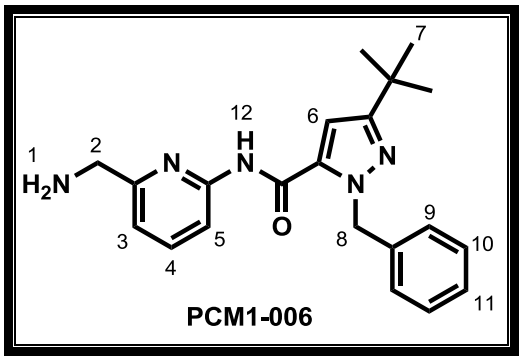

***N*-(6-(Aminomethyl)pyridin-2-yl)-1-benzyl-3-*tert*-butyl-1*H*-pyrazole-5-carboxamide (PCM1-006)**

Brown solid (0.0200 g, 62%), m.p. 137-140 °C; R_f (CH_3OH-CH_2Cl_2 1:9) 0.5; IR ν_{max}(KBr)/cm^{-1} 3323 (N-H, 1° amine), 2959 (C-H, *tert*-butyl CH_3), 1682 (C=O, amide), 1583 (C=C, aromatic); δ_H (400 MHz; $CDCl_3$) 8.25 (1H, br s, H_{12}), 8.03 (1H, d, J = 8.3 Hz, H_5), 7.59 (1H, t, J = 7.9 Hz, H_4), 7.23-7.12 (5H, m, H_9, H_{10}, H_{11}), 6.93 (1H, d, J = 7.9 Hz, H_3), 6.60 (1H, s, H_6), 5.72 (2H, s, H_8), 3.85 (2H, s, H_2), 1.56 (2H, br s, H_1), 1.28 (9H, s, H_7); δ_C ($CDCl_3$) 161.0, 159.1, 151.0, 151.1, 139.9 (2C), 138.0, 134.0, 128.4 (2C), 127.6 (2C), 117.2, 114.8, 105.3, 54.9, 44.5, 32.0, 30.5 (3C) ; EI-*m/z* found 363.1597 (100%, M^+), ($C_{21}H_{25}N_5O$ requires M 363.2059); HPLC purity: 98% (t_r = 13.3 min).

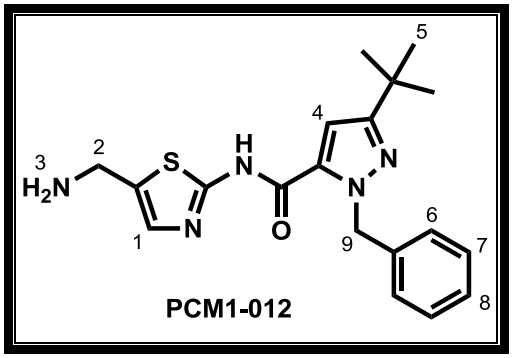

***N*-(5-(Aminomethyl)thiazol-2-yl)-1-benzyl-3-*tert*-butyl-1*H*-pyrazole-5-carboxamide (PCM1-012)**

Brown solid (0.1100 g, 32%), m.p. 83-85 ^{o}C; R_f (CH_3OH-CH_2Cl_2 1.5 : 8.5) 0.5; IR ν_{max}(KBr)/cm^{-1} 3366 (N-H, 1° amine), 2966 (C-H, *tert*-butyl CH_3), 2918 (C-H, aminomethyl CH_2), 1673 (C=O, amide), 1558 (C=C, aromatic); δ_H (400 MHz; $CDCl_3$) 7.22-7.11 (5H, m, H_6, H_7, H_8), 6.96 (1H, s, H_1), 6.64 (1H, s, H_4), 5.71 (2H, s, H_9), 3.91 (2H, s, H_2), 1.24 (9H, s, H_5); δ_C ($CDCl_3$) 161.0, 158.1, 157.5, 137.5, 133.5 (2C), 129.1, 128.4 (2C), 127.5 (2C), 105.5, 54.6, 38.5, 30.4 (3C), 29.9; EI-*m/z* found 368.9970 (56.6%, M^+), ($C_{19}H_{23}N_5OS$ requires M 369.1623); HPLC purity: 99% (t_r = 13.2 min).

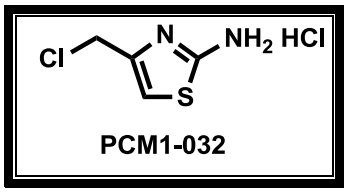

5.5 Synthesis of 4-(chloromethyl)thiazol-2-amine hydrochloride (PCM1-032)

A solution of thiourea (2.59 g, 34.0 mmol) in acetone (80 mL) was added drop wise to a solution of 1, 3-dichloroacetone (4.24 g, 33.4 mmol) in acetone (16 mL). The reaction mixture was stirred at room temperature for 48 h before being concentrated *in vacuo*. Absolute ethanol (32 mL) was added to the resulting residue and left to stir at room temperature for 6 h. The white precipitate that formed was removed by filtration. The filtrate was then concentrated *in vacuo* and the residue was washed with dichloromethane to afford **PCM1-032** as a white hydrochloride salt (2.06 g, 33%), EI-*m/z* found 149.8571(13.4%, M^+), ($C_4H_6ClN_2S$ requires M 148.9935).

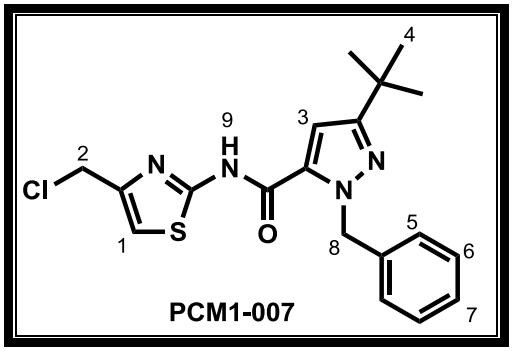

5.6 Synthesis of 1-benzyl-3-*tert*-butyl-*N*-(4-(chloromethyl)thiazol-2-yl)-1*H*-pyrazole-5 carboxamide (PCM1-007)

EDCI (4.66 g, 24.31 mmol) was added to a solution of 1-benzyl-3-(*tert*-butyl)-1*H*-pyrazole-5-carboxylic acid (4.61 g, 17.83 mmol) and hydroxybenzotriazole (HOBt) (3.29 g, 24.31 mmol) in dichloromethane (20 mL). After stirring the reaction mixture for 45 min, a solution of 4-(chloromethyl)thiazol-2-amine hydrochloride (**PCM1-032**) (3.00 g, 16.21 mmol) and *N*,*N*-diisopropylethylamine (DIEA) (5.65 mL, 32.42 mmol) in dichloromethane (4 mL) was added in small portions. The reaction mixture was stirred for 15 h before being washed with saturated aqueous solutions of $NaHCO_3$ (4 × 50 mL), NH_4Cl (2 × 50 mL), and NaCl (2 × 50 mL). The organic layer was dried ($MgSO_4$), filtered, concentrated *in vacuo* and purified by column chromatography (SiO_2, EtOAc-hexane, 10:90) to give the intermediate chloro compound **PCM1-007** (3.15 g, 50%) as a white solid, δ_H (400 MHz; $CDCl_3$) 9.96 (1H, br s, H_9), 7.26-7.13 (5H, m, H_5, H_6, H_7), 6.90 (1H, s, H_1), 6.47 (1H, s, H_3), 5.72 (2H, s, H_8), 4.34 (2H, s, H_2), 1.24 (9H, s, H_4).

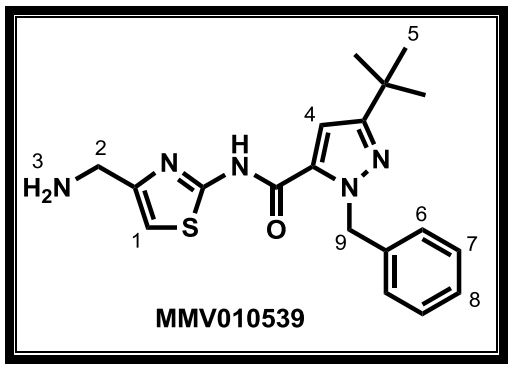

5.7 Synthesis of *N*-(4-(aminomethyl)thiazol-2-yl)-1-benzyl-3-*tert*-butyl-1*H*-pyrazole-5-carboxamide (MMV010539)

NaN_3 (0.33 g, 5.14 mmol) was slowly added to a solution of 1-benzyl-3-*tert*-butyl-*N*-(4-(chloromethyl)thiazol-2-yl)-1*H*-pyrazole-5-carboxamide **PCM1-007** (0.10 g, 0.26 mmol) in DMF (1 mL) and reaction mixture stirred at 80 ^{o}C for 26 h before being concentrated *in vacuo*.

The resulting residue was taken up in dichloromethane and washed with deionised water (10 mL). The organic layer was dried ($MgSO_4$), filtered, concentrated *in vacuo*, and purified by column chromatography (SiO_2, EtOAc-hexane, 30:70) to afford the azide substituted compound **PCM1-008** which was confirmed by EI-MS, EI-*m/z* found 395.0193(52.9%, M^+), ($C_{19}H_{21}N_7OS$ requires M 395.1528). To reduce the azide intermediate to the corresponding amine, water (0.0024 g, 0.13 mmol) and triphenylphosphine (0.05 g, 0.20 mmol) were added to a solution of *N*-(4-(azidomethyl)thiazol-2-yl)-1-benzyl-3-*tert*-butyl-1*H*-pyrazole-5-carboxamide **PCM1-008** (0.05 g, 0.13 mmol) in THF (2 mL). The reaction mixture was stirred for 24 h before being concentrated under reduced pressure. The remaining residue was dissolved in dichloromethane (6 mL), washed with deionised water (5 mL), dried ($MgSO_4$), filtered and concentrated *in vacuo.* Purification by column chromatography (SiO_2, CH_3OH-CH_2Cl_2, 5:95) afforded **MMV010539** (0.0337 g, 68%) as a white solid, δ_H (300 MHz; $CDCl_3$) 7.31-7.17 (5H, m, H_6, H_7, H_8), 6.67 (1H, s, H_1), 6.65 (1H, s, H_4), 5.80 (2H, s, H_9), 3.75 (2H, s, H_2), 1.32 (9H, s, H_5); EI-*m/z* found 369.1398(64.1%, M^+), ($C_{19}H_{23}N_5OS$ requires M 369.1623); HPLC purity: 99.9% (t_r = 13.2 min).

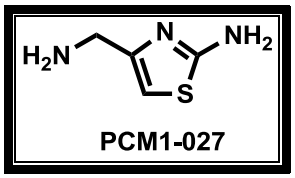

PCM1-027

5.8 Synthesis of 4-(aminomethyl)thiazol-2-amine (PCM1-027)

Ammonia solution in methanol (7*N*) (54 mL, 378 mmol) was added to 4-(chloromethyl)thiazol-2-amine hydrochloride **PCM1-032** (2.06 g, 11.20 mmol) and the reaction mixture stirred in a sealed tube at room temperature. After stirring for 72 h, the reaction mixture was concentrated *in vacuo* to afford intermediate **PCM1-027** as a yellow solid which was used without further purification.

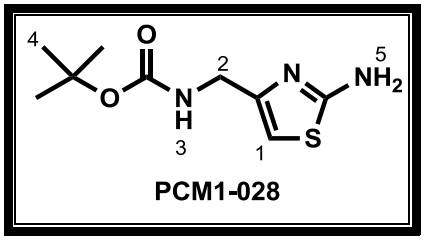

PCM1-028

5.9 Synthesis of *tert*-butyl (2-aminothiazol-4-yl)methylcarbamate (PCM1-028)

Boc_2O (2.13 g, 9.80 mmol) was added in small portions to a suspension of 4-(aminomethyl)thiazol-2-amine **PCM1-027** (1.26 g, 9.80 mmol) and triethylamine (4.0 mL, 29 mmol) in DMF (30 mL) at 0 ^{o}C. The reaction mixture was left to warm to room temperature and stirred for 24 h. Cold deionised water (25 mL) at 0 ^{o}C was added and the mixture extracted with ethyl acetate (4 × 85 mL). The combined organic layers were washed with deionised water (4 × 170 mL), and saturated aqueous NaCl (85 mL), dried ($NaSO_4$), filtered and concentrated *in vacuo*. Purification by column chromatography (SiO_2, 0-60% EtOAc/Hexane) furnished **PCM1-028** (0.72 g, 32%) as a yellowish solid, δ_H (400 MHz; $CDCl_3$) 6.29 (1H, s, H_1), 5.16 (1H, br s, H_3), 4.14 (2H, br s, H_5), 3.73 (2H, s, H_2), 1.43 (9H, s, H_4).

5.10 General procedure for the synthesis of thiazole methylcarbamates (PCM1-081, PCM1-084, PCM1-086 and PCM1-029 - PCM1-049)

The synthesis of the thiazole methylcarbamates **PCM1-081**, **PCM1-084**, **PCM1-086** and **PCM1-029 - PCM1-049** was achieved by following a protocol already described in sub-section 5.2 of the experimental section. The synthesis basically involved coupling many carboxylic acid derivatives to a common amino intermediate **PCM1-028** in presence of EDCI and DMAP to afford the appropriate thiazole methylcarbamates. However, reaction mixtures for analogues **PCM1-029 - PCM1-049**, were not subjected to aqueous work up procedures but were directly chromatographed to give the title compounds. The remaining analogues were otherwise subjected to aqueous work up before further purification by column chromatography as described in section 5.2.

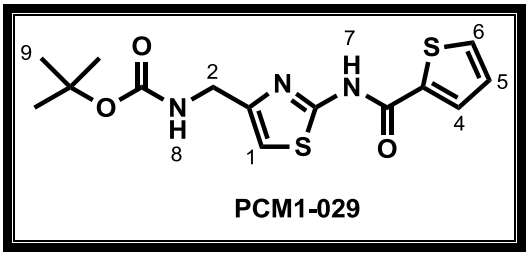

***tert*-Butyl (2-(thiophene-2-carboxamido)thiazol-4-yl)methylcarbamate (PCM1-029)**

White solid (0.07 g, 93%), δ_H (400 MHz; $CDCl_3$) 9.16 (1H, br s, $H_{8,}$), 8.24 (1H, d, J = 3.7 Hz, H_4), 7.53 (1H, d, J = 4.9 Hz, H_6), 6.91 (1H, t, J = 6.9 Hz, H_5), 6.70 (1H, s, H_1), 4.14 (2H, d, J = 6.6 Hz, H_2), 1.47 (9H, s, H_9).

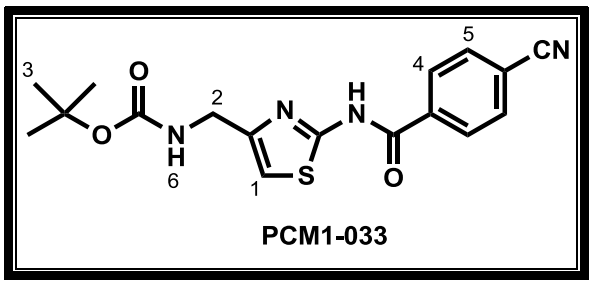

***tert*-Butyl (2-(4-cyanobenzamido)thiazol-4-yl)methylcarbamate (PCM1-033)**

Brown solid (0.2491 g, 94%), δ_H (400 MHz; $CDCl_3$) 8.17 (2H, d, J = 8.7 Hz, H_4), 7.78 (2H, d, J = 8.7 Hz, H_5), 6.96 (1H, s, H_1), 4.98 (1H, br s, H_6), 4.23 (2H, s, H_2), 1.45 (9H, s, H_3).

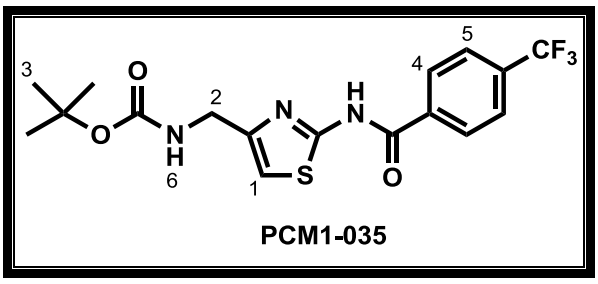

***tert*-Butyl (2-(4-(trifluoromethyl)benzamido)thiazol-4-yl)methylcarbamate (PCM1-035)**

White solid (0.2477 g, 78%), δ_H (400 MHz; $CDCl_3$) 8.17 (2H, d, J = 8.3 Hz, H_5), 7.86 (2H, d, J = 8.2 Hz, H_4), 7.16 (1H, s, H_1), 4.98 (1H, br s, H_6), 4.13 (2H, s, H_2), 1.47 (9H, s, H_3).

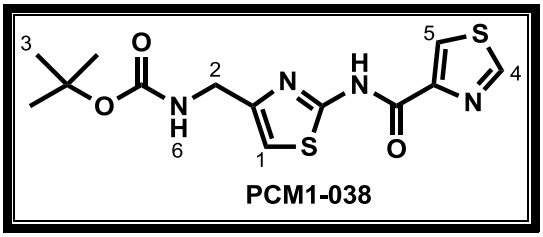

***tert*-Butyl (2-(thiazole-4-carboxamido)thiazol-4-yl)methylcarbamate (PCM1-038)**

White solid (0.2234 g, 94%), δ_H (400 MHz; $CDCl_3$) 9.12 (1H, s, H_4), 8.48 (1H, s, H_5), 7.06 (1H, s, H_1), 4.98 (1H, br s, H_6), 4.14 (2H, s, H_2), 1.45 (1H, s, H_3).

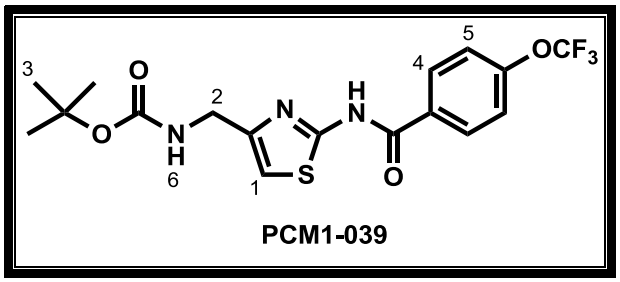

***tert*-Butyl (2-(4-(trifluoromethoxy)benzamido)thiazol-4-yl)methylcarbamate (PCM1-039)**

White solid (0.1722 g, 55%), δ_H (400 MHz; $CDCl_3$), 8.20 (2H, d, J = 8.4 Hz, H_4), 7.19 (2H, d, J = 7.5 Hz, H_5), 6.74 (1H, s, H_1), 4.95 (1H, t, J = 6.7 Hz, H_6), 4.15 (2H, d, J = 6.8 Hz, H_2), 1.44 (9H, s, H_3).

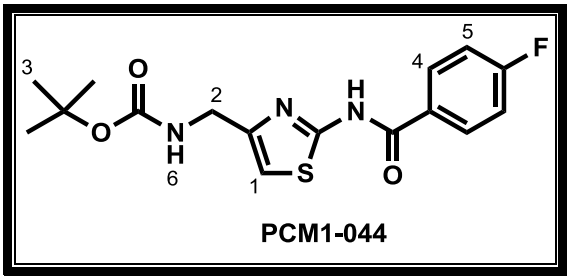

***tert*-Butyl (2-(4-fluorobenzamido)thiazol-4-yl)methylcarbamate (PCM1-044)**

White solid (0.1555 g, 68%), δ_H (400 MHz; $CDCl_3$), 8.26 (2H, m, H_4), 7.10 (2H, t, J = 8.6 Hz, H_5), 6.79 (1H, s, H_1), 4.94 (1H, t, J = 8.0 Hz, H_6), 4.22 (2H, d, J = 8.0 Hz, H_2), 1.49 (9H, s, H_3).

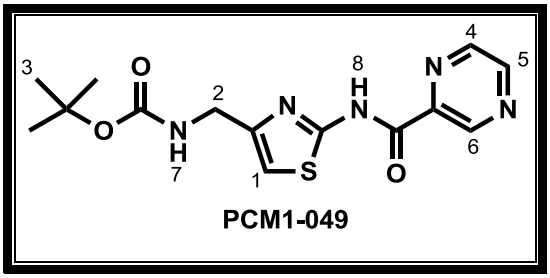

***tert*-Butyl (2-(pyrazine-2-carboxamido)thiazol-4-yl)methylcarbamate (PCM1-049)**

Yellow solid (0.2040 g, 98%), δ_H (400 MHz; $CDCl_3$) 10.78 (1H, br s, H_8), 9.44 (1H, s, H_6), 8.79 (1H, s, H_5), 8.56 (1H, s, H_4), 6.80 (1H, s, H_1), 4.99 (1H, br s, H_7), 4.29 (2H, s, H_2), 1.38 (9H, s, H_3).

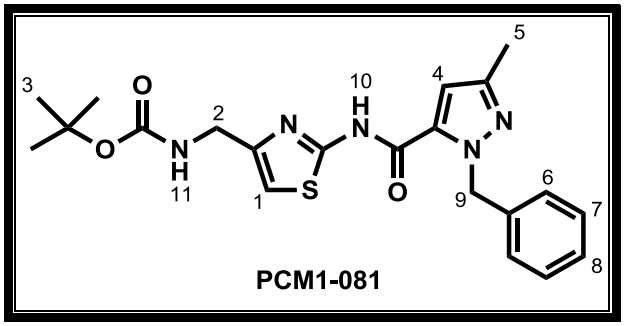

***tert*-Butyl (2-(1-benzyl-3-methyl-1*H*-pyrazole-5-carboxamido)thiazol-4-yl)methylcarbamate (PCM1-081)**

White solid (0.3049 g, 82%) , δ_H (400 MHz; $CDCl_3$) 12.47 (1H, br s, H_{10}), 8.98 (1H, br s, H_{11}), 7.34-7.16 (6H, m, H_1, H_6, H_7, H_8), 6.76 (1H, s, H_4), 5.80 (2H, s, H_9), 4.18 (2H, s, H_2), 2.27 (3H, s, H_5), 1.53 (9H, s, H_3).

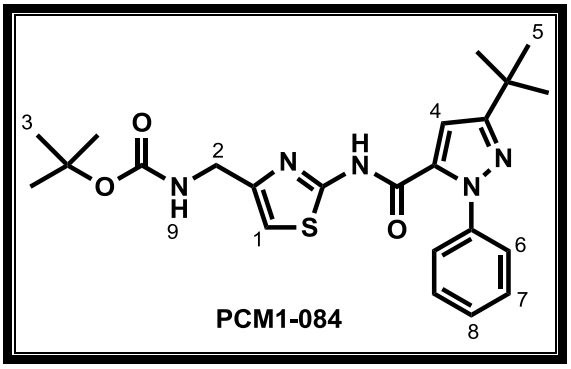

***tert*-Butyl (2-(3-tert-butyl-1-phenyl-1H-pyrazole-5-carboxamido)thiazol-4-yl)methylcarbamate (PCM1-084)**

Colourless oil (0.3474 g, 88%), δ_H (400 MHz; $CDCl_3$) 7.56-7.46 (3H, m, H_7, H_8), 7.37 (2H, d, J = 8.1 Hz, H_6), 6.84 (1H, s, H_1), 6.69 (1H, s, H_4), 5.11 (1H, br s, H_9), 4.26 (2H, d, J = 5.2 Hz, H_2), 1.42 (9H, s, H_3), 1.20 (9H, s, H_5).

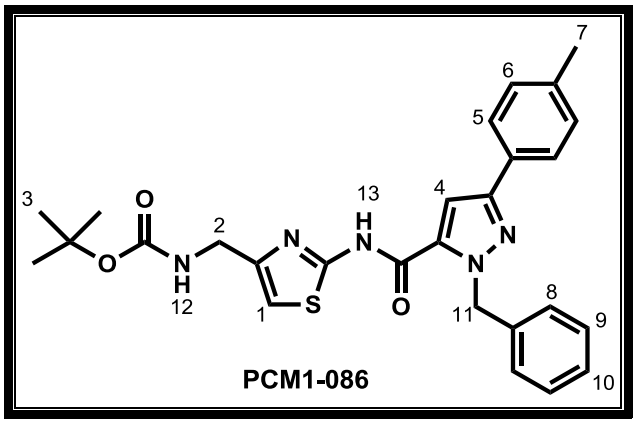

***tert*-Butyl (2-(1-benzyl-3-*p*-tolyl-1*H*-pyrazole-5-carboxamido)thiazol-4-yl)methylcarbamate (PCM1-086)**

White solid (0.1417 g, 88%), δ_H (400 MHz; $CDCl_3$) 9.09 (1H, br s, H_{13}), 7.73 (2H, d, J = 7.9 Hz, H_5), 7.64 (1H, s, H_1), 7.40-7.11 (7H, m, H_6, H_8, H_9, H_{10}), 6.78 (1H, s, H_4), 5.91 (2H, s, H_{11}), 5.08 (1H, br s, H_{12}), 4.20 (2H, s, H_2), 2.37 (3H, s, H_7), 1.52 (9H, s, H_3).

5.11 General synthetic procedure for the aminomethylthiazole carboxamides and aminomethylthiazole benzamides (PCM1-083, PCM1-085, PCM1-087 and PCM1-031-PCM1-051)

The final target compounds **PCM1-083**, **PCM1-085**, **PCM1-087** and **PCM1-031-PCM1-051** were finally obtained by an *N*-boc-deprotection step using TFA. A generic procedure described

under section 5.4 of this dissertation was followed and the title compounds were obtained in poor to good yields (13 – 84%).

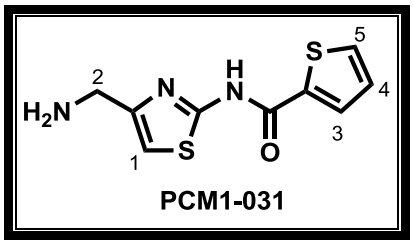

***N*-(4-(Aminomethyl)thiazol-2-yl)thiophene-2-carboxamide (PCM1-031)**

White solid (0.0095 g, 19%), m.p. 174-176 ^{o}C; R_f (CH_3OH-CH_2Cl_2 1.5 : 8.5) 0.14; IR ν_{max}(KBr)/cm^{-1} 3405 (N-H, 1° amine), 2922 (C-H, aminomethyl CH_2), 1690 (C=O, amide), 1551 (C=C, aromatic); δ_H (400 MHz; CD_3OD) 7.93 (1H, s, H_3), 7.80 (1H, s, H_5), 7.21 (1H, s, H_4), 7.06 (1H, s, H_1), 4.02 (2H, s, H_2), δ_C (CD_3OD) 179.2, 159.9, 147.3, 144.5, 133.1, 130.2, 128.5, 112.1, 39.8; EI-*m/z* found 238.9879 (26.9%, M^+), ($C_{10}H_{10}N_3OS$ requires M 239.0187); HPLC purity: 99.4% (t_r = 7.6 min).

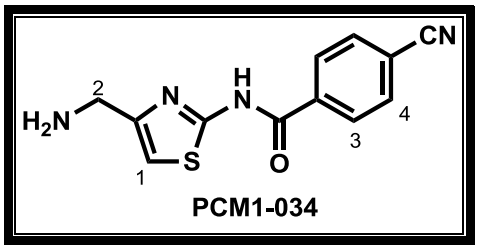

***N*-(4-(Aminomethyl)thiazol-2-yl)-4-cyanobenzamide (PCM1-034)**

Yellow solid (0.15 g, 84%); m.p. 214-216 ^{o}C; R_f (CH_3OH-CH_2Cl_2 1.5 : 8.5) 0.24; IR ν_{max}(KBr)/cm^{-1} 3418 (N-H, 1° amine), 2922 (C-H, aminomethyl CH_2), 2228 (CN, cyano), 1697 (C=O, amide), 1551 (C=C, aromatic); δ_H (400 MHz; CD_3OD) 8.16 (2H, d, J = 8.3 Hz, H_3), 7.88 (2H, d, J = 8.1 Hz, H_4), 7.08 (1H, s, H_1), 4.03 (2H, s, H_2); δ_C (CD_3OD) 165.4, 161.3, 145.8, 137.5, 132.2(3C), 128.4(2C), 117.6, 110.8, 39.6; EI-*m/z* found 258.0575 (43.2%, M^+), ($C_{12}H_{10}N_3OS$ requires M 258.0575); HPLC purity: 97.6% (t_r = 8.1 min).

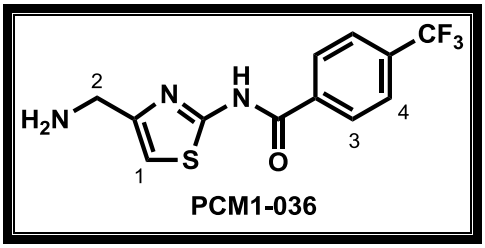

***N*-(4-(Aminomethyl)thiazol-2-yl)-4-(trifluoromethyl)benzamide (PCM1-036)**

White solid (0.15 g, 83%); m.p. 213-214 ^{0}C; R_f (CH_3OH-CH_2Cl_2 1.0 : 9.0) 0.10; IR ν_{max}(KBr)/cm^{-1} 3426 (N-H, 1° amine), 2918 (C-H, aminomethyl CH_2), 1694 (C=O, amide), 1551 (C=C, aromatic) ; δ_H (400 MHz; CD_3OD) 8.17 (2H, d, J = 8.1 Hz, H_3), 7.87 (2H, d, J = 8.2 Hz, H_4), 7.18 (1H, s, H_1), 4.12 (2H, s, H_2); δ_C (CD_3OD) 169.5, 159.1, 143.5, 136.0, 133.5, 128.3(3C), 126.0(2C), 112.5, 38.7; EI-*m/z* found 301.0507 (30.8%, M^+), ($C_{12}H_{10}F_3N_3OS$ requires M 301.0497); HPLC purity: 99.9% (t_r = 11.4 min).

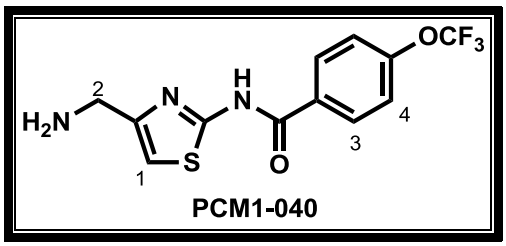

***N*-(4-(Aminomethyl)thiazol-2-yl)-4-(trifluoromethoxy)benzamide (PCM1-040)**

Brown solid (0.0395 g, 78%); m.p. 182-186 ^{0}C; R_f (CH_3OH-CH_2Cl_2 1.5:8.5) 0.10; IR ν_{max}(KBr)/cm^{-1} 3426 (N-H, 1° amine), 2922 (C-H, aminomethyl CH_2), 1690 (C=O, amide), 1555 (C=C, aromatic); δ_H (400 MHz; CD_3OD) 8.7 (2H, d, J = 8.7 Hz, H_3), 7.45 (2H, d, J = 8.5 Hz, H_4), 7.08 (1H, s, H_1), 4.02 (2H, s, H_2); δ_C (CD_3OD) 165.0, 160.0, 153.0, 144.5, 131.5, 129.8(3C), 120.6(2C), 111.0, 39.1; EI-*m/z* found 317.0639 (29.2%, M^+), ($C_{12}H_{10}F_3N_3O_2S$ requires M 317.0446); HPLC purity: 95.2% (t_r = 11.8 min).

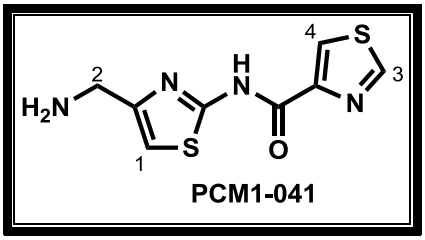

***N*-(4-(Aminomethyl)thiazol-2-yl)thiazole-4-carboxamide (PCM1-041)**

Brown solid (0.044 g, 28%); m.p. 151-153 ^{o}C; R_f (CH_3OH-CH_2Cl_2 1.5 : 8.5) 0.20; IR ν_{max}(KBr)/cm^{-1} 3405 (N-H, 1° amine), 2922 (C-H, aminomethyl CH_2), 1677 (C=O, amide), 1551 (C=C, aromatic) ; δ_H (400 MHz; CD_3OD) 9.11 (1H, s, H_3), 8.49 (1H, s, H_4), 7.07 (1H, s, H_1), 4.01 (2H, s, H_2); δ_C (CD_3OD) 159.1(2C), 154.8, 149.0, 146.5, 125.7, 110.7, 39.8; EI-*m/z* found 240.0140 (62.5%, M^+), ($C_8H_8N_4OS_2$ requires M 240.0140); HPLC purity: 99.9% (t_r = 3.7 min).

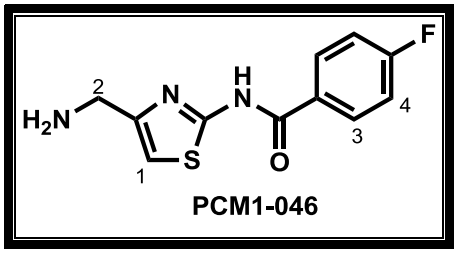

***N*-(4-(Aminomethyl)thiazol-2-yl)-4-fluorobenzamide (PCM1-046)**

Brown solid (0.0702 g, 63%); m.p. 209-210 ^{o}C; R_f (CH_3OH-CH_2Cl_2 1.5 : 8.5) 0.10; IR ν_{max}(KBr)/cm^{-1} 3418 (N-H, 1° amine), 2924 (C-H, aminomethyl CH_2), 1671 (C=O, amide), 1542 (C=C, aromatic); δ_H (400 MHz; CD_3OD) 8.07 (2H, dd, J = 5.0, 8.7 Hz, H_3), 7.29 (2H, t, J = 8.7 Hz, H_4), 7.17 (1H, s, H_1), 4.13 (2H, s, H_2); δ_C (CD_3OD) 167.5, 165.0, 159.9, 144.5, 130.0(2C), 129.0, 115.5(2C), 111.5, 39.5; EI-*m/z* found 250.9708 (34.6%, M^+), ($C_{11}H_{10}FN_3OS$ requires M 251.0529); HPLC purity: 99.1% (t_r = 9.2 min).

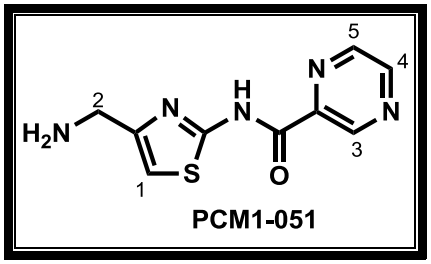

***N*-(4-(Aminomethyl)thiazol-2-yl)pyrazine-2-carboxamide (PCM1-051)**

Yellow solid (0.08 g, 57%); m.p. 176-180 ^{o}C; R_f (CH_3OH-CH_2Cl_2 2.0 : 8.0) 0.10; IR ν_{max}(KBr)/cm^{-1} 3422 (N-H, 1° amine), 2924 (C-H, aminomethyl CH_2), 1675 (C=O, amide), 1546

(C=C, aromatic); δ_H (400 MHz; [D_6]DMSO) 9.30 (1H, s, H_3), 8.88 (2H, s, H_4), 8.79 (1H, s, H_5), 7.15 (1H, s, H_1), 3.95 (2H, s, H_2); δ_C ([D_6]DMSO) 162.9, 159.5, 148.6, 140.0, 144.6(2C), 144.2, 111.6, 39.7; EI-*m/z* found 234.8896 (100%, M^+), ($C_9H_9N_5OS$ requires M 235.0528); HPLC purity: 99.9% (t_r = 3.4 min).

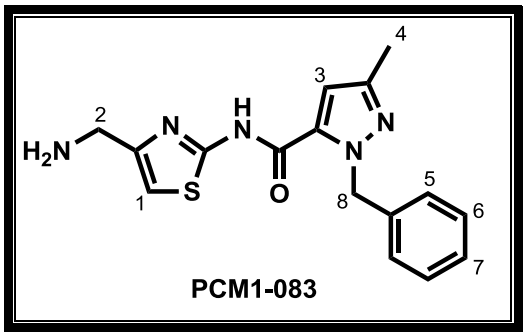

***N*-(4-(Aminomethyl)thiazol-2-yl)-1-benzyl-3-methyl-1*H*-pyrazole-5-carboxamide (PCM1-083)**

White solid (0.0814 g, 35%), m.p. 158-160 ^{o}C; R_f (CH_3OH-CH_2Cl_2 1.0 : 9.0) 0.17; IR ν_{max}(KBr)/cm^{-1} 3431 (N-H, 1° amine), 3060 (C-H, aromatic), 2931 (C-H, aminomethyl CH_2), 1669 (C=O, amide), 1549 (C=C, aromatic); δ_H (400 MHz; CD_3OD) 7.29-7.16 (5H, m, H_5, H_6, H_7), 7.07 (1H, s, H_1), 6.84 (1H, s, H_3), 5.73 (2H, s, H_8), 4.03 (2H, s, H_2), 2.30 (3H, s, H_4); δ_C (CD_3OD) 159.5, 158.1, 147.9, 145.5, 137.5, 134.7, 128.1 (2C), 127.3 (2C), 127.0, 113.7, 108.1, 53.9, 39.4, 11.8; EI-*m/z* found 327.0607 (100.0%, M^+), ($C_{16}H_{17}N_5OS$ requires M 327.1154); HPLC purity: 97.4% (t_r = 10.23 min).

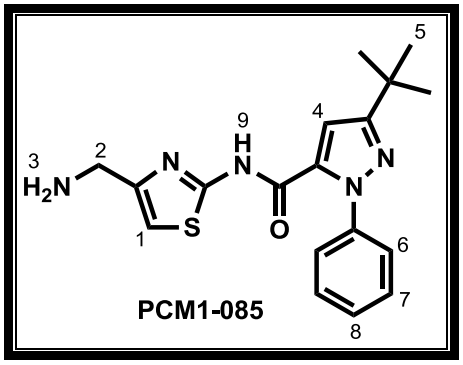

***N*-(4-(Aminomethyl)thiazol-2-yl)-3-*tert*-butyl-1-phenyl-1*H*-pyrazole-5-carboxamide (PCM1-085)**

Brown solid (0.1446 g, 54%), m.p. 85-88 ^{o}C; R_f (CH_3OH-CH_2Cl_2 1.0 : 9.0) 0.31; IR ν_{max}(KBr)/cm^{-1} 3379 (N-H, 1° amine), 3056 (C-H, aromatic), 2970 (C-H, *tert*-butyl CH_3), 2927 (C-H, aminomethyl CH_2), 1680 (C=O, amide), 1542 (C=C, aromatic); δ_H (400 MHz; $CDCl_3$) 7.56-7.43 (3H, m, H_7, H_8), 7.31 (2H, d, J = 7.5 Hz, H_6), 7.26 (1H, s, H_9), 6.81 (1H, s, H_1), 6.61 (1H, s, H_4), 4.92 (2H, br s, H_3), 3.77 (2H, s, H_2), 1.18 (9H, s, H_5); δ_C ($CDCl_3$) 159.7, 158.7, 156.0, 146.6, 141.3, 129.9, 128.8 (2C), 128.3 (3C), 110.4, 105.4, 40.2, 32.2, 30.5 (3C); EI-*m/z* found 355.1451 (98.5%, M^+), ($C_{18}H_{21}N_5OS$ requires M 355.1467); HPLC purity: 99.1% (t_r = 13.79 min).

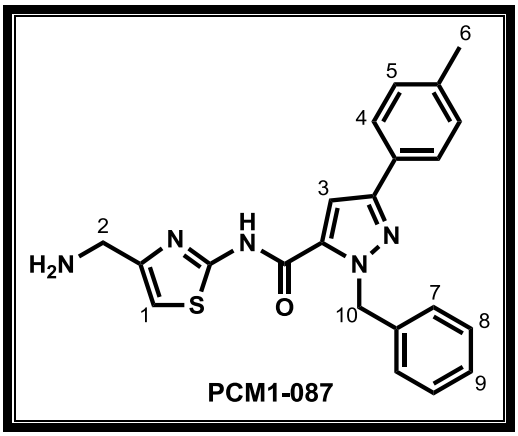

***N*-(4-(Aminomethyl)thiazol-2-yl)-1-benzyl-3-*p*-tolyl-1*H*-pyrazole-5-carboxamide (PCM1-087)**

Brown solid (0.0921 g, 14%), m.p. 85-87 ^{o}C; R_f (CH_3OH-CH_2Cl_2 1.0 : 9.0) 0.30; IR ν_{max}(KBr)/cm^{-1} 3414 (N-H, 1° amine), 2953 (C-H, methyl), 2922 (C-H, aminomethyl CH_2), 1678 (C=O, amide), 1551 (C=C, aromatic); δ_H (300 MHz; CD_3OD) 7.74 (2H, d, J = 8.2 Hz, H_4), 7.38 (1H, s, H_1), 7.33-7.13 (8H, m, H_3, H_5, H_7, H_8, H_9), 5.84 (2H, s, H_{10}), 4.14 (2H, s, H_2), 2.36 (3H,

s, H_6); δ_C (CD_3OD) 162.0, 159.9, 158.9, 151.0, 143.9, 139.9, 138.8, 129.9, 129.0 (2C), 128.1 (2C), 127.1 (2C), 125.3 (3C), 112.5, 105.4, 54.5, 38.7, 19.9; EI-*m/z* found 403.0529 (27.1%, M^+), ($C_{22}H_{21}N_5OS$ requires M 403.1467); HPLC purity: 95.9% (t_r = 7.30 min).

5.22 General procedure for the synthesis of pyrazole thiazole methylcarbamates (PCM1-054 and PCM1-082)

The pyrazole thiazole methylcarbamates (**PCM1-054** and **PCM1-082**) were prepared following a general procedure detailed in section 5.10 with slight modifications. The reactions typically involved coupling of the appropriate pyrazole carboxylic acid to the amino intermediate **PCM1-028** (section 5.9) in presence of EDCI and DMAP. After completion of reaction as signalled by TLC, the reaction mixture for analogue **PCM1-054** was concentrated *in vacuo* and directly subjected to column chromatography (SiO_2, 0 – 40% EtOAc/Hexane) to give the desired product as a white solid. The aqueous work up in this case was deliberately avoided to circumvent the opportunity of losing part of the desired product into the aqueous phase. Due to poor solubility of the pyrazole carboxylic acid starting material, intermediate **PCM1-082** was prepared by carrying out the reaction in DMF followed by precipitation of the product by addition of deionised water. The precipitate was filtered and sequentially washed with deionised water, hexane, and a minimal amount of EtOAc to deliver the pyrazole intermediate **PCM1-082** as a brown solid.

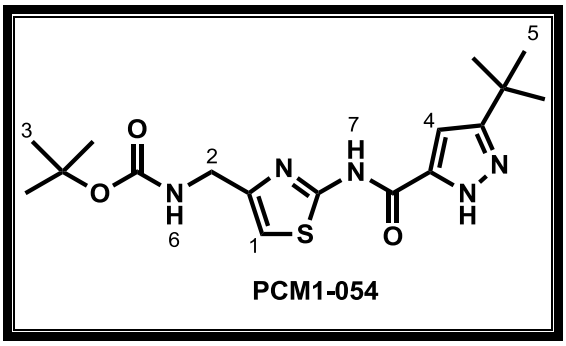

PCM1-054

***tert*-Butyl (2-(3-*tert*-butyl-1*H*-pyrazole-5-carboxamido)thiazol-4-yl)methylcarbamate (PCM1-054)**

White solid (1.0244 g, 42%), δ_H (400 MHz; $CDCl_3$) 7.35(1H, s, H_7), 6.80 (1H, s, H_1), 6.72 (1H, s, H_4), 5.24 (1H, br s, H_6), 4.50 (2H, br s, H_2), 1.48 (9H, s, H_3), 1.34 (9H, s, H_5).

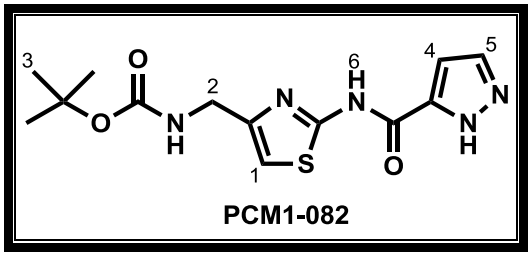

***tert*-Butyl (2-(1*H*-pyrazole-5-carboxamido)thiazol-4-yl)methylcarbamate (PCM1-082)**

Brown solid (0.3875 g, 55%), δ_H (400 MHz; [D_6]DMSO) 7.83(1H, br s, H_6), 7.24 (1H, br s, H_5), 7.02 (1H, br s, H_4), 6.84 (1H, s, H_1), 4.14 (2H, s, H_2), 1.39 (9H, s, H_3).

5.23 General procedure for the synthesis of benzyl pyrazole thiazole methylcarbamates (PCM1-055, PCM1-057, PCM1-064, PCM1-067, PCM1-071 and PCM1-088)

The methylcarbamate intermediates **PCM1-055** - **PCM1-071** and **PCM1-088** were synthesised by respectively stirring the pyrazole precursors **PCM1-054** and **PCM1-082** (1.0 eq) with the appropriate benzyl bromide (2.0 eq) in presence of K_2CO_3 (2.0 eq) base in DMF or acetonitrile at room temperature. Save for **PCM1-055** and **PCM1-057** whose reactions were performed in acetonitrile, DMF was used in all the reactions. The reaction mixture was stirred for 12 – 48 h, concentrated *in vacuo*, and partitioned between deionised water and dichloromethane. The organic layer was dried ($MgSO_4$), concentrated *in vacuo*, and subjected to column chromatography (SiO_2, 0-30% EtOAc/hexane) to afford the title compounds. **PCM1-071** was, however, further purified by preparative-TLC in 30% EtOAc/hexane after failed column chromatographic separation.

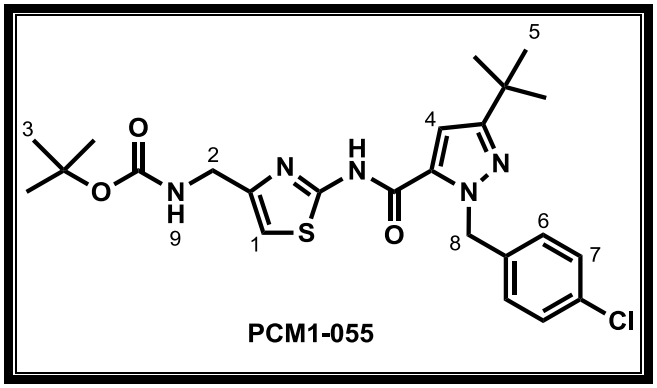

***tert*-Butyl (2-(3-*tert*-butyl-1-(4-chlorobenzyl)-1*H*-pyrazole-5-carboxamido)thiazol-4 yl) methylcarbamate (PCM1-055)**

White solid (0.0713 g, 26%), δ_H (400 MHz; $CDCl_3$) 7.25-7.14 (4H, m, H_6, H_7), 6.78 (1H, s, H_1), 6.63 (1H, s, H_4), 5.98 (2H, s, H_8), 4.90 (1H, br s, H_9), 4.28 (2H, s, H_2), 1.45 (9H, s, H_3), 1.33 (9H, s, H_5).

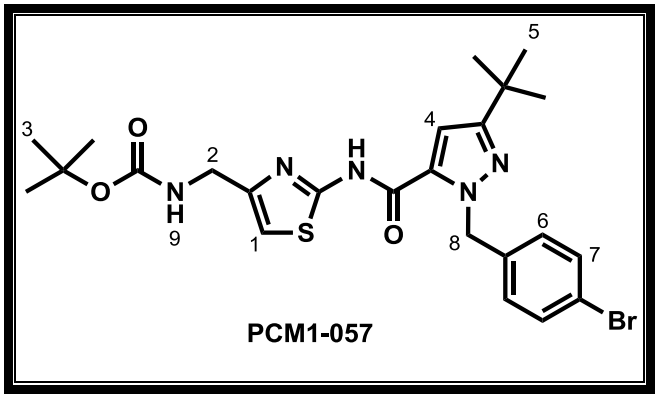

***tert*-Butyl (2-(1-(4-bromobenzyl)-3-*tert*-butyl-1*H*-pyrazole-5-carboxamido)thiazol-4yl) methylcarbamate (PCM1-057)**

White solid (0.1040 g, 48%), δ_H (400 MHz; $CDCl_3$) 7.35 (2H, d, J = 8.5 Hz, H_7), 7.20 (1H, s, H_1), 7.08 (2H, d, J = 8.5 Hz, H_6), 6.50 (1H, s, H_4), 6.08 (2H, s, H_8), 4.09 (2H, s, H_2), 1.44 (9H, s, H_3), 1.31 (9H, s, H_5).

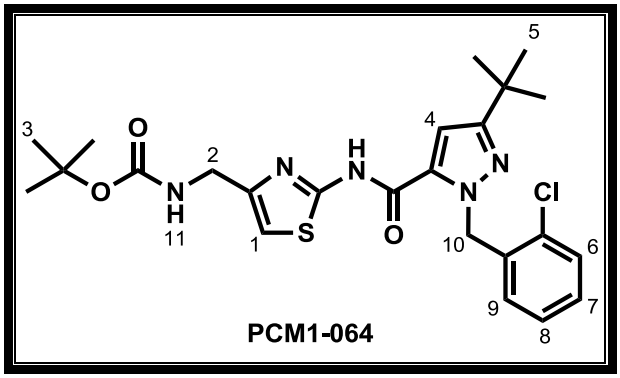

***tert*-Butyl (2-(3-*tert*-butyl-1-(2-chlorobenzyl)-1*H*-pyrazole-5-carboxamido)thiazol-4-yl)methylcarbamate (PCM1-064)**

White solid (0.0417 g, 18%), δ_H (400 MHz; $CDCl_3$) 7.38 (1H, dd, J = 8.5, 1.4 Hz, H_6), 7.20-7.08 (2H, m, H_7, H_8), 7.00 (1H, d, J = 7.7 Hz, H_9), 6.81 (1H, s, H_1), 6.53 (1H, s, H_4), 6.03 (2H, s, H_{10}), 4.94 (1H, br s, H_{11}), 4.24 (2H, d, J = 8.0 Hz, H_2), 1.43 (9H, s, H_3), 1.29 (9H, s, H_5).

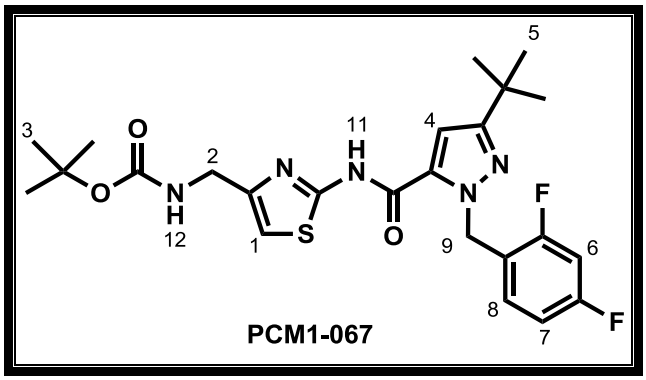

***tert*-Butyl (2-(3-*tert*-butyl-1-(2,4-difluorobenzyl)-1*H*-pyrazole-5-carboxamido)thiazol-4-yl)methylcarbamate (PCM1-067)**

White solid (0.0651 g, 27%), δ_H (400 MHz; $CDCl_3$) 7.26 (1H, s, H_1), 7.12 (1H, m, H_6), 6.90-6.67 (2H, m, H_7, H_8), 6.64 (1H, s, H_4), 5.99 (2H, s, H_9), 4.94 (1H, br s, H_{12}), 4.26 (2H, s, H_2), 1.45 (9H, s, H_3), 1.34 (9H, s, H_5).

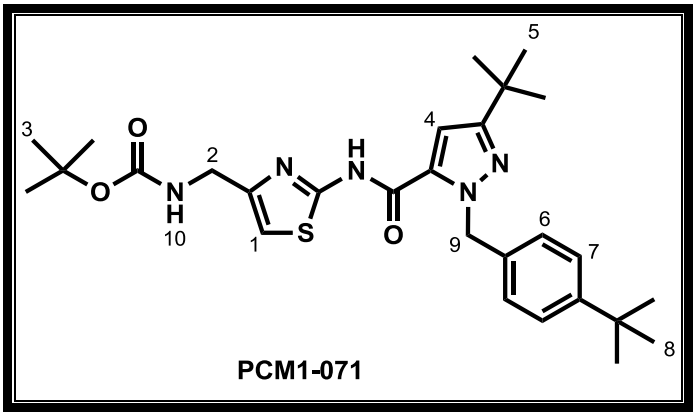

***tert*-Butyl (2-(3-*tert*-butyl-1-(4-*tert*-butylbenzyl)-1*H*-pyrazole-5-carboxamido)thiazol-4-yl)methylcarbamate (PCM1-071)**

White solid (0.0683 g, 28%), δ_H (400 MHz; $CDCl_3$) 7.25 (2H, d, J = 8.0 Hz, H_6), 7.15 (2H, d, J = 8.0 Hz, H_7), 6.79 (1H, s, H_1), 6.57 (1H, s, H_4), 5.95 (2H, s, H_9), 4.98 (1H, br s, H_{10}), 4.30 (2H, br s, H_2), 1.45 (9H, s, H_3), 1.31 (9H, s, H_5), 1.26 (9H, s, H_8).

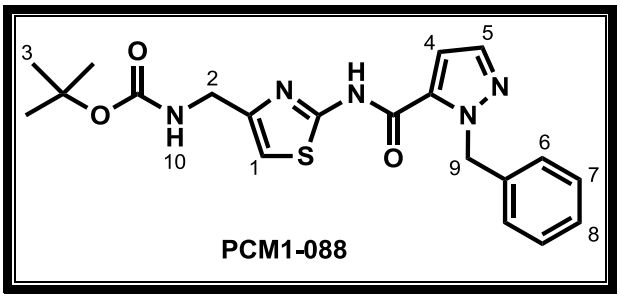

***tert*-Butyl (2-(1-benzyl-1*H*-pyrazole-5-carboxamido)thiazol-4-yl)methylcarbamate (PCM1-088)**

Whitish oil (0.1709 g, 34%), δ_H (400 MHz; $CDCl_3$) 7.54 (1H, s, H_5), 7.48-7.05 (6H, m, H_4, H_6, H_7, H_8), 6.93 (1H, s, H_1), 5.95 (2H, s, H_9), 4.95 (1H, br s, H_{10}), 4.32 (2H, br s, H_2), 1.45 (9H, s, H_3).

5.24 General procedure for the synthesis of aminomethylthiazole pyrazole carboxamides (PCM1-056 - PCM1-073 and PCM1-089)

The final target compounds **PCM1-056 - PCM1-073** and **PCM1-089** were synthesised by deprotection of their *N*-boc-protected precursors (**PCM1-055**, **PCM1-057**, **PCM1-064**, **PCM1-067**, **PCM1-071** and **PCM1-088**) by treatment with TFA. A general procedure described in section 5.4 of this dissertation was followed.

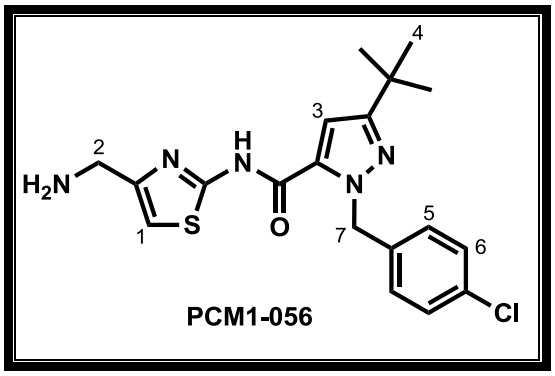

***N*-(4-(Aminomethyl)thiazol-2-yl)-3-*tert*-butyl-1-(4-chlorobenzyl)-1*H*-pyrazole-5-carboxamide (PCM1-056)**

White solid (0.0181 g, 22%), m.p. 115-117 ^{o}C; R_f (CH_3OH-CH_2Cl_2 1.0 : 9.0) 0.07; IR ν_{max}(KBr)/cm^{-1} 3435 (N-H, 1° amine), 3103 (C-H, aromatic), 2966 (C-H, *tert*-butyl CH_3), 1667 (C=O, amide); δ_H (400 MHz; CD_3OD) 7.22 (2H, d, J = 8.6 Hz, H_6), 7.20 (1H, s, H_1), 7.14 (2H, d, J = 8.7 Hz, H_5), 6.50 (1H, s, H_3), 6.09 (2H, s, H_7), 4.06 (2H, s, H_2), 1.32 (9H, s, H_4); δ_C (CD_3OD) 165.1, 160.9 (2C), 143.8, 136.8, 132.0, 129.8, 128.3 (2C), 128.0 (2C), 113.5, 104.2, 50.7, 39.2, 30.5, 29.0 (3C); EI-*m/z* found 403.0546 (24.9%, M^+), ($C_{19}H_{22}ClN_5OS$ requires M 403.1234); HPLC purity: 98.7% (t_r = 7.52 min).

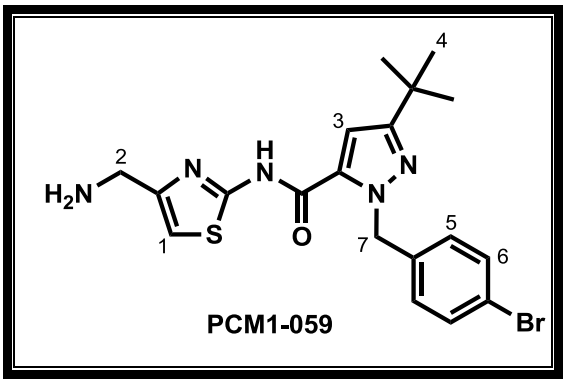

***N*-(4-(Aminomethyl)thiazol-2-yl)-1-(4-bromobenzyl)-3-*tert*-butyl-1*H*-pyrazole-5-carboxamide (PCM1-059)**

Brown solid (0.0138 g, 16%), m.p. 92-94 ^{o}C; R_f (CH_3OH-CH_2Cl_2 1.0 : 9.0) 0.21; IR ν_{max}(KBr)/cm^{-1} 3414 (N-H, 1° amine), 3099 (C-H, aromatic), 2961 (C-H, *tert*-butyl CH_3), 2927 (C-H, aminomethyl CH_2), 1667 (C=O, amide); δ_H (400 MHz; CD_3OD) 7.36 (2H, d, J = 8.5 Hz, H_6), 7.21 (1H, s, H_1), 7.09 (2H, d, J = 8.5 Hz, H_5), 6.50 (1H, s, H_3), 6.08 (2H, s, H_7), 4.09 (2H, s, H_2), 1.32 (9H, s, H_4); δ_C (CD_3OD) 164.1, 160.9 (2C), 143.3, 137.3, 131.2, 130.9 (2C), 129.0

(2C), 120.3, 113.7, 104.3, 50.9, 39.1, 29.3, 29.1 (3C); EI-*m/z* found 447.0108 (24.1%, M^+), ($C_{19}H_{22}BrN_5OS$ requires M 447.0728); HPLC purity: 98.1% (t_r = 8.02 min).

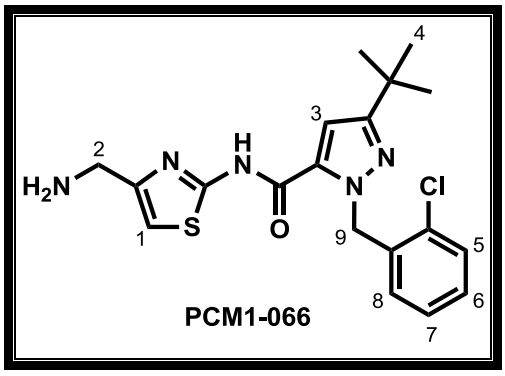

***N*-(4-(Aminomethyl)thiazol-2-yl)-3-*tert*-butyl-1-(2-chlorobenzyl)-1*H*-pyrazole-5-carboxamide (PCM1-066)**

White solid (0.0160 g, 50%), m.p. 143-145 ^oC; R_f (CH_3OH-CH_2Cl_2 1.0 : 9.0) 0.25; IR ν_{max}(KBr)/cm^{-1} 3422 (N-H, 1° amine), 3086 (C-H, aromatic), 2961 (C-H, *tert*-butyl CH_3), 1637 (C=O, amide); δ_H (400 MHz; CD_3OD) 7.37 (1H, d, J = 7.9 Hz, H_5), 7.29 (1H, s, H_1), 7.22-7.11 (2H, m, H_6, H_7), 6.90 (1H, d, J = 7.7 Hz, H_8), 6.43 (1H, s, H_3), 4.09 (2H, s, H_2), 1.26 (9H, s, H_4); δ_C (CD_3OD) 161.1, 142.4 (2C), 135.5, 132.0, 129.0 (2C), 127.8 (2C), 126.7, 126.4, 114.5, 104.0, 50.1, 38.7, 30.5, 29.0 (3C); EI-*m/z* found 403.0250 (37.1%, M^+), ($C_{19}H_{22}ClN_5OS$ requires M 403.1234); HPLC purity: 96.6% (t_r = 7.14 min).

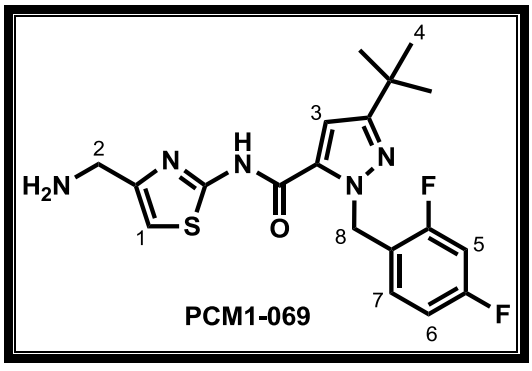

***N*-(4-(Aminomethyl)thiazol-2-yl)-3-*tert*-butyl-1-(2,4-difluorobenzyl)-1*H*-pyrazole-5-carboxamide (PCM1-069)**

White solid (0.0130 g, 68%), m.p. 149-153 ^oC; R_f (CH_3OH-CH_2Cl_2 1.4 : 8.6) 0.40; IR ν_{max}(KBr)/cm^{-1} 3427 (N-H, 1° amine), 3091 (C-H, aromatic), 2966 (C-H, *tert*-butyl CH_3), 1671 (C=O, amide); δ_H (400 MHz; CD_3OD) 7.21 (1H, s, H_1), 7.05 (1H, m, H_5), 6.95-6.73 (2H, m, H_6,

H_7), 6.52 (1H, s, H_3), 6.11 (2H, s, H_8), 4.05 (2H, s, H_2), 1.32 (9H, s, H_4); EI-*m/z* found 405.1111 (39.7%, M^+), ($C_{19}H_{21}F_2N_5OS$ requires M 405.1435); HPLC purity: 97.3% (t_r = 7.95 min).

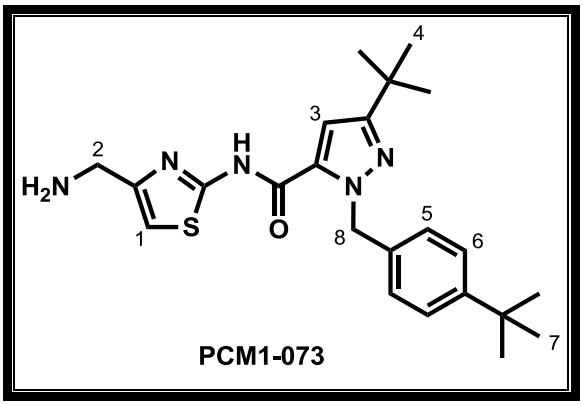

***N*-(4-(Aminomethyl)thiazol-2-yl)-3-*tert*-butyl-1-(4-*tert*-butylbenzyl)-1*H*-pyrazole-5-carboxamide (PCM1-073)**

Brown solid (0.0285 g, 52%), m.p. 118-120 °C; R_f (CH_3OH-CH_2Cl_2 1.0 : 9.0) 0.20; IR ν_{max}(KBr)/cm^{-1} 3435 (N-H, 1° amine), 2957 (C-H, *tert*-butyl CH_3), 2927 (C-H, aminomethyl CH_2) 1669 (C=O, amide); δ_H (400 MHz; CD_3OD) 7.26 (2H, d, *J* = 8.3 Hz, H_5), 7.18 (1H, s, H_1), 7.04 (2H, d, *J* = 8.3 Hz, H_6), 6.40 (1H, s, H_3), 6.04 (2H, s, H_8), 4.06 (2H, s, H_2), 1.30 (9H, s, H_4), 1.25 (9H, s, H_7); δ_C (CD_3OD) 161.2, 149.9, 144.8, 143.0, 134.8, 126.9, 126.2 (2C), 125.0 (2C), 113.3, 103.9, 51.0, 39.3, 33.1, 31.3, 30.3 (3C), 29.0 (3C); EI-*m/z* found 425.1754 (26.5%, M^+), ($C_{23}H_{31}N_5OS$ requires M 425.2249); HPLC purity: 95.4% (t_r = 7.69 min).

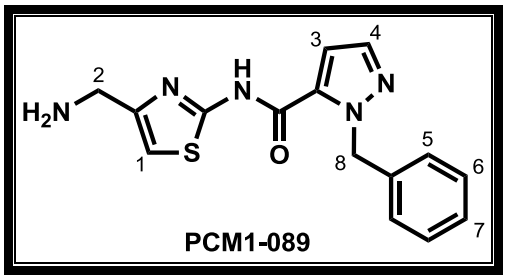

***N*-(4-(Aminomethyl)thiazol-2-yl)-1-benzyl-1*H*-pyrazole-5-carboxamide (PCM1-089)**

Yellow solid (0.0300 g, 23%), m.p. 166-169 °C; R_f (CH_3OH-CH_2Cl_2 1.0 : 9.0) 0.25; δ_H (400 MHz; CD_3OD) 7.80 (1H, s, H_4), 7.44-7.05 (6H, m, H_3, H_5, H_6, H_7), 6.93 (1H, s, H_1), 5.48 (2H, s, H_8), 4.11 (2H, s, H_2); δ_C (CD_3OD) 160.3, 159.1, 144.4, 143.3, 136.2, 132.4, 128.5 (2C), 128.0 (2C), 127.4, 112.1, 107.4, 56.0, 38.8; EI-*m/z* found 313.0404 (100.0%, M^+), ($C_{15}H_{15}N_5OS$ requires M 313.0997); HPLC purity: 97.2% (t_r = 6.42 min).

5.25 Procedure for biological assays

Compounds were tested in triplicate against chloroquine-sensitive (CQS) strain of *Plasmodium falciparum* (NF54). A modified method of Trager and Jensen[1] was used to maintain continuous *in vitro* cultures of asexual erythrocyte stages of *P. falciparum*. Antiplasmodial activity *in vitro* was quantitatively assessed via the parasite lactate dehydrogenase assay using a modified method described by Makler *et al*.[2] For each sample a 20 mg/ml stock solution in DMSO was prepared and sonicated to enhance solubility. Samples were tested as a suspension if not completely dissolved. Stock solutions were stored at -20 ºC and further diluted on the day of the experiment. Chloroquine (CQ) and artesunate were used as the reference drugs.

5.26 References

1. Trager, W.; Jensen, J.B. *Science*. **1976**, *193*, 673-675.
2. Makler, M.T.; Ries, J.M.; Williams, J.A.; Bancroft, J.E.; Piper, R.C.; Gibbins, B.L.; Hinrichs, D.J. *Am. Soc. Trop. Med. Hyg*. **1993**, *48*, 739-741.